TECHNICAL REPORT
NATICK/TR-00/010

AD_____

PASSIVE AIRBAG VENT CONTROL VALVE STUDY

by
Nicholas P. Rosato

December 1999

Final Report
October 1996 - December 1998

Approved for Public Release; Distribution is Unlimited

U.S. Army Soldier and Biological Chemical Command
Soldier Systems Center
Natick, Massachusetts 01760-5017

DISCLAIMERS

The findings contained in this report are not to be construed as an official Department of the Army position unless so designated by other authorized documents.

Citation of trade names in this report does not constitute an official endorsement or approval of the use of such items.

DESTRUCTION NOTICE

For Classified Documents:

Follow the procedures in DoD 5200.22-M, Industrial Security Manual, Section II-19 or DoD 5200.1-R, Information Security Program Regulation, Chapter IX.

For Unclassified/Limited Distribution Documents:

Destroy by any method that prevents disclosure of contents or reconstruction of the document.

REPORT DOCUMENTATION PAGE

Form Approved
OMB No. 0704-0188

1. REPORT DATE *(DD-MM-YYYY)*	2. REPORT TYPE	3. DATES COVERED *(From - To)*
13-12-1999	Final Report	Oct 96-Dec 98

4. TITLE AND SUBTITLE

PASSIVE AIRBAG VENT CONTROL VALVE STUDY

5a. CONTRACT NUMBER

5b. GRANT NUMBER

5c. PROGRAM ELEMENT NUMBER
1L162786

6. AUTHOR(S)

Nicholas P. Rosato

5d. PROJECT NUMBER
D283

5e. TASK NUMBER
D

5f. WORK UNIT NUMBER
AA

7. PERFORMING ORGANIZATION NAME(S) AND ADDRESS(ES)

U.S. Army Soldier Biological Chemical Command
Soldier Systems Center
Kansas Street Attn: AMSSB-RAD-T (N)
Natick, MA 01760-5017

8. PERFORMING ORGANIZATION REPORT NUMBER

NATICK-TR-00-010

9. SPONSORING/MONITORING AGENCY NAME(S) AND ADDRESS(ES)

10. SPONSOR/MONITOR'S ACRONYM(S)

11. SPONSOR/MONITOR'S REPORT NUMBER(S)

12. DISTRIBUTION/AVAILABILITY STATEMENT

13. SUPPLEMENTARY NOTES

14. ABSTRACT

The U.S. Army currently uses paper honeycomb material to both dissipate the ground impact energy and to cushion parachute delivered airdropped payload from damage. This report documents exploring the use of pressurized airbags with passively controlled exhaust vents as a means to mitigate ground impact landing shock. The results of both computational and experimental research that examined the performance of passively controlled venting candidates are presented. The venting candidates studied consisted of two different linear spring check valve designs, a magnetostatic check valve design, along with two precision release blowout vents configured using a four pole magnetic valve seat design.

15. SUBJECT TERMS

AIRBAGS	AIRDROP OPERATIONS	GROUND SHOCK
GROUND IMPACT	IMPACT ATTENUATION	GROUND IMPACT ATTENUATION
CUSHIONING	ENERGY ABSORPTION	SHOCK MITIGATION

16. SECURITY CLASSIFICATION OF:			17. LIMITATION OF ABSTRACT	18. NUMBER OF PAGES	19a. NAME OF RESPONSIBLE PERSON
a. REPORT	b. ABSTRACT	c. THIS PAGE			Nicholas Rosato
Unclassified	Unclassified	Unclassified	SAR	81	19b. TELEPHONE NUMBER *(Include area code)* 508-233-5909

TABLE OF CONTENTS

LIST OF FIGURES

LIST OF FIGURES (Cont'd)

LIST OF FIGURES (Cont'd)

LIST OF FIGURES (Cont'd)

PREFACE AND ACKNOWLEDGEMENTS

The present investigation, Passive Airbag Vent Control Study, was performed by the author in the Experimental Research Team of the Mobility Directorate, Science & Technology Group. This report documents work accomplished in the study of airbag vent control valves for the airdrop cargo delivery application. The report serves to document the data required for the initial part of a Cooperative Research and Development Agreement effort between Marrotta Scientific Controls, Inc. and the Natick Soldier Center, (Natick) Soldier Systems Center, U.S. Army Soldier and Biological Chemical Command.

The efforts of many individuals were required in order to create and produce the equipment used for this study. The data contained in this document is due to their diligent work efforts. The author wishes to thank Zvi Horwitz from Federal Fabrics-Fibers Inc. for furnishing a seamless woven scale model airbag for the testing portion of the research. The fabrication of the prototype passive valves, scale model airbag system and valve test chamber were performed through the skill of several individuals at Natick under the guidance of Randy Natches. The author wishes to thank Junior Christmas, Lionel Lafleur, Ralph Routh and Ken Rowe from the Prototype Fabrication Office for their knowledge and skill in fabricating the equipment used in the experimental part of the research study. A special thanks goes to John Doucette from the Testing Team in support of the experimental test of the scale model airbag system.

The research study was funded under a Soft Landing Airdrop Technology, Science & Technology Objective program. The work was conducted from October 1, 1996 through December 31, 1998 under Program Element: 1L162786, Project No. D283, Work Unit: AA-D, and Aggregate Code: T/B 1513.

PASSIVE AIRBAG VENT CONTROL VALVE STUDY

Introduction

This report presents the results of computational and experimental research that examined the performance of passive control valve candidates for use with airborne cargo style airbag cushioning systems. Past methods to improve the performance of airbags for airdrop were conducted by Lee[1], who determined methods to optimize energy absorption through airbag vent-control and gas-injection techniques. A parachute-suspended platform descending toward the ground at terminal velocity carrying a payload with an airbag ground shock attenuation system, can in theory be designed to effectively limit the magnitude of the applied G-force sustained during landing. The U.S. Army current standard uses a paper honeycomb material to dissipate the ground impact energy and to cushion the airdropped payload from damage.

The intent of the current research was to explore the possibility of using passive exhaust vented pressurized airbags to perform shock mitigation as effectively as the dynamic response of paper honeycomb. An airbag system model describing the gas dynamic compression in response to a simplified one degree of freedom impact was used to calculate the response of the inertial forces applied to the airdropped payload.
Analytical research of the performance of various airbag system configurations being subjected to impacts was conducted using a digital computer model. The computer model was created to simulate the compression of a pre-pressurized airbag having check valve styled air-release vents, or precision blow out patches to relieve internal bag pressure. Experimental research was conducted using hardware designed specifically to function as close to the ideal calculated behavior as possible. The empirical study of the behavior was conducted on a scale model system to further reveal system incalculable performance and to validate the digital simulated results.

The airbag system used for the experimentation contained a tank of compressed air connected to a ventable airbag through an electrically actuated solenoid valve. The solenoid valve normally remained open after initiation coupling the bag volume to the filling tank volume during the impact. This allowed free flow exchange between the two volumes. Two different types of proportioning check valves were invented, prototyped, and tested on a scale model airbag system. The first valve consisted of a simple linear spring-loaded poppet design. The second design featured a magneto-statically loaded poppet valve with adjustable release and return set points. The normally closed check valve style venting provided air-release to the environment as a function of airbag internal pressure.

An alternative method was invented to passively release internal airbag pressure. The performance of this prototyped device was experimentally examined using the scale model airbag system. The method consisted of using a slightly pre-pressurized airbag containing a precision magnetic blow out patch created by using the seat and stem components of the aforementioned magneto-static check valve.

Tseng[2] previously explored the concept of using a plastic film to burst at prescribed pressure levels and vent the airflow from an airbag. This method was abandoned due to the unpredictable variation of the pressure level required to rupture the membrane. The new technique is based upon the level of magnetic attractive force that attaches the valve stem to the valve seat. This force level can be designed to release at a very precise level of applied pressure. The consistency of the vent release point that this technique provides furnishes precision control over the exit area opening process.

Airbag System Model Description

A digital computer model describing the performance of an airborne airbag landing system was originally devised 35 years ago[3]. The Browning model contained air bags designed as shock absorbers with fixed venting orifices. Mathematical computer studies by Ross[4] investigated control laws to be used to optimize airbag platform landings. Ross studies involved conceptual simulated open loop as well as feedback controller design. Another prior digital computer model developed by Lai[5] established guidelines for the application of airbags as alternative energy dissipaters to soft land parachute delivered loads. The Lai model explored the improvement in efficiency achieved through added mass gas-injection into the airbag. The purpose of the current digital computer model development (ABAG6.FOR found in Appendix A.) was to create a simplified numerical tool to explore the effects of various exhaust methods that enhance pre-pressurized airbag cushioning performance.

The current digital computer model ABAG6.FOR developed in FORTRAN source code calculates the airbag internal pressure response, the mass rates of flow into and out of the airbag, the deceleration level of the attached landing platforms payload and the vertical velocity and displacement of the airbag.

The model was created to simulate the one-dimensional compression of an airbag system with various exhaust vent features. The model can be configured to explore the performance of airbag systems possessing different types of exhaust venting. The system response of passively controlled exhaust methods such as ideal blow out patches and check valves can be determined. The model was developed to gain an understanding of the required passive air-release vent performance of an airbag system attached to a platform undergoing a parachute descent landing. Pressurizing the airbag eliminates the airbag stroke lost during the initial part of the compression. Pre-pressured airbags immediately upon landing start producing significant shock attenuation work against the incoming kinetic energy of the payload.

The current computer model contains some features previously examined by Lai[2]. The model has the provision to control the mass rates of flow into and out of the airbag. This feature was used by Lai to explore the improvements in airbag efficiency caused by direct gas-injection during the compression cycle. The goal was to be able to size a gas generation system to allow an airbag with a small stroke to behave as efficiently as a large stroke simple vent airbag. The Lai model used a simple airbag with

fully opened fixed exhaust vents. The theoretical derivation of the computer model used in this report is found in Appendix C. The focus of the current modeling was to first understand how various levels of gas-injection could control the airbag impact pressure response. Then to validate the models ability to reproduce the previously arrived at conclusions by studying the effects of injecting mass into the volume of a non-pressurized open exhaust vent system.

The current digital computer modeling focuses on studying the behavior of an initially pressurized closed volume airbag system with non-powered exhaust vents. The method of solution is by direct simple integration of the nonlinear differential equation describing the time rate of change of the pressure ratio solved simultaneously with a force balance applied to the landing platform. The computer simulation studied the effects of the systems response to the landing impacts using spring loaded and magnetically loaded proportioning exhaust vents, as well as magnetically secured precision release blow out patches.

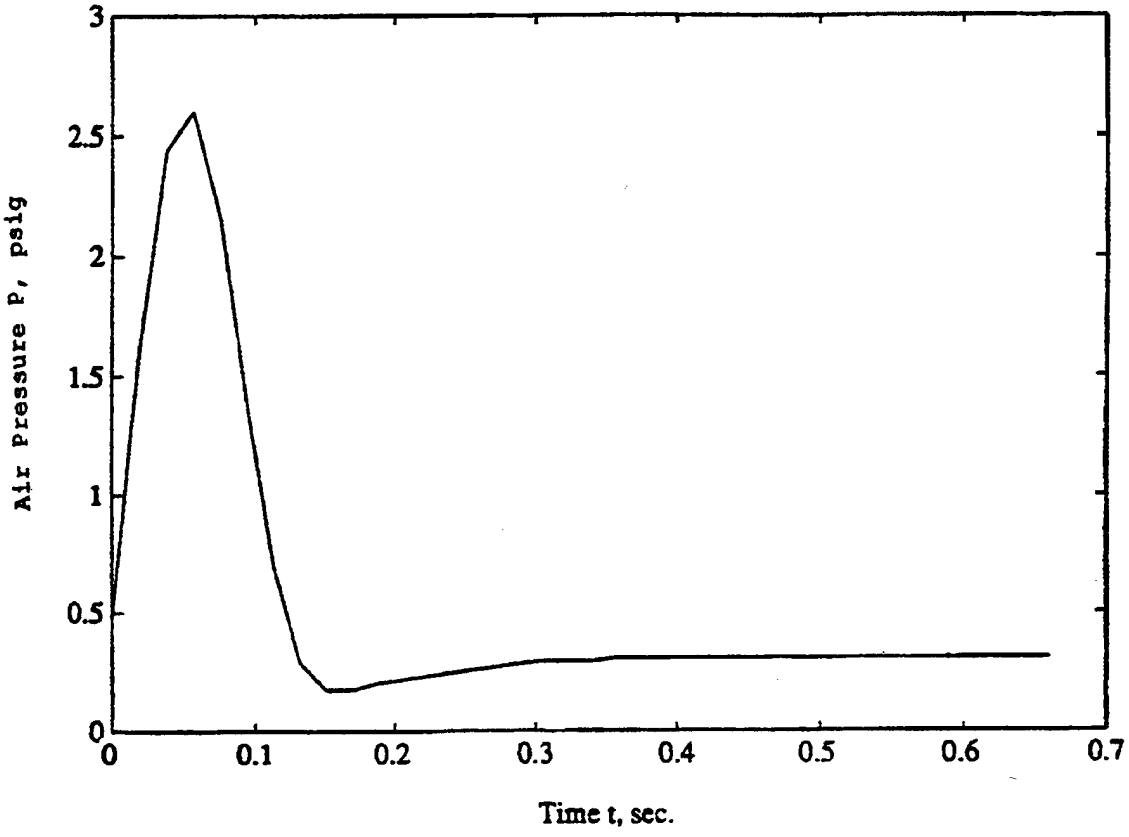

Figure 1. Analytically Determined Pressure Response of a Simple 8'x4'x4' Airbag, H=7 ft, M=1390 lbs, A_v=1.39 ft^2 (Figure 12B p41. Ref. 1)

Model Evaluation Study

After completion of the development of the Fortran Source Code, a small exercise was undertaken to define its performance as compared with past published analytical analysis. The computer model was configured to produce a 21 ft/sec impact of a simple (8x4x4) ft rectangular airbag supporting a 1390 lb payload with a 1.39 ft^2 fixed open vent area. This case was previously reported by Lee[1] and is shown again as Fig 1.

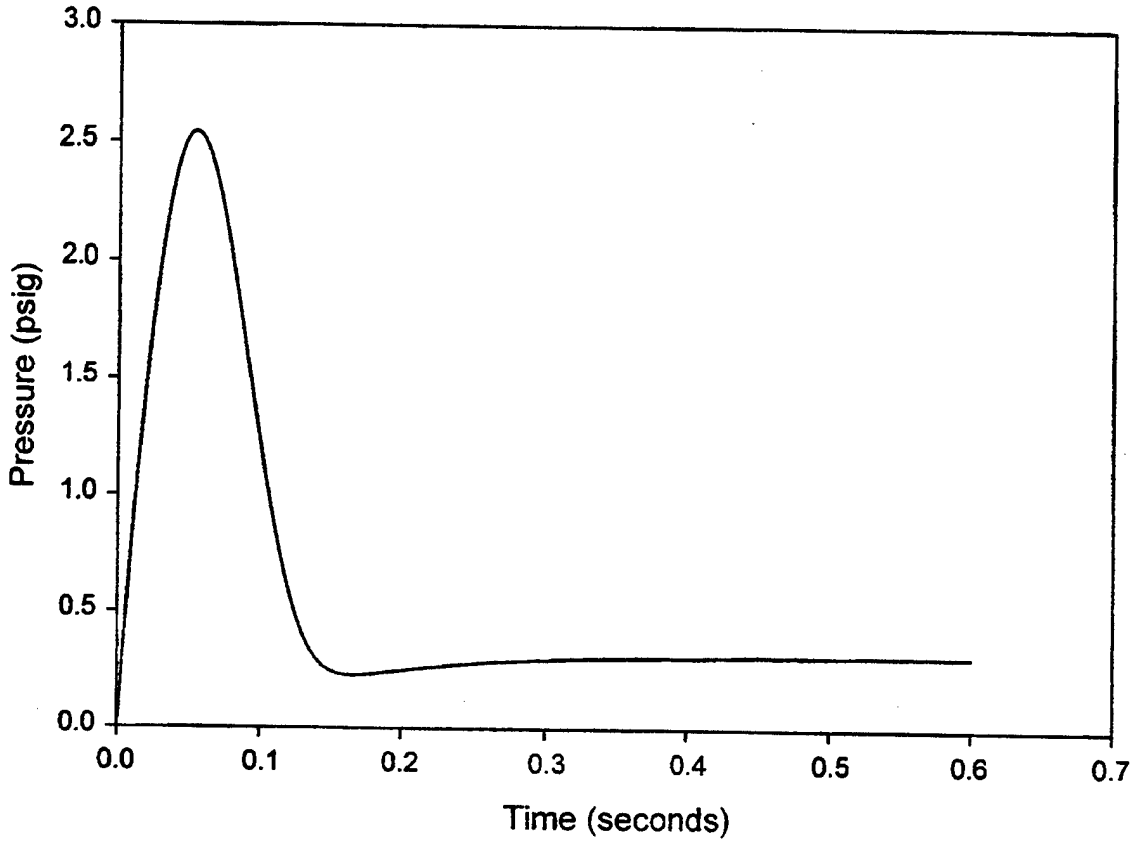

Figure 2. ABAG4.FOR Computer Simulated Pressure Response for a Simple 8' x 4'x 4' Airbag, V=21 ft/sec, W=1390 lbs, $A_v = 1.39\ ft^2$

The computer simulated pressure response output for this case is found in Fig. 2. This response appears to be a smoother version of Lee's results. The shape and magnitude of the airbag pressure response appears identical. The model was then configured to evaluate the ability of the computer to match previous results obtained during Gas-Injection analytical studies of airbag performance. The second case, examined the pressure response of a 9' x 4'x 2' airbag with a 1.74 ft^2 vent opening undergoing a 7 ft drop with a 1490 lb payload. The results of the computer simulation are shown in Fig. 3.

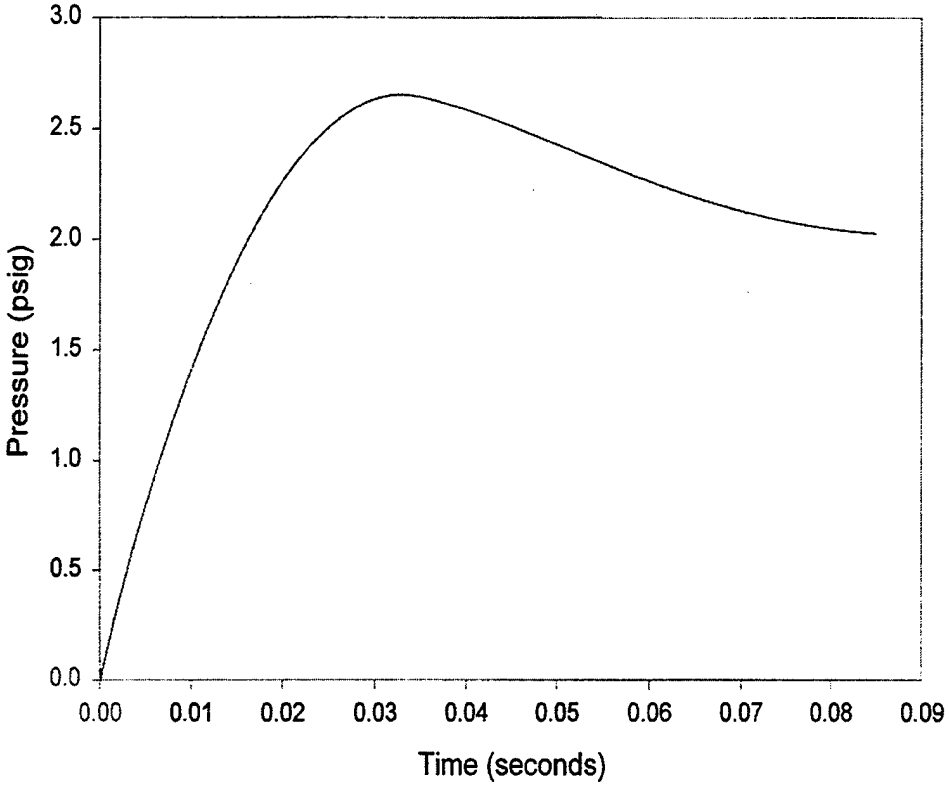

Figure 3. ABAG4.FOR Computer Simulated Pressure Response for a Gas-Injected 9'x 4'x 2' Airbag, H=7 ft, W=1490 lbs, A_v=1.74 ft^2

The approximated input flow applied to the airbag for this case consisted of a 35 ms time delayed ramp function with a magnitude of 16.5 lb/sec/sec. The results published by Lee shown by Fig. 4 can be compared with the case found in Fig. 3. Lee's result shows a distinct pressure drop of approximately 1 psig from the 2.5 psig peak level centered at 25 ms with a pronounced point of inflection occurring in the first 40 ms region of the pressure response curve. After this point in time the pressure transitions to a 30 ms region with a slight upwardly sloped pressure response. The pressure increases to a value of approximately 1.9 psig at 0.07 seconds, where another point of inflection is noticed. The slope over the final 15 milliseconds of the pressure response becomes very close to zero only a small negative tendency appears visibly noticeable.

The pressure response calculated using the computer simulation has some very significant shape differences when compared to the previously obtained results found in Fig. 4. The most striking of which is the vanishing of the first inflection point in the pressure response curve. This may be due to the different techniques used in the modeling of the injection phenomena and the algorithms used to perform the numerical integration calculation.

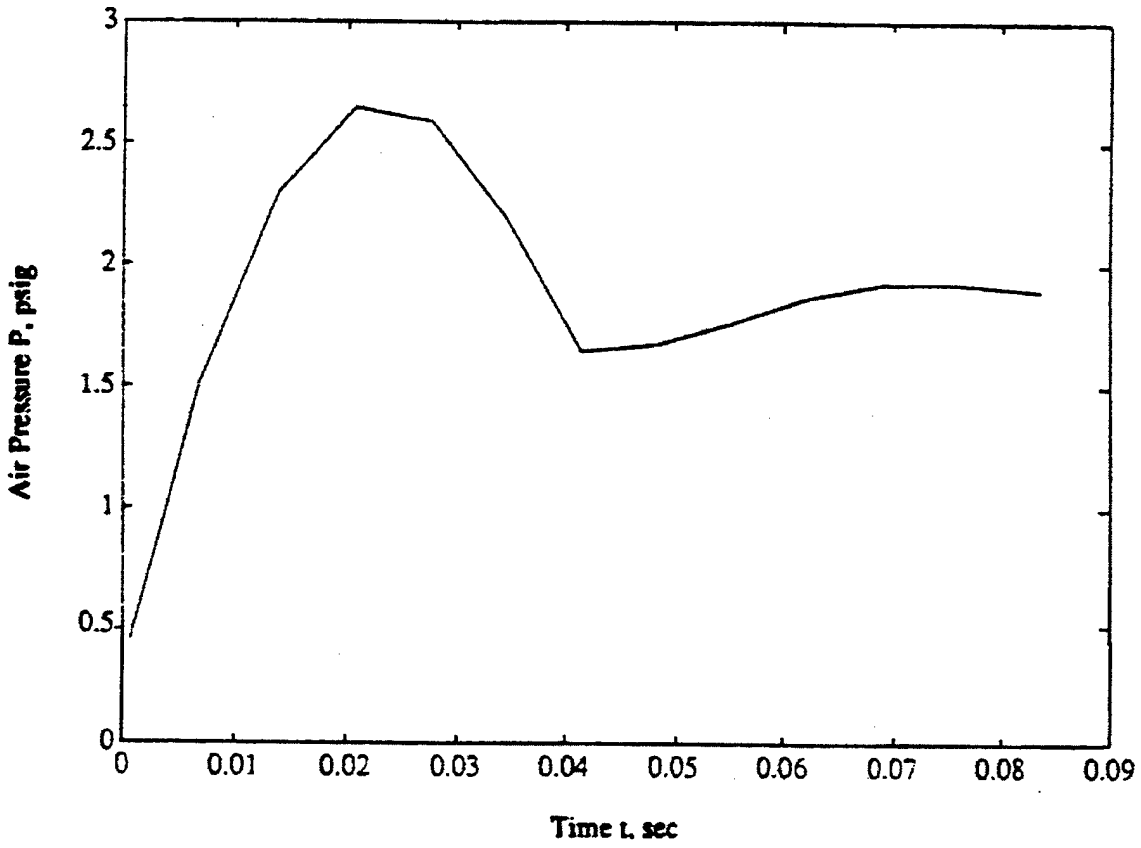

Figure 4. Analytically Determined Pressure Response of a Gas-Injected 9'x4'x2' Airbags, H=7 ft, M=1490 lbs, Av=1.74 ft^2 (Figure 42. p73. Ref 1.)

The influence that the input mass injected rate of flow has on the calculation of pressure response is found to be greater using the Lee analysis. Both models had identical continuity equations describing the conservation of mass. The solutions presented by Lee [1] assumed that the velocity profile of the airbag was a fourth order polynomial. The unknown parameters were m_{in} the mass rate of input flow and the vent exhaust area A_v along with the internal pressure of the airbag P(t). The Lee[1] model calculates for each assumed vent area value, a mass rate of inflow profile and the internal pressure response m_{in} and P(t) that satisfies the assumed fourth order velocity profile u(t). The ABAG6.FOR models the set of system equations directly using a linear piecewise approximation to the mass rate of inflow forcing function. The model then uses simple rectangular integration to directly solve the differential equations.

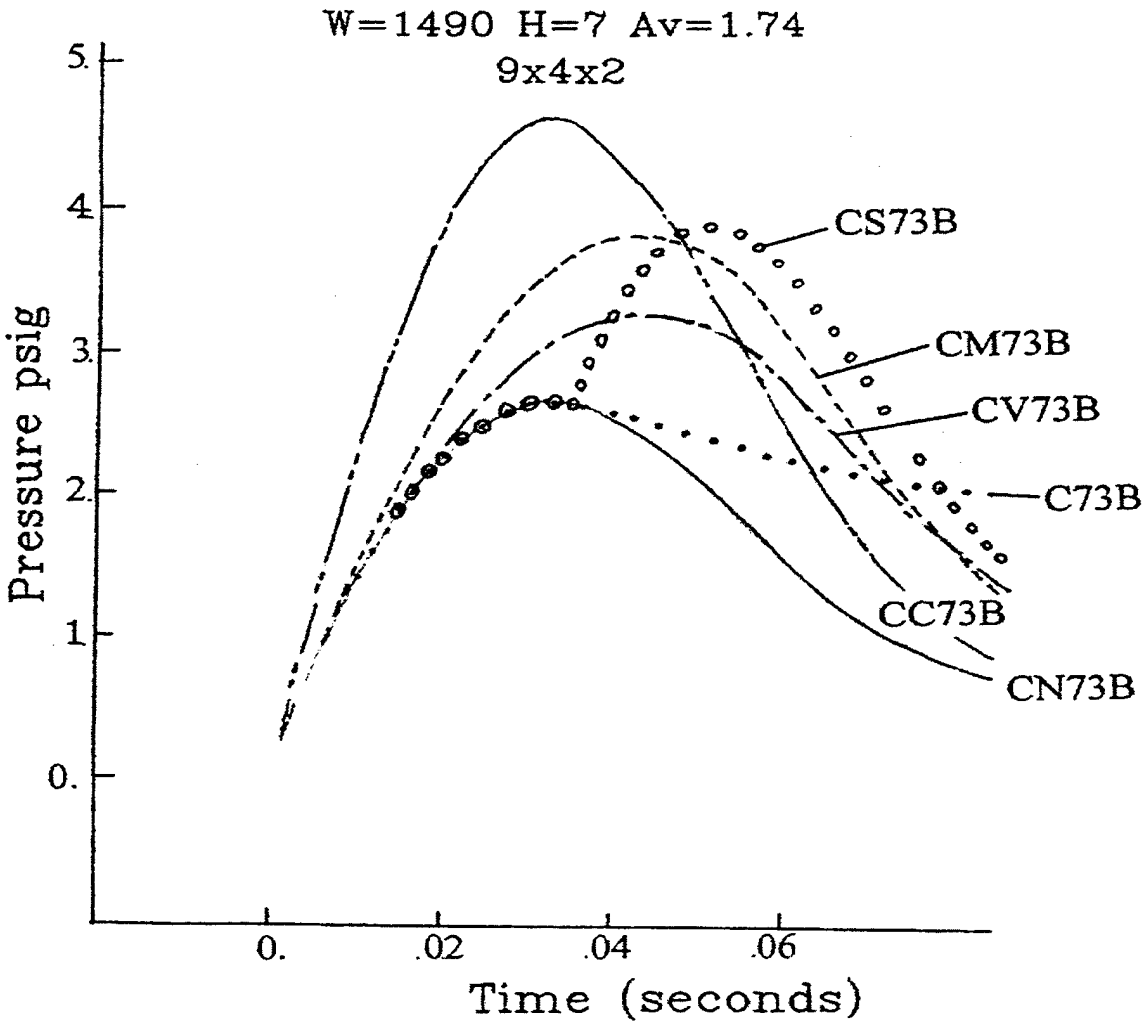

Figure 5. ABAG4.FOR Computer Simulated Airbag Pressure Response from various Applied Gas-Injection Profiles, 9'x4'x2' Airbag, W=1490 lbs, H=7 ft

The current model was used to study the effects that Gas-Injection control had on the airbag pressure response. Figure 5 shows the superposition of five different gas injection input flow profiles with a simple airbag pressure response. The airbag chosen for the study was a 9'x 4'x 2' rectangular shaped airbag impacting at 21 ft/sec with a payload weight of 1490 lbs and an open vent area of 1.74 ft^2. The simple airbag response case is labeled as CN73B this case did not contain any injected mass flow. The next case labeled as C73B is the same response shown in Fig. 3. The pressure results from injecting a ramped mass rate of inflow into the airbag after 35 ms of time have elapsed. The next case CC73B applied a constant 26.5 lbm/sec input flow level instantaneously at impact.

Applying a ramped inflow function instantaneously at impact produced the CM73B pressure response. The vent area was then opened to 2 ft^2 and the ramped inflow reapplied to produce the case labeled as CV73B. The last case tested applied a 35 ms

delayed constant 26.57 lbm/sec step function in the airbag's mass rate of inflow. The result of this delayed mass inflow step input is found in the figure labeled CS73B.

The analysis of Fig. 5 shows that the dynamic effect that served to optimize the energy absorbing efficiency of the airbag was the injection of a time delayed ramp in inflow. The injection of a ramp in mass inflow applied immediately after the occurrence of the maximum in the mass rate of outward airflow transforms the appearance of the airbag pressure pulse to more of a rectangular shape. The magnitude of the input mass rate of flow is determined by an equal an opposite sloped valve of the outflow experienced from a simple airbag exhausting through the same fixed orifice. The same time rate of change or slope of the outward airflow efflux should be equated to the injection rate, this has the effect of lifting the pressure response curve. The restructuring of the pressure curves shape approaches a more flattened or rectangular appearance. Since the inflow is applied after the peak in pressure occurred no increase in pressure results. The added mass flow then serves to help maintain the pressure, for the remainder of the compression cycle.

The shape of the airbag pressure response is effected by both the profile of the mass injection input function and the point in time when it is applied. The study reveals that in order to optimize the energy absorption process a synchronized time dependent application of mass gas inflow must occur.

Computer Simulation Study of an Ideal Check Valve

The digital computer models original Fortran source code was modified to allow the pressure ratio P defining the fraction of bag internal pressure relative to the surrounding ambient pressure to be readily changed prior to impact. This reflects the effect produced by a high pressure source filling the airbag to some prescribed pressure level before ground impact. The level was arbitrarily chosen as 1.034 representing a 0.5 psig bag pressurization level.

An ideal check valve without hysteresis was modeled as a simple step function in exhaust area. When the airbag internal pressure exceeded the gage pressure level PSET, the flow exhaust area was changed from a value of AMIN1 to AMAX. The value of AMIN1 was usually chosen as zero (i.e. no exit flow area). The valve is scheduled to remain shut until the model parameters BJ & PSET are established.

The scale model airbag used for the simulation consisted of a 1.325 cubic foot airbag having a 1.5 ft diameter with a 0.75 ft height. This airbag was subjected to vertical impacts at approximately 21.2 ft/sec with a 100 lb weight, the initial kinetic energy of impact being 700 ft-lbs.

The first case explored CBP1A gave the system three 1" diameter ideal check valves set to open at a 2.0 psig pressure level. The total flow exit area for the sum of the three valves was 0.0164 ft^2, each valve having an open exit area of 0.785 square inches.

The pressure response found in Fig. 6 resulting from this simulated impact shows a pronounced flattening of the peak occurring at the 12.5 psig pressure level.

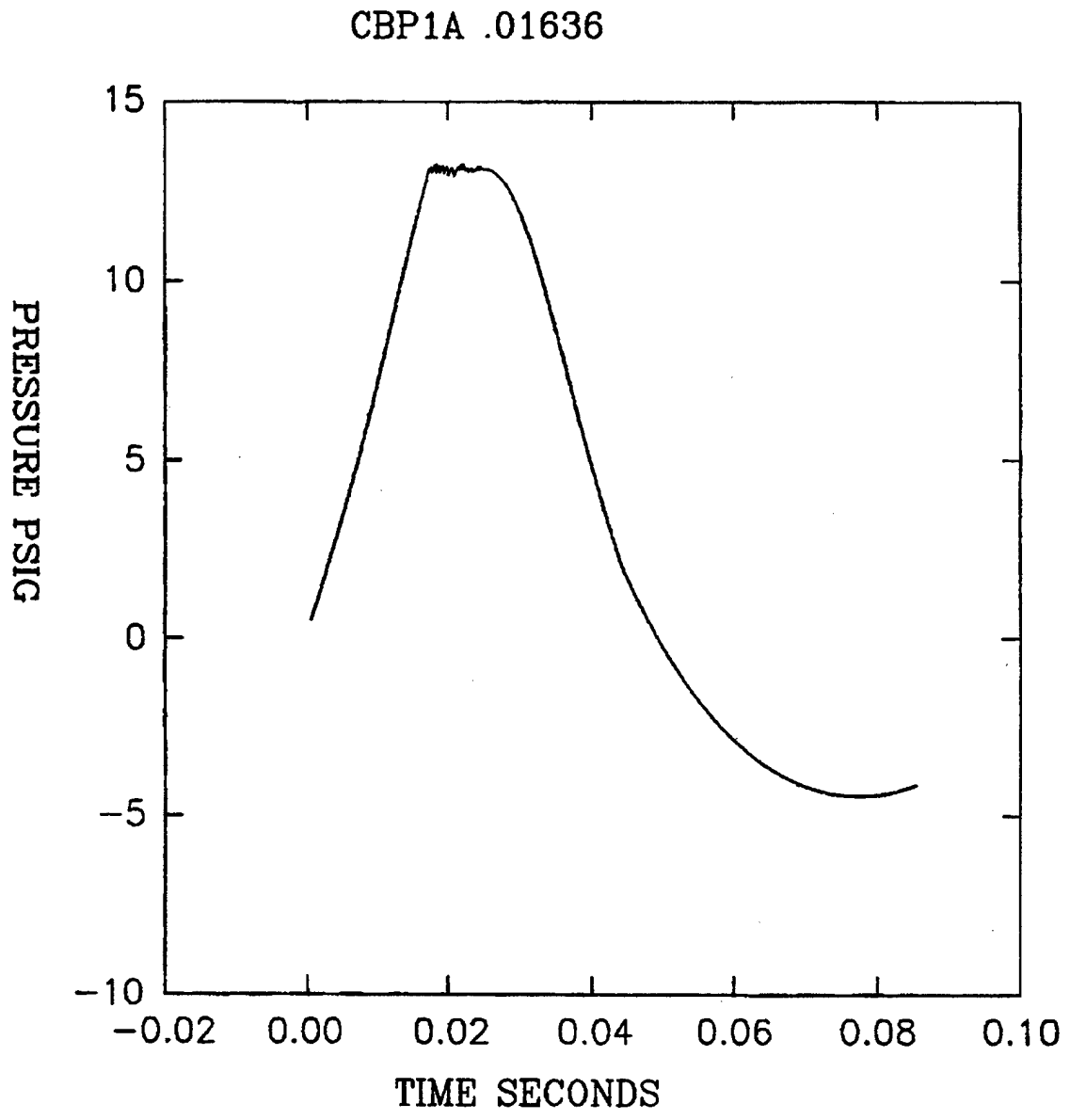

Figure 6. Airbag Pressure Response, V = 21 ft/sec, PSET = 2.0 psig, A_v = 0.01636 ft^2

The 0.0164 ft^2 exhaust area for this case was insufficient to maintain a 2.0 psig internal airbag pressure as specified by the valve set point. Even when the valve was wide open the internal pressure of the airbag kept rising as a function of time.

The vent area was then increased by an approximate order of magnitude to a 0.196 ft^2 value, which represented a single 6 inch diameter outlet opening or three 3.46 inch diameter openings. The same set point level of 2.0 psig was chosen and the second

case CBP2A was simulated. These results appear in Fig. 7 and show a distinct 2.0 psig modulation of the airbag pressure time history.

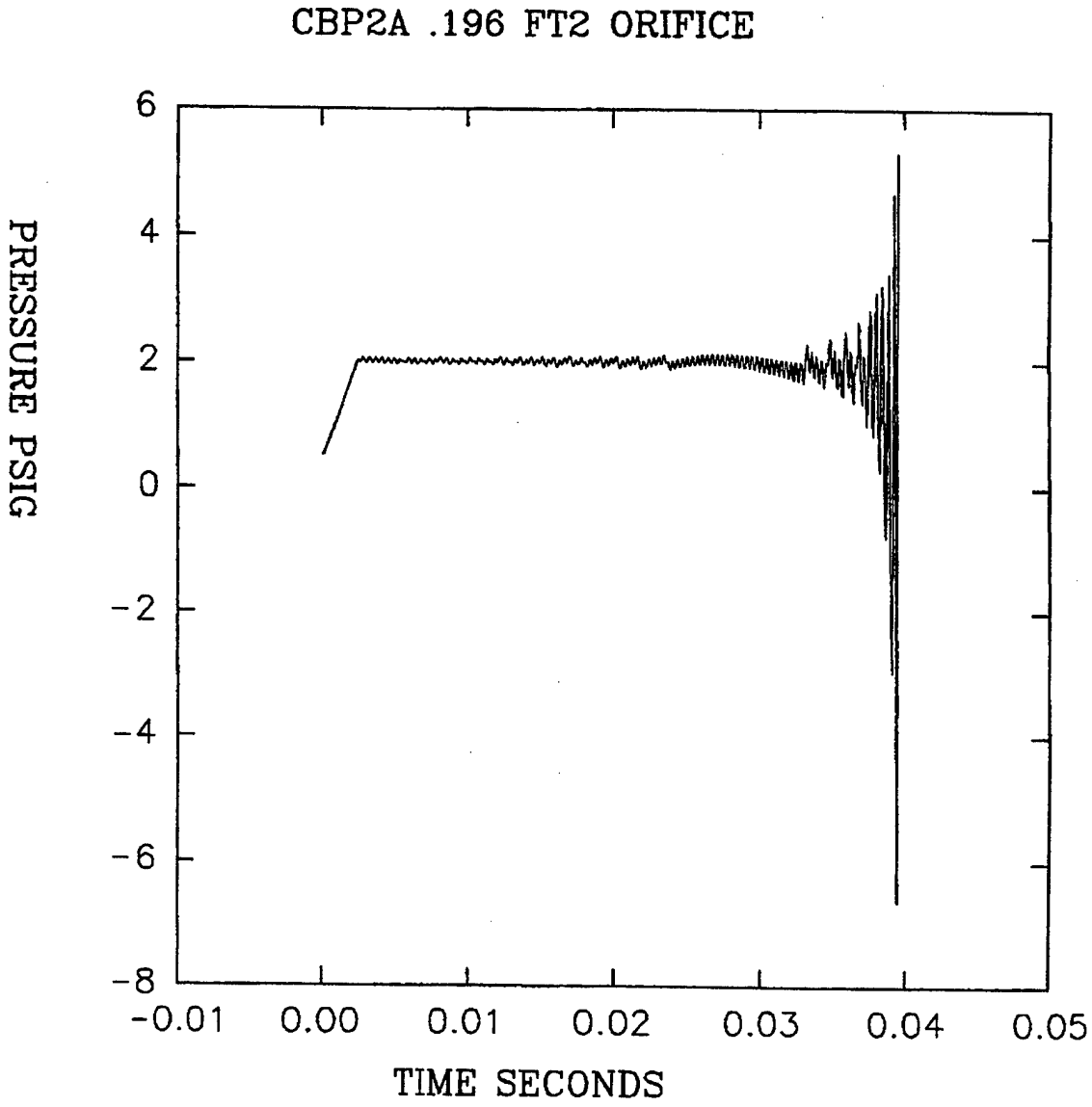

Figure 7. Airbag Pressure Response, V = 21 ft/sec, PSET = 2.0 psig, $A_v = 0.196$ ft^2

The 0.196 ft^2 exhaust area was sufficient to vent the resulting flow and maintained the airbag pressure at the 2.0 psig set point level. The resulting pressure becomes numerically unstable after 35 milliseconds of simulation. The constant pressure characteristic results from the modeling assumption that the check valve has an infinite speed of response. In order to realize this abstraction the valve must be infinitely powered and both friction free and massless.

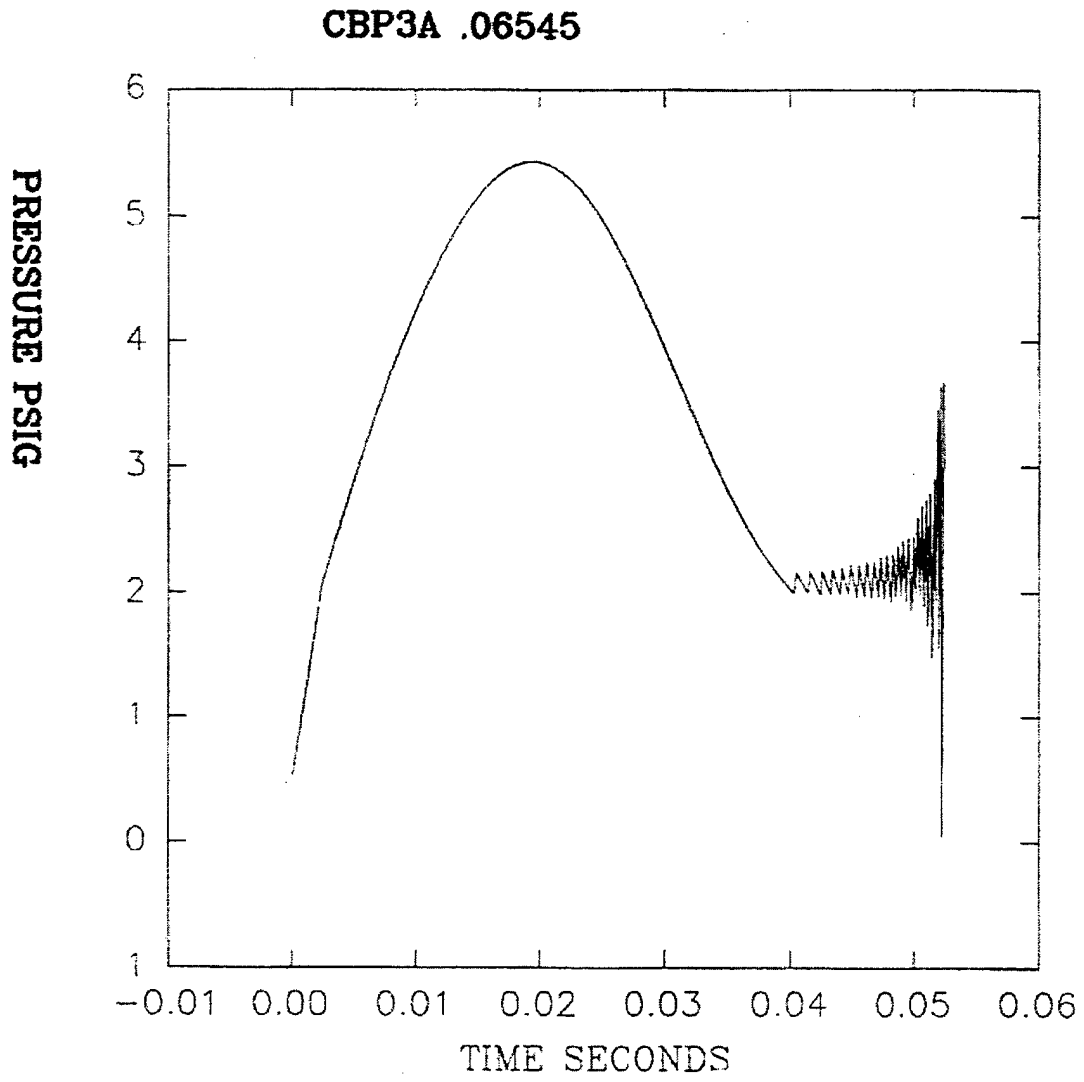

Figure 8. Airbag Pressure Response, V = 21 ft/sec, PSET = 2.0 psig, A_v = 0.06545 ft^2

The results of the third case CBP3A are found in Fig. 8. The graph shows the pressure response of the system with a 2.0 psig set point containing an exhaust valve with 0.0655 ft^2 of open flow area, which represents three 2 inch diameter orifices. This valve is undersized for the impact and can not maintain a flat 2.0 psig pressure level. The pressure passes through the set point level and peaks at 5.5 psig. When the pressure returns to the 2.0 psig threshold the area becomes sufficient to modulate the flow and maintain the airbag pressure quasi-constant.

The fourth numerically simulated case CBP4A examined the scale model airbags response to the same 700 ft-lb impact with the pressure set point level of the check valve determined from the basic principle of the conservation of energy. The calculation assumed a 70% crush of the 9 inch tall airbag having a constant internal pressure. The work performed by the airbag, the integral of force with respect to stroke minus the potential energy of the payload was set equal to the payload kinetic energy.

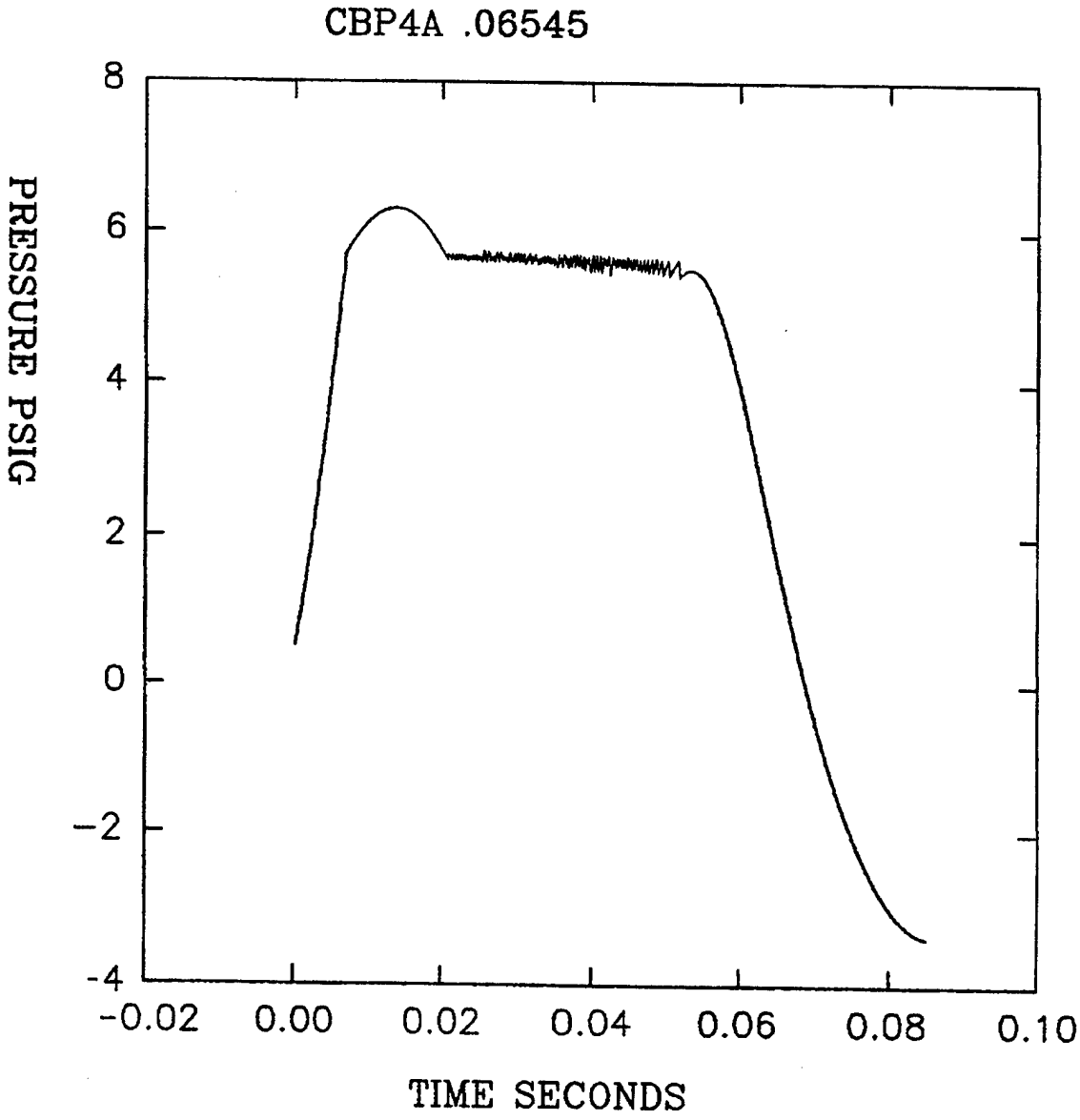

Figure 9. Airbag Pressure Response, V = 21 ft/sec, PSET = 5.63 psig, $A_v = 0.06545$ ft^2

Equation (1) was solved for the airbag pressure level using a 100 LB payload weight and a 700 ft-LB kinetic energy level acting on an airbag with a 1.767 ft^2 surface area.

$$\text{Equation (1)} \quad [144.0 * A * P_{bag} - W] * 0.7 * (.75) = 700.0$$

The airbag pressure and subsequent set point level was determined by Equation (1) to be 5.63 psig. The pressure response of the impact found in Fig. 9 shows the

pressure slightly overshooting this set point level but then returning to and modulating about the level. The shape of this response is similar to the dynamic impact response of a payload cushioned by paper honeycomb.

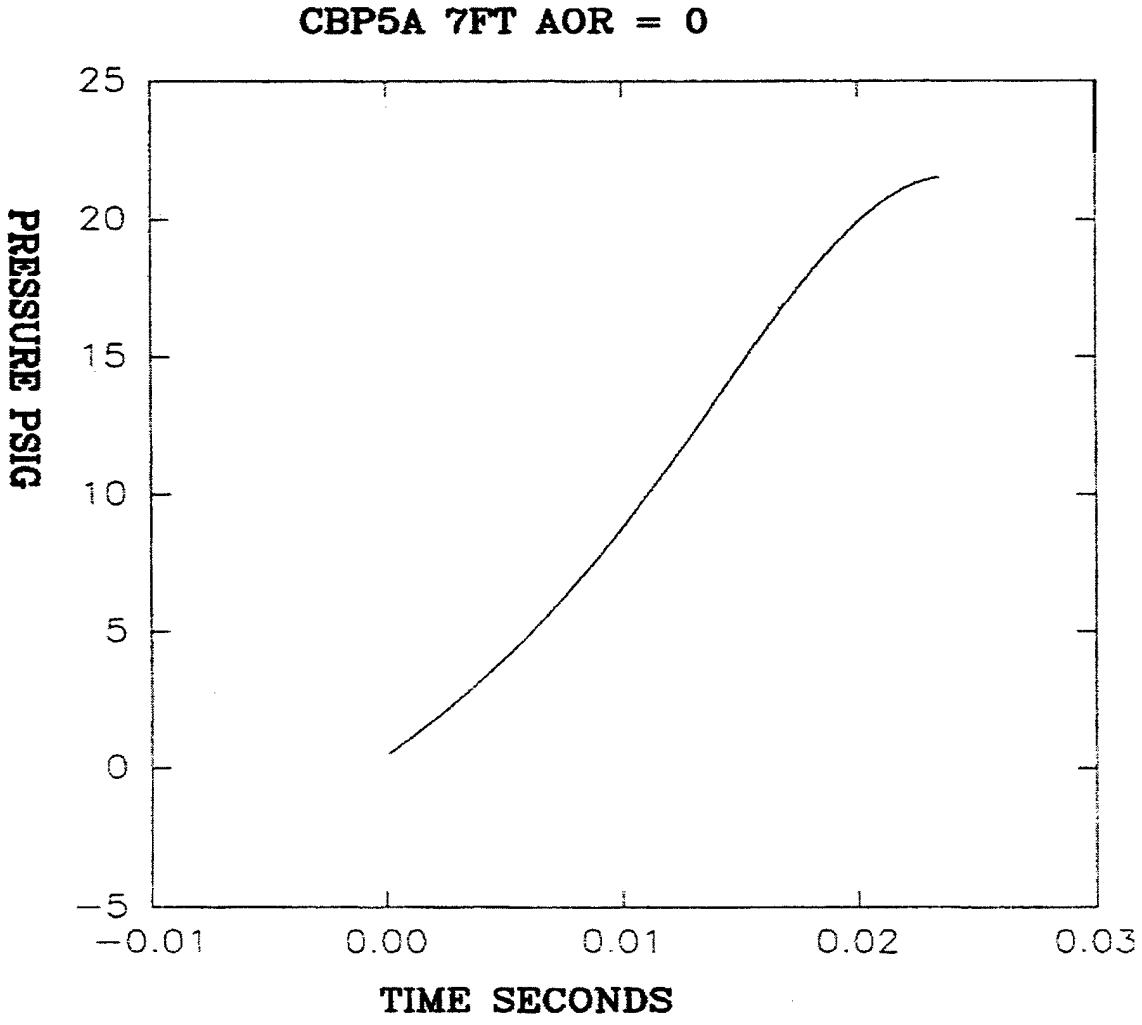

Figure 10. Closed Exhaust Vent Airbag Pressure Response, $A_v = 0.$, V = 21 ft/sec

The rectangular impact response generated by paper honeycomb is currently the most efficient practiced method of ground shock mitigation. Figure 9 represents the perfect reusable alternative to the paper honeycomb method of cargo impact protection.

The fifth case CBP5A subjected the simulated scale model airbag to the same 7 ft impact with a closed exhaust vent area. This was done to test the digital model. The model parameters AMIN1 and AMAX were set to zero and remained at zero during the simulation. The airbag pressure set point level PSET for this case was fixed at 1.0 psig. The results of the simulation are found in Fig. 10. The figure shows that the airbag pressure reached a 22 psig level after 0.025 seconds have elapsed. Using this pressure in conjunction with the model determined airbag stroke multiplied by the airbags area raised

to the 1.4 power, the product of PV^{γ} was calculated. This product was calculated at random time steps during the compression and was found to be the quasi-constant value of approximately 3230. This implies that the modeled pressure response exhibits true polytropic air compression when the airbag vent is closed.

The numerical simulation suggests that when the area is insufficient the modulation of pressure occurs after the peak in pressure is realized on the return to zero pressure set point threshold crossing section of the pressure time history. This is believed to be due to the magnitude of the kinetic energy maintaining the velocity in conjunction with the rate of change of pressure inside the airbag with respect to time.

The next two cases simulated CBP6A and CBP7A were for the pressure set points of 3.0 psig and 4.0 psig, respectively, with an exhaust open vent area of .06545 ft^2. These two cases together with the previous last two cases CBP3A and CBP4A for the 2.0 psig and 5.63 psig set point levels form a response family for the airbag venting through a 3.5 inch diameter ideal check valve. Contained in Fig. 11 is the plot of this family of pressure responses caused by a 7 ft impact. Examining the graph shows that the lower the valve of pressure set point the higher the overshoot of airbag pressures response prior to successful valve modulation. This figure also shows that the bag experiences polytropic compression until the check valve pressure set point level is reached, at which time the valve opens and releases the flow.

When the set point is low, the pressure-volume work level is low and the residual difference in payload kinetic energy is large. The velocity is reduced as the pressure-volume work is applied as time elapses during the compression process. For high values of the pressure set point, the residual kinetic energy of the payload is significantly lowered. The reduction in the velocity and work acting upon the bag helps to allow the check valve to vent the flow and reduce the pressure. In the subsonic region of flow, the higher the check valve pressure difference, the greater the flow through the orifice. The lower set point levels yield overshooting pressure responses until the velocity of the system is reduced and the valve begins to modulate and maintain the pressure quasi-constant at the set point level. The model simulation results suggest that for a given vent size there exits an optimum velocity level were the airbag pressure will experience a minimum in set point level overshoot.

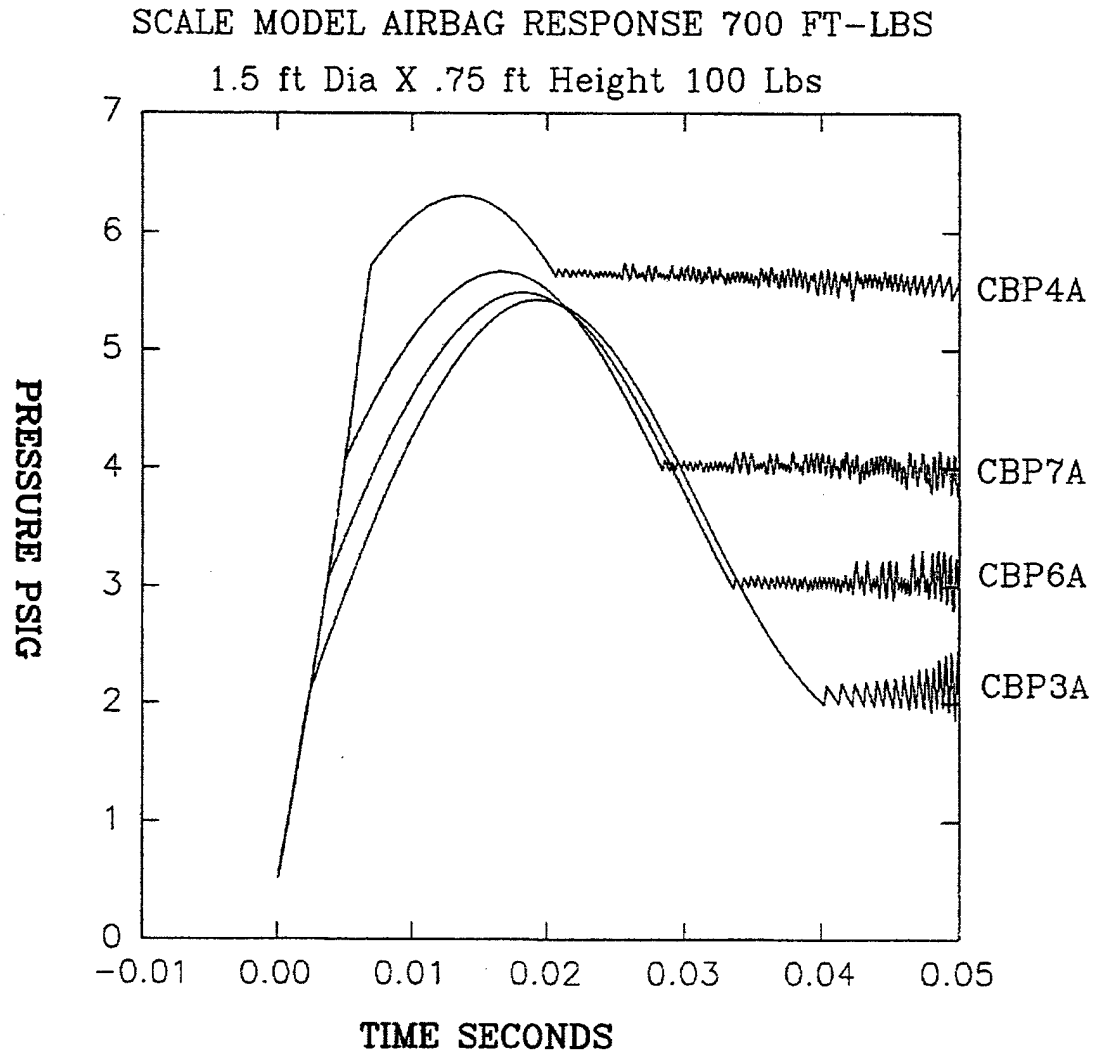

Figure 11. Plot of a family of Simulated Airbag Pressure Responses Conducted at Various Check Valve Set Point Pressure Levels

Exceeding this velocity level produces large values of pressure overshoot. The effects of impact velocity magnitude on airbag pressure response were then studied using the same 3.5 inch diameter ideal styled check valve model. The cases CBP3A, CBP8A and CPB9A contain the simulated airbag pressure response for different levels of impact velocities. These cases possess the identical initial 0.5 psig pressurization level, and a 0.0655 ft^2 orifice vent opening area. The velocity levels 21.2 ft/sec, 17.9 ft/sec and 13.9 ft/sec were chosen in order to produce 700 ft-lbs, 500 ft-lbs, and 300 ft-lbs, of payload kinetic impact landing energy to the airbag. The 21.2 ft/sec impact case CBP3A exhibits airbag pressure overshoot greater than twice the 2.0 psig pressure set point level. A flattening of the overshoot pulse shape and a shortening of the check valve modulation time occurs when the impact velocity and subsequent kinetic energy becomes reduced.

The superposition of the pressure response curves can be found in Fig. 12. This plot shows that there exists a 10 millisecond modulation time difference between the largest and smallest velocity cases.

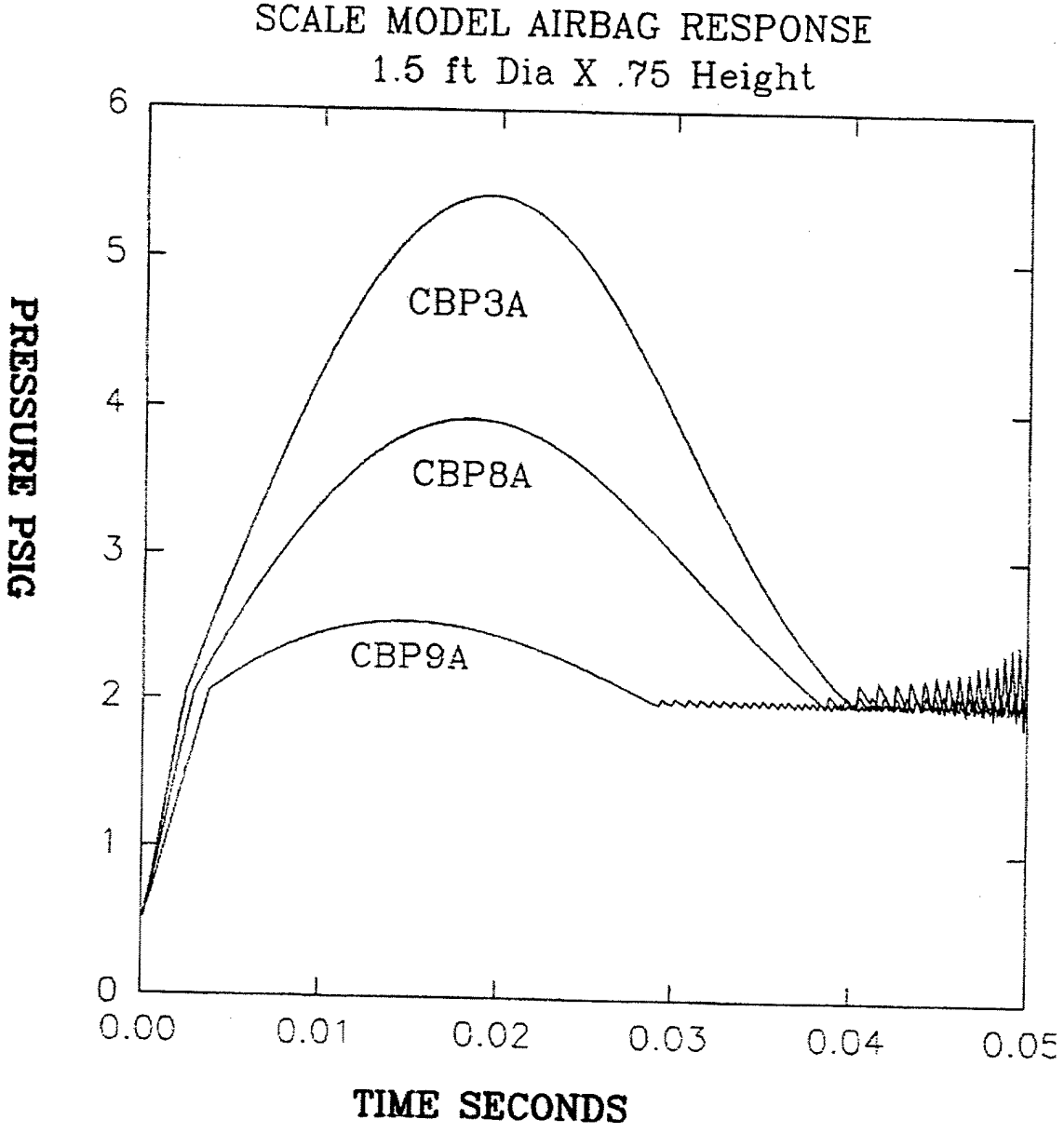

Figure 12. Plot of a family of Airbag Pressure Responses for an Ideal Check Valve for V = 21.2 ft/sec, V = 17.9 ft/sec & V = 13.9 ft/sec Impacts

Theoretical Calculated Valve Performance

The digital computer model was modified from the previous version that simulated the performance of the pressure release valve by an ideal step function. The subroutine CKVALVE was used to explore the theoretical behavior of a spring loaded

check valve connected to a scale model airbag undergoing a purely vertical impact with the ground. The subroutine represents a more reasonable model of the physically realizable check valve hardware. The airbag modeled had 50 lbs of payload weight, contained 1.767 ft^2 of projected surface area and an initial height of 9 inches. The typical spring loaded check valve was designed theoretically with a set of helical wound wire compression springs possessing a spring rate of 14.5 lb/inch of deflection with a 1.5 inch free length and a 0.975 inch allowable total deflection. Compressing the springs by 0.468 inch produces a 2.12 psig initial pre-load level.

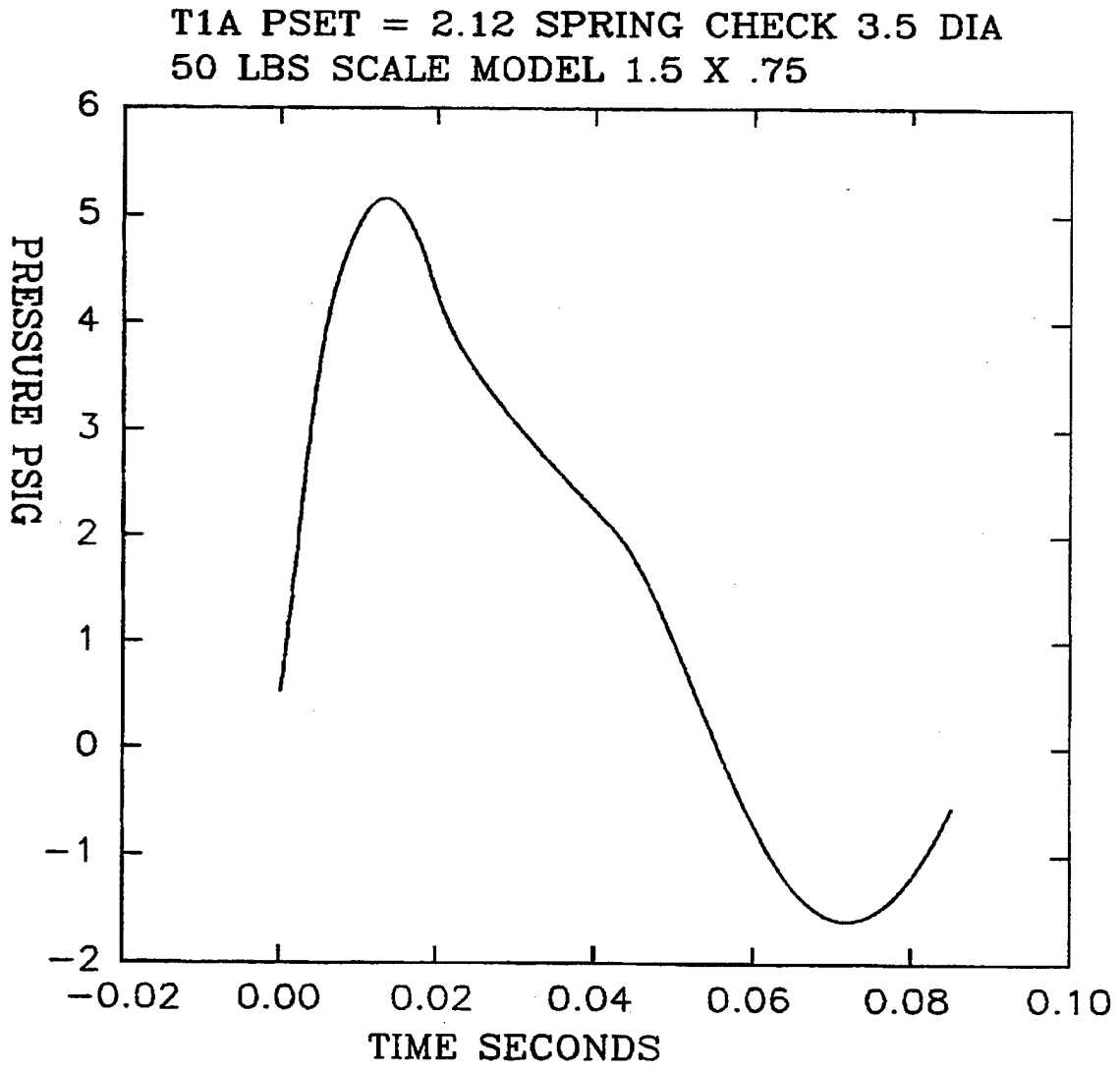

Figure 13. Simulated Airbag Pressure Response of a Spring Loaded Check Valve, D= 3.5 in, LD = 5.5 in, PSET = 2.12 psig, W = 50 lb, V = 21 ft/sec

The valve flow escape area varies linearly with spring deflection and valve body diameter, until the springs reach their solid height.

The subroutine CKVALVE describes the exit flow are as a function of valve body underside average pressure. This pressure was assumed to be equal to the airbags internal pressure. No correction due to flow was applied in this model. Six cases that explored the behavior of the airbags pressure response to the spring loaded valve model were simulated. The first result achieved was the pressure response to a 7 ft drop height. The data is contained in the plot labeled Fig. 13.

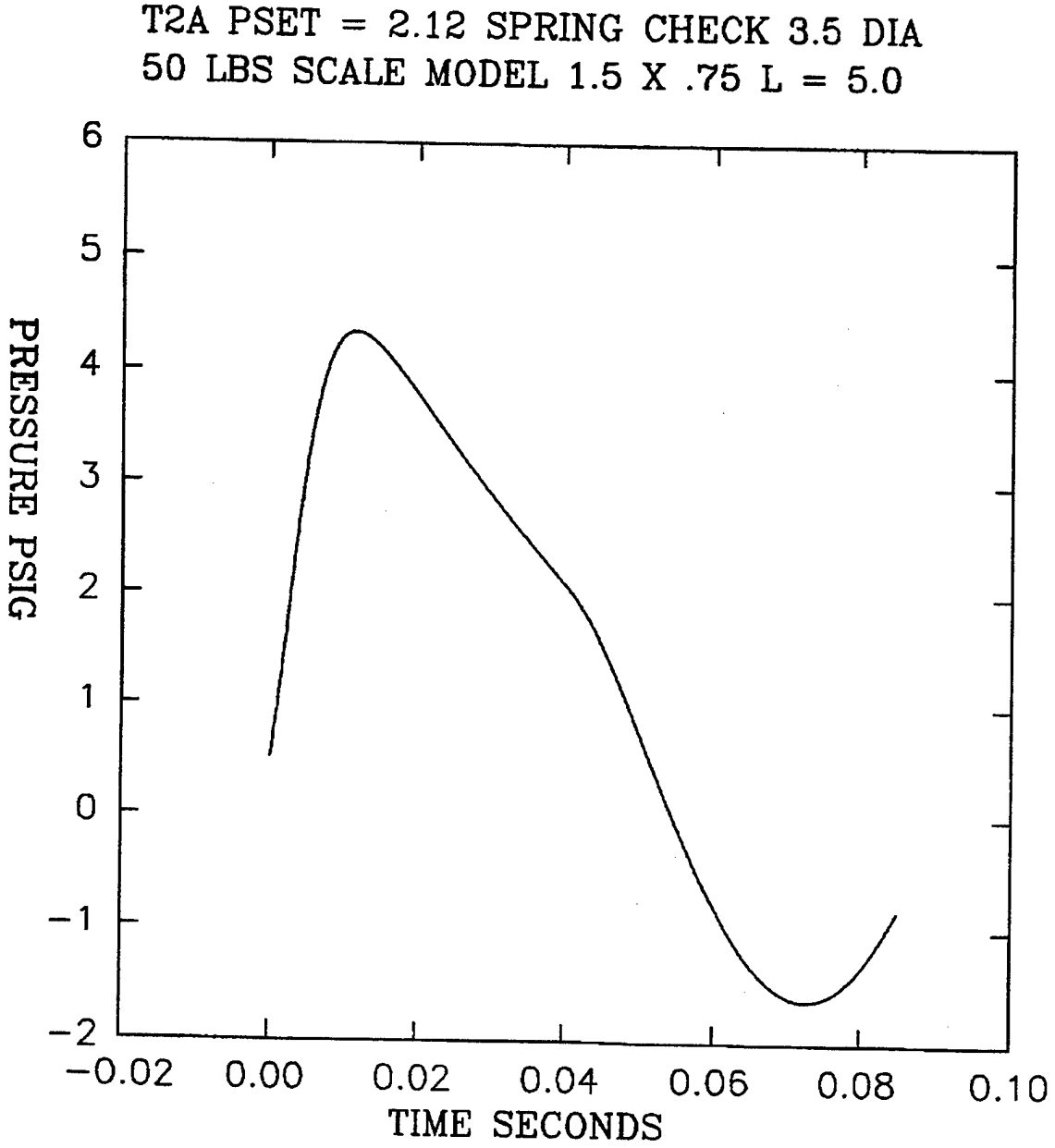

Figure 14. Simulated Airbag Pressure Response of a Spring Loaded Check Valve, D = 3.5 in, LD = 5.5 in, PSET = 2.12 psig, W = 50 lb, V = 17.9 ft/sec

After the pressure inside the airbag reached the peak a distinct unsymmetrical change is noticed as the pressure returns to zero. The slope of the pressure time impact history

appears to contain two points of inflection defining a somewhat linear segment of decreasing pressure. The model was then set to simulate a 17.94 ft/sec impact, the pressure response is found in Fig. 14. The airbag valve system has to only dissipate 250 ft-lbs of kinetic energy for this case. The plot shows at this reduced level of impact that the valve full open area was sufficient to produce a distinct linear pressure decaying slope as it returns to zero.

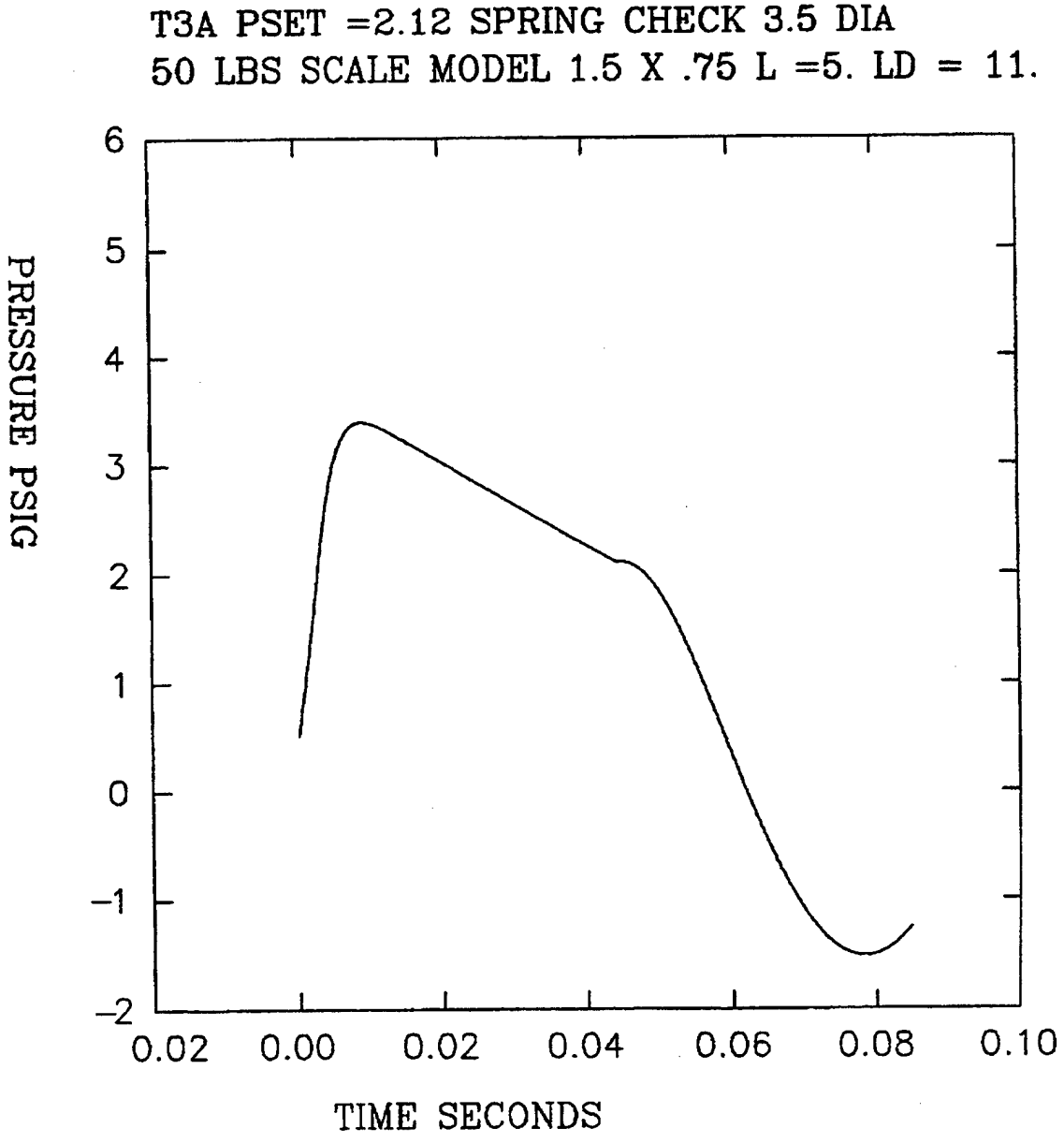

Figure 15. Simulated Airbag Pressure Response of a Spring Loaded Check Valve, D = 3.5 in, LD = 11 in, PSET = 2.12 psig, W = 50 lb, V = 17.9 ft/sec

The check valve body diameter was then doubled from the initial simulated value of 5.5 inches to an 11 inch diameter. This provided a flow outlet area of 0.118 ft^2 when

the spring experiences approximately one half inch of deflection. The simulation results displayed in Fig. 15 show that a decrease in the peak pressure along with a widening of the transient pressure pulse has occurred. The slope after the peak in pressure that is realized is higher for the larger valve body diameter. When the pressure decreases to 2.12 psig the second inflection point shows a discontinuity. This is clearly visible as an infinitesimal segment of approximately zero slope or constant pressure due to the area changing in the simulation.

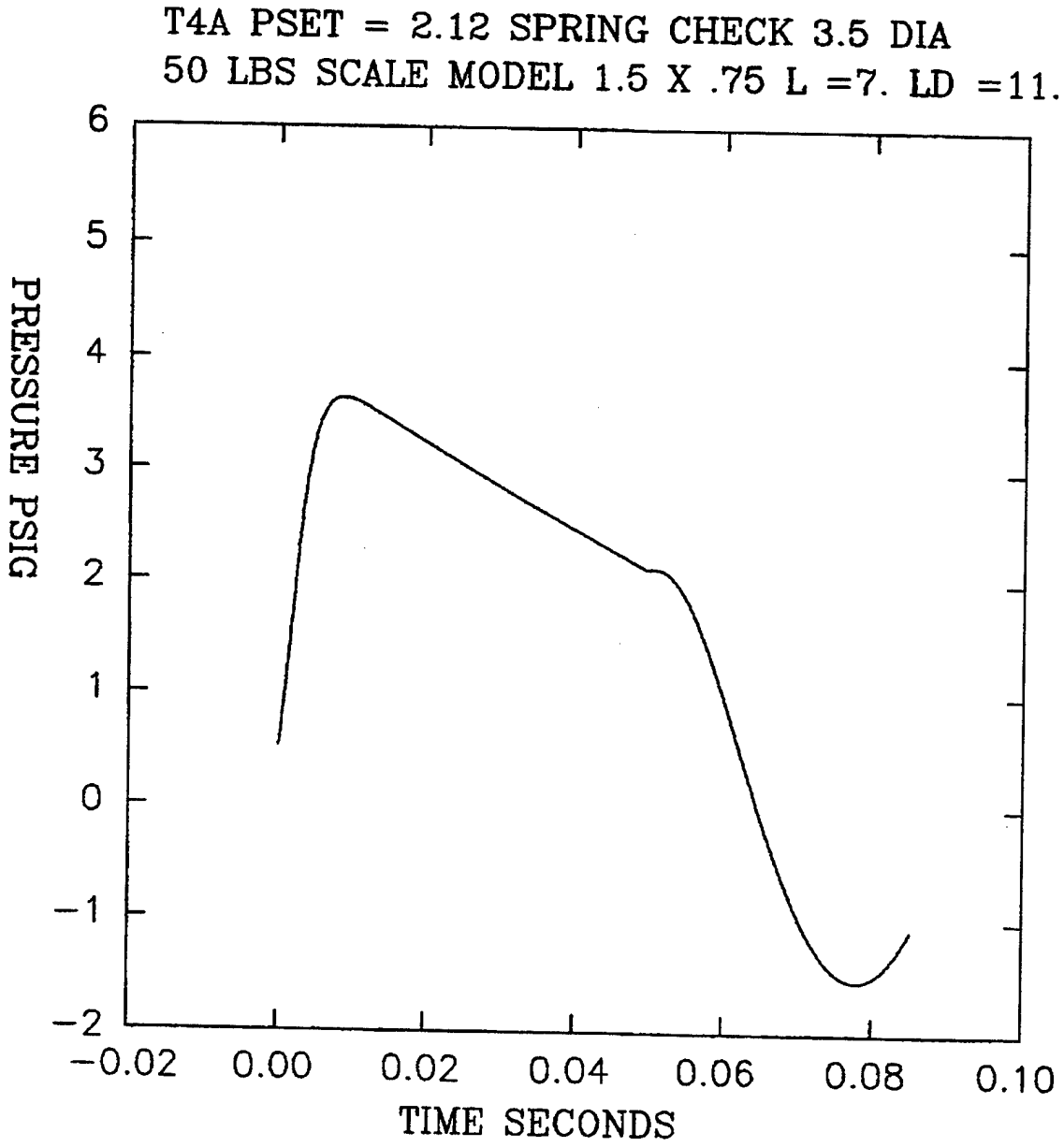

Figure 16. Simulated Airbag Pressure Response of a Spring Loaded Check Valve, D = 3.5 in, LD = 11 in, PSET = 2.12 psig, W = 50 lb, V = 21 ft/sec

The identical performance was obtained at 21.2 ft/sec using the 11 inch diameter valve body. The pressure time history found in Fig. 16 is slightly higher and wider than that of the 5 ft drop case. In order to show the effect of a 50% increase over the original 5.5 inch diameter design, two other cases Fig. 17 and Fig. 18 were simulated using an 8.25 inch diameter valve body.

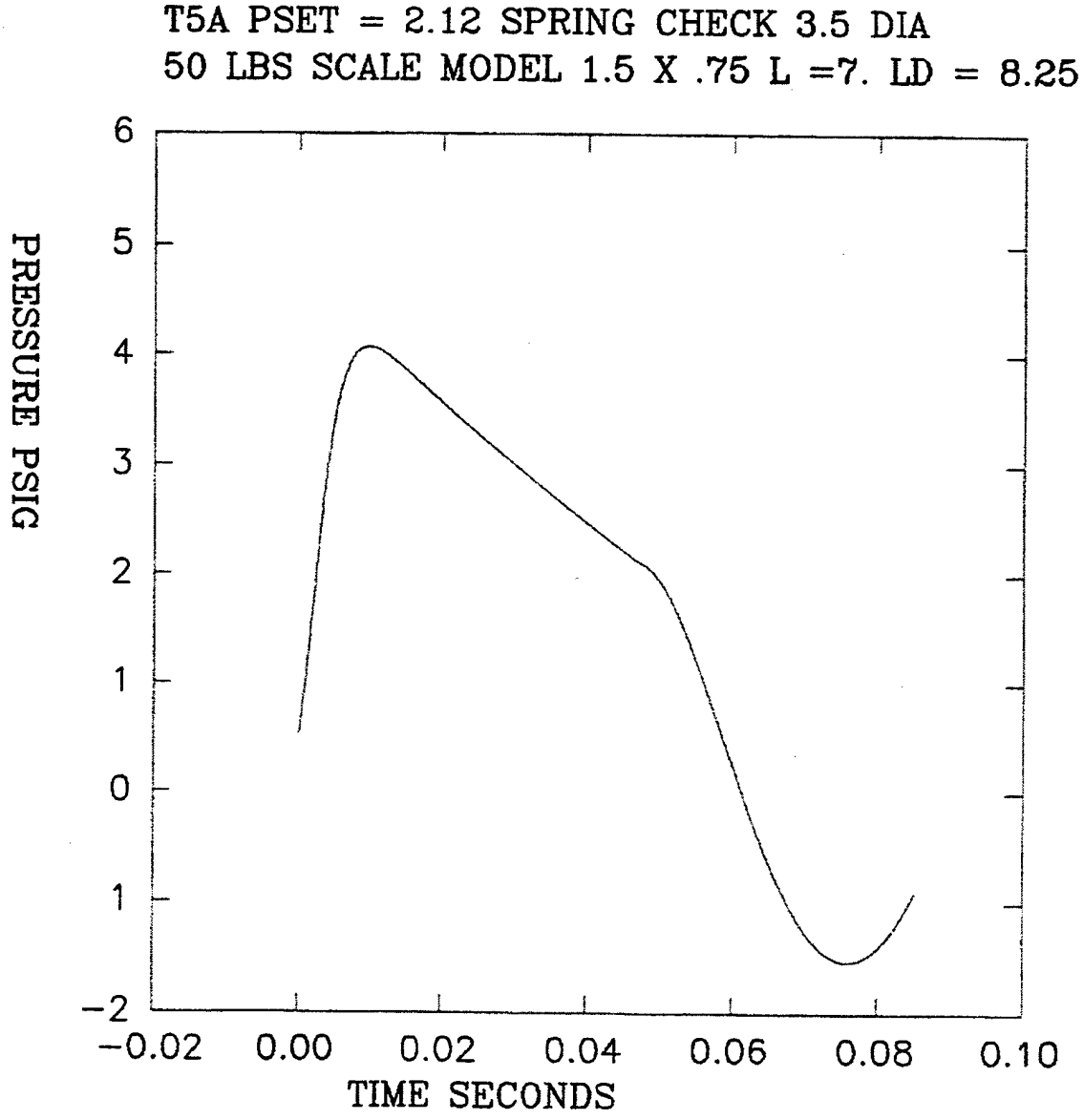

Figure 17. Simulated Airbag Pressure Response of a Spring Loaded Check Valve, D = 3.5 in, LD = 8.25 in, W = 50 lb, V = 21 ft/sec

The pressure responses have the same shape as previously produced for the 5 ft and 7 ft impacts. A common characteristic of this style valve shown by all of the pressure response curves is negative pressure. It appears that during the return to zero pressure

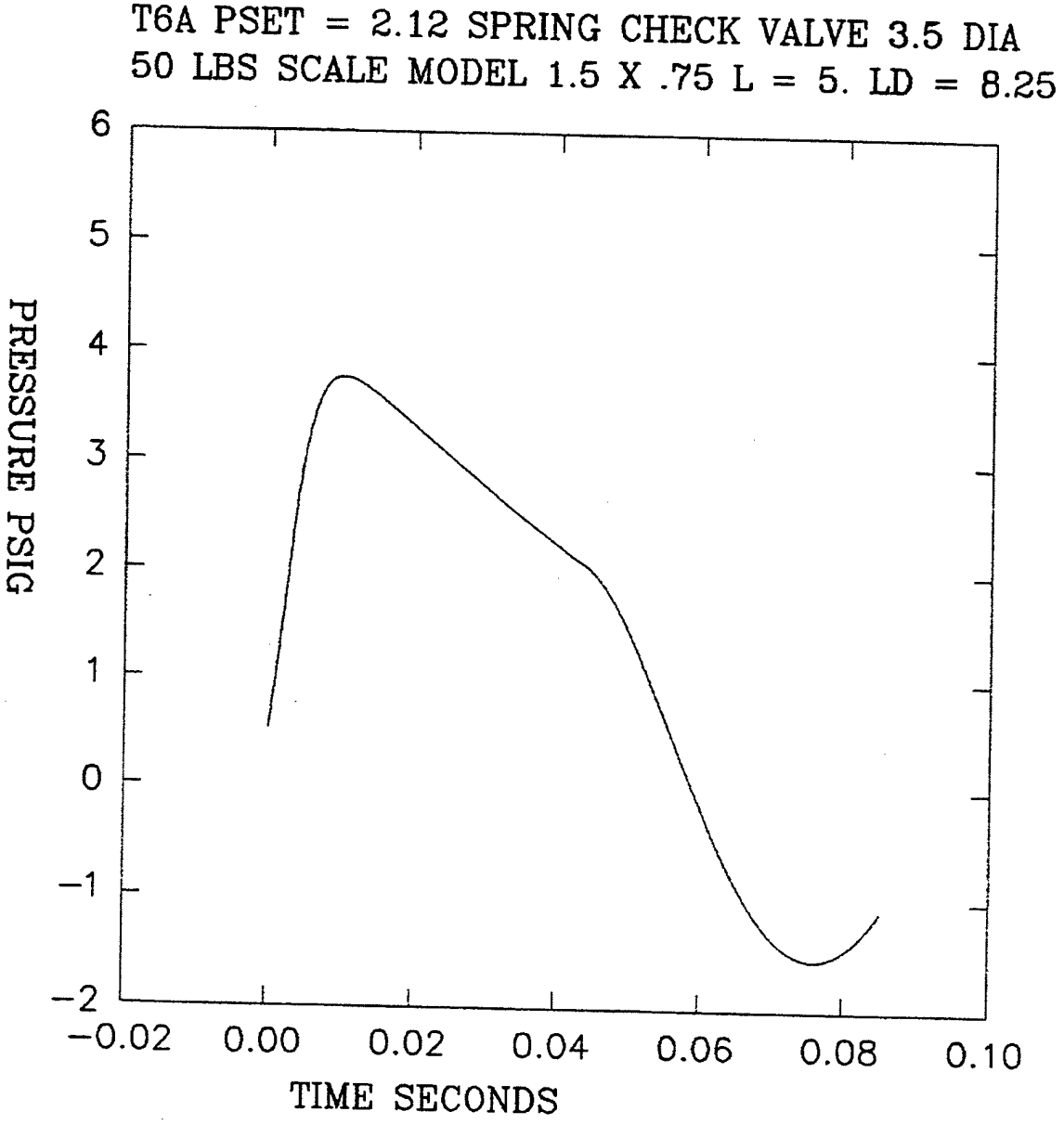

Figure 18. Simulated Airbag Pressure Response of a Spring Loaded Check Valve, D = 3.5 in, LD = 8.25 in, W = 50 lb, V = 17.9 ft/sec

phase of the impact transient, a vacuum is being created inside the airbag. This is assumed to be due to the rebounding of the payload weight, when the bag is in the collapsed state.

The computer model was configured to simulate the same scale model airbag system with a fixed open vent. The vent used had a 0.067 ft^2 orifice. The simulation was conducted for a 50 lb payload impacting at 21 ft/sec. The pressure time history for this case is contained in Fig. 19. The plot of the pressure time history is more symmetric than formerly produced by the 8.25 and 11 inch diameter spring loaded check valves.

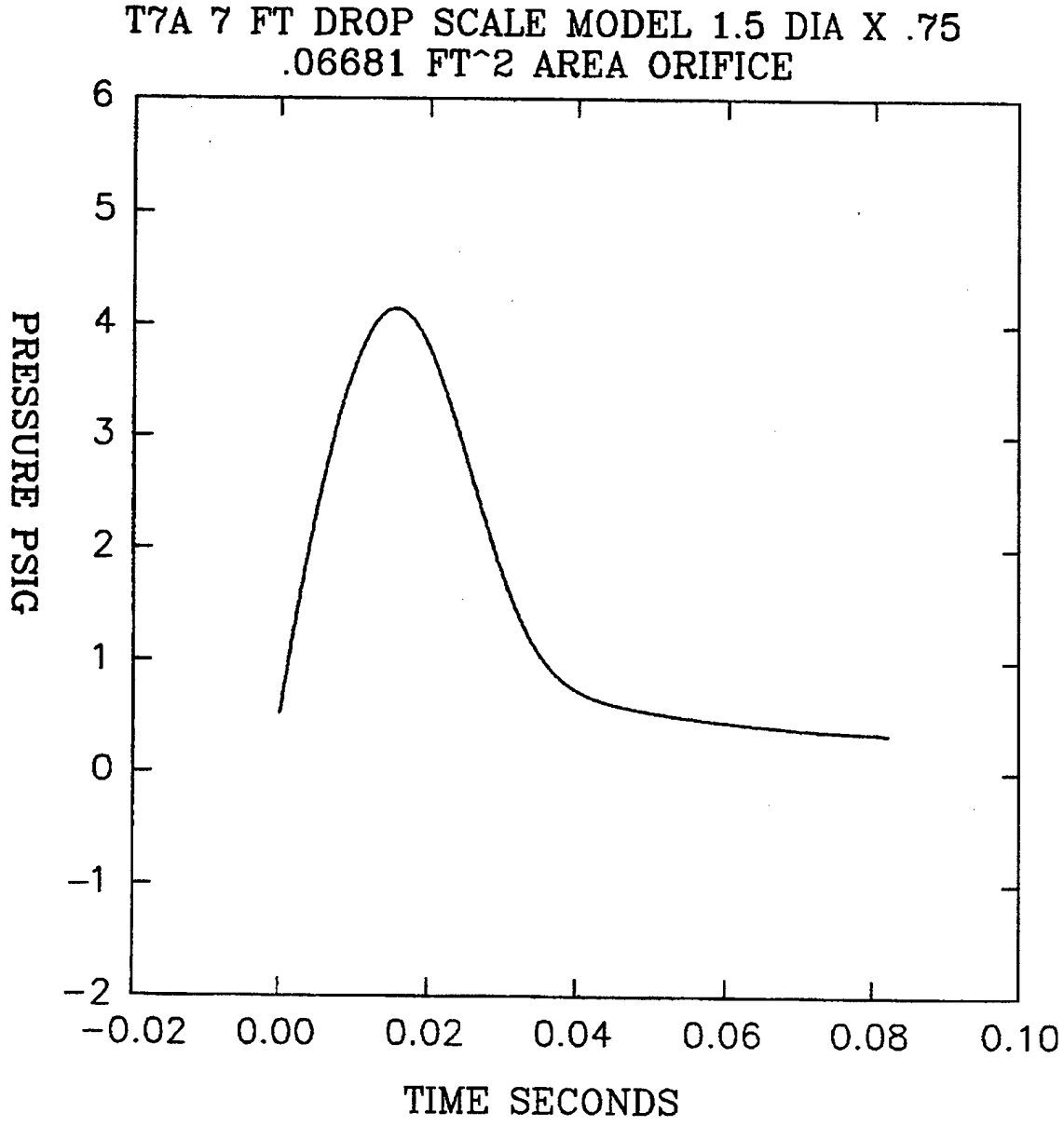

Figure 19. Simulated Airbag Pressure Response using a Fixed 0.06681 ft^2 Open Vent

The check valve output flow area as a function of time for the 7 ft drop with a valve having a body diameter of 11 inches is found in Fig.20. This plot represents the valve area characteristic used during the previously conducted simulation case found in Fig. 16. A slight modulation is noticeable in the 50 millisecond region of the graph. The airbags internal pressure responds by severely overshooting the 2.12 psig set point level. The area change is directly reflected in the slope of the pressure trace for this simulation. The valve body seems to chatter on the return to zero when the pressure is low. A graph

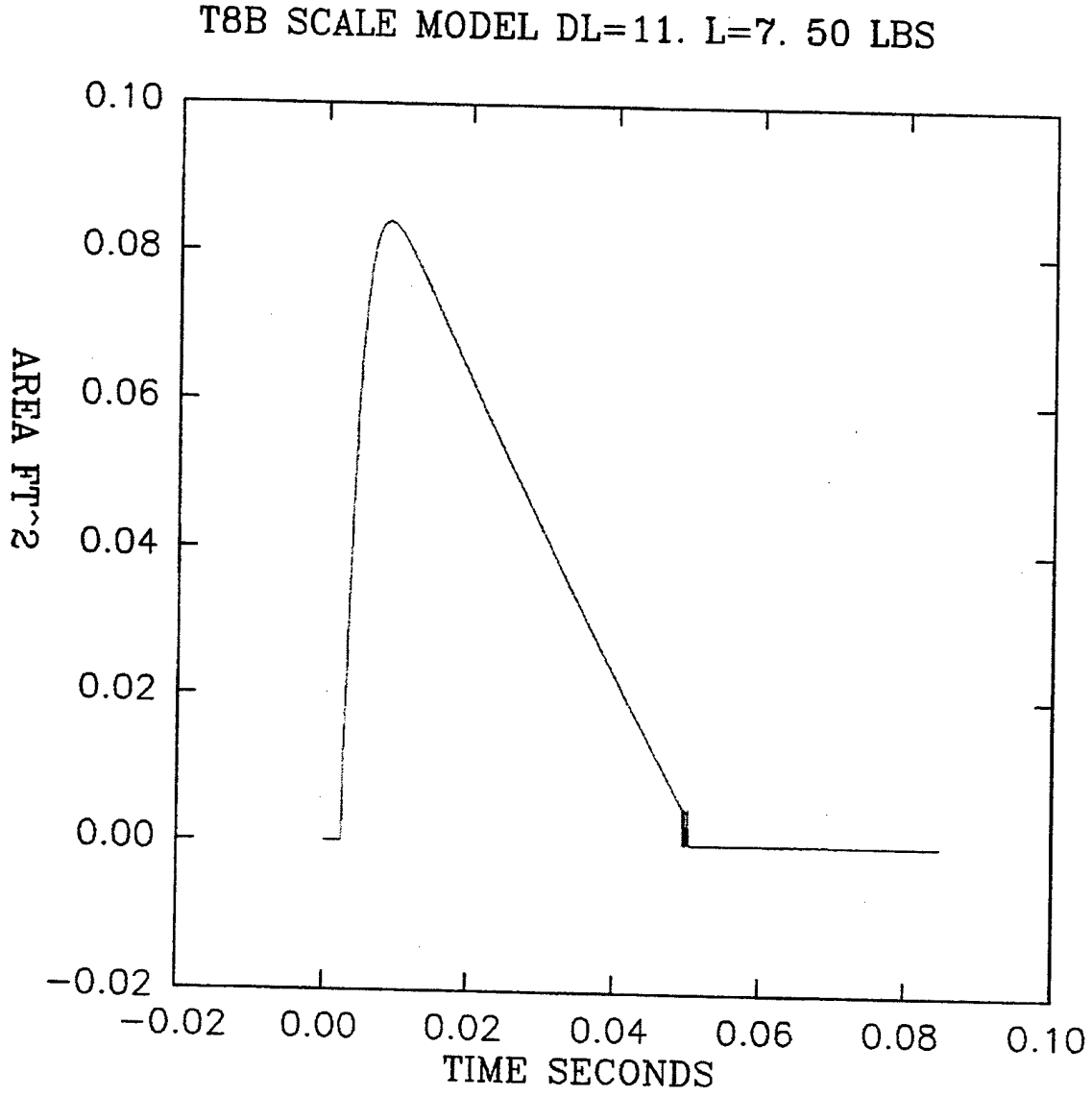

Figure 20. Spring Loaded Check Valve Area as a Function of Time, V= 21 ft/sec

superimposing the computer calculated pressure responses with the ideally modeled spring loaded check valve is found in Fig. 21.

Passive Valve Prototype Design

Three different prototype airbag check valves were invented for the experimental research study. The first two candidates consisted of linearly spring-loaded designs using compression springs. The original design shown in Fig. 22 is very simple and easy to fabricate. The valve seat has three equally spaced studs on a 5.5 inch diameter bolt circle and possesses a 3.5 inch diameter center hole with a 1/8 inch 45-degree seat chamfer. The

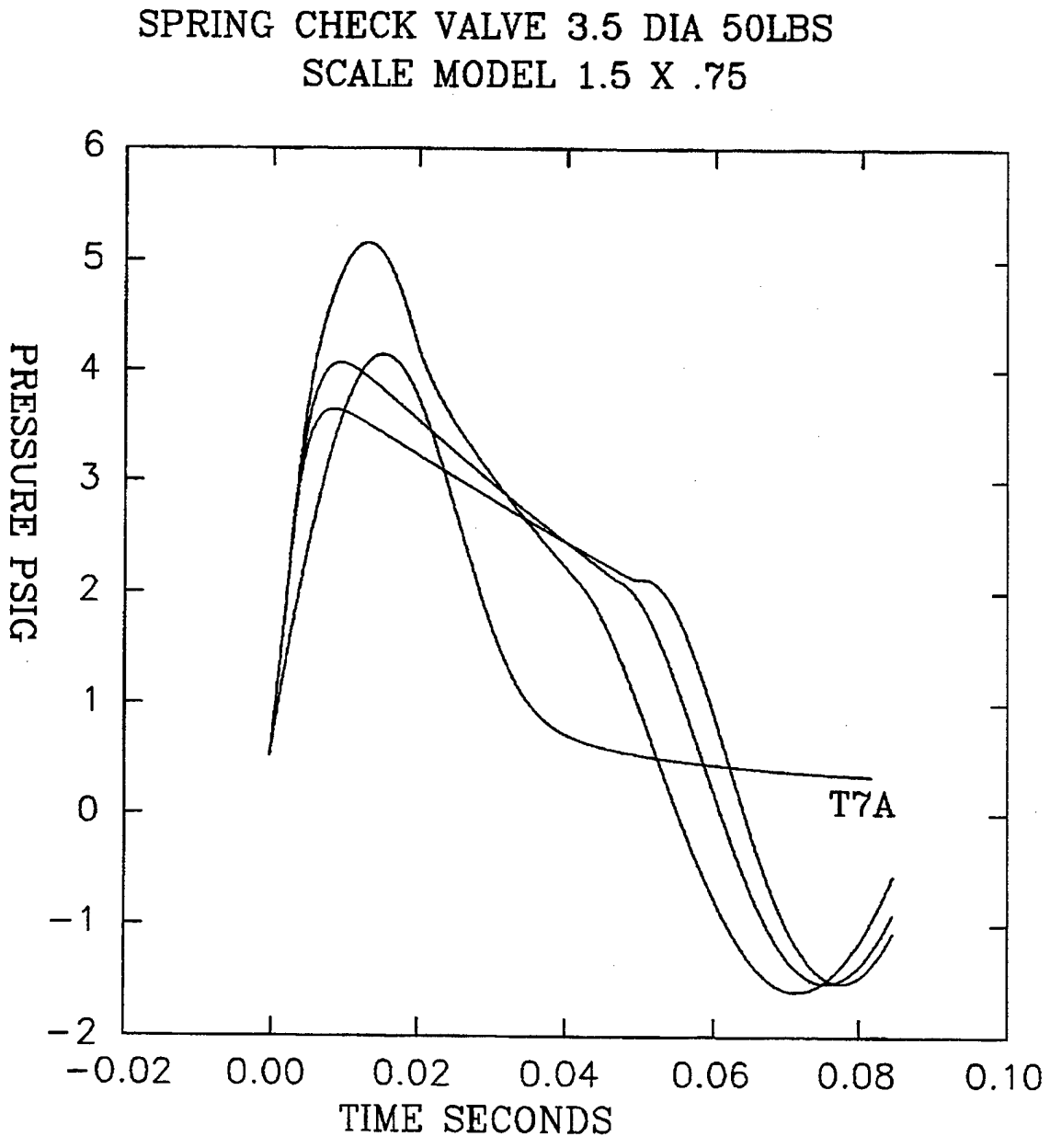

Figure 21. Superposition of the Computer Simulated Airbag Pressure Response Curves for the Spring Loaded Ideally Modeled Check Valve

valve body consists of a circular plastic cover with stud matching in line through holes. Three compression springs are placed on top of the valve cover and secured by washers and lock nuts. The pressure set point level for the valve is variable. The design does not allow for a precision adjustment of the prescribed preload force setting level. Increasing the preload level of the valve is achieved by tightening the lock nuts and compressing the unstretched length of the springs. The valve body is a simple circular plate covering the

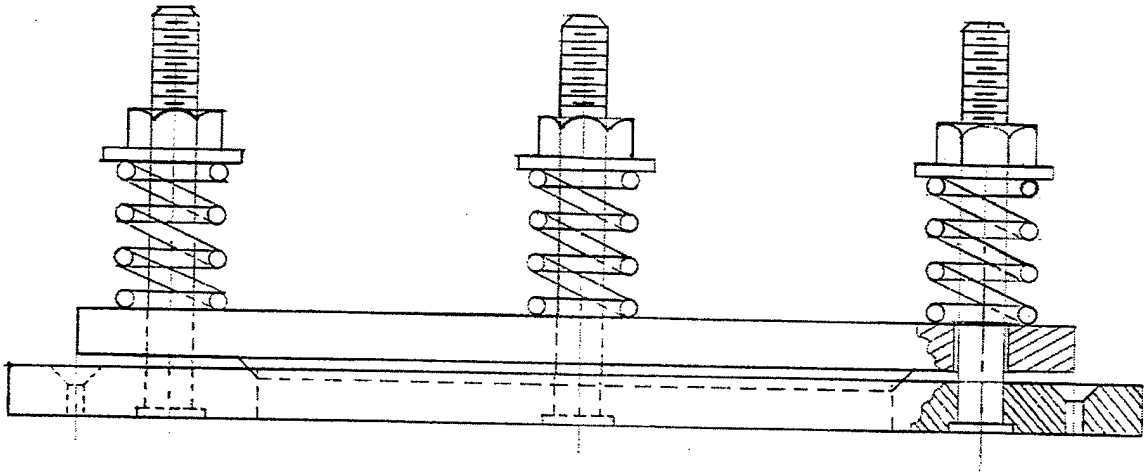

Figure 22. Sketch of the simple Three Spring Check Valve Design

valve seat center outlet hole. The fabrication is uncomplicated with virtually no significant manufacturing tolerances. Figure 23 contains a graph of the theoretical determined outlet flow area of the spring loaded check valve as a function of pressure for a family of various spring rates.

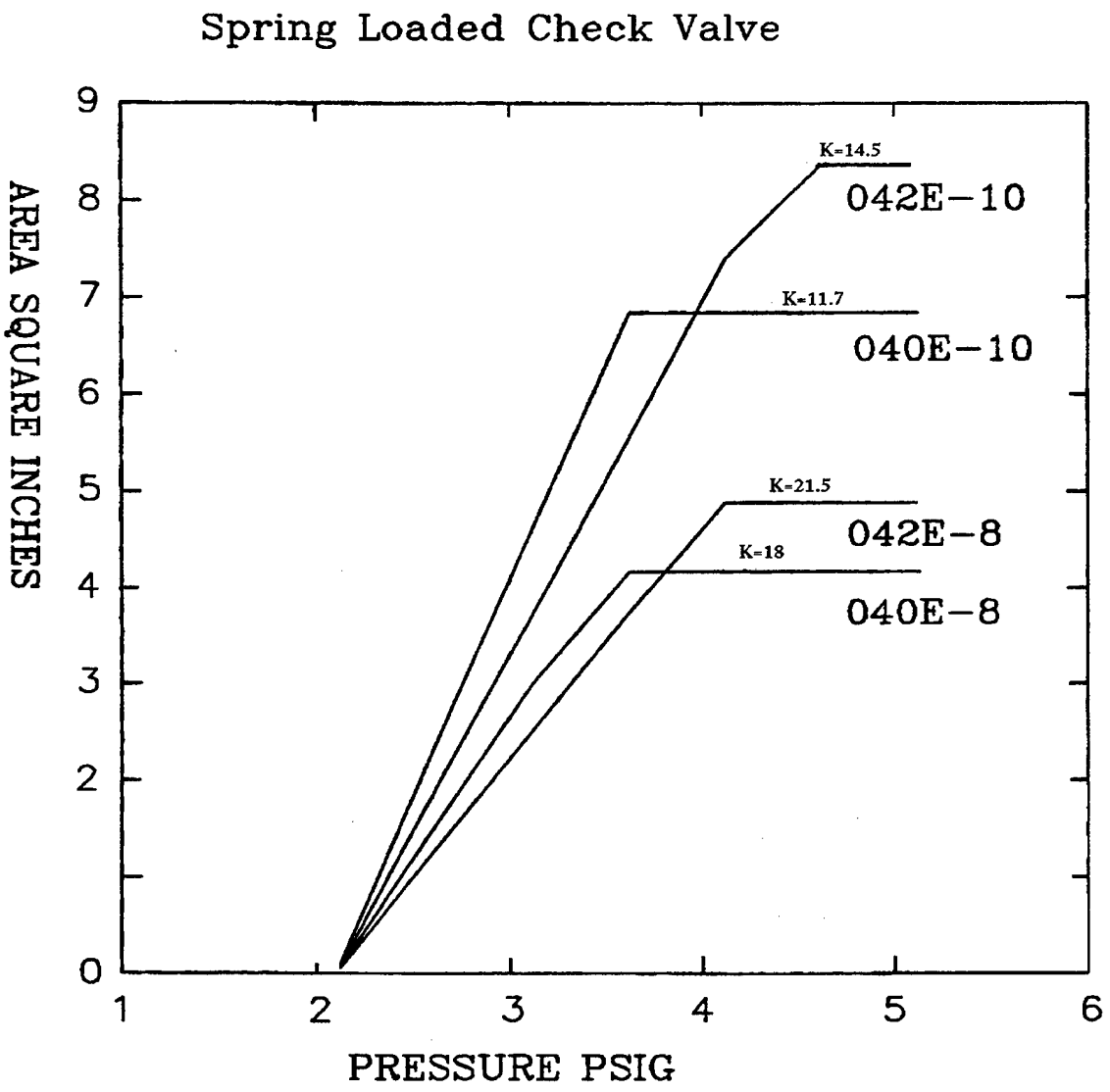

Figure 23. Graph of Flow Area as a Function of Pressure for Various Ideal Spring Rates

However, this design allows the valve to open and vent flow in several modes. The cover plate is free to oscillate about its center axes because of the clearance between the hole and the stud diameter. The pressure set point at which the valve first cracks open is not well controlled because the valve does not translate purely linearly. Each spring can be subjected to different displacements depending on the angular tilt of the valve cover. Since the valve cover design has three parallel springs, the pre-load and the equivalent spring rate becomes approximately the sum of each of the individual spring contributions for large displacements.

The second prototype design had a guide to constrain the valve to move normal to the valve seat and contained a single linear spring. This poppet type design is shown in Fig. 24. The valve possesses a 45-degree chamfer that mates with the sharp edged valve seat. The single spring is sandwiched between the lower surface of the valve guide plate

and the upper surface of the circular plate valve body. The guide is attached to the valve seat using three equally spaced studs covered by spacing bushings. The amount of pre-load required initially to seat the valve can be adjusted by changing the height of the spacing bushings. This design requires greater tolerance and precision in the machining of the valve components. The ability to scale this design up for larger flow exit area is difficult. The single spring design is less efficient in applying large loads to the valve, than the parallel spring design.

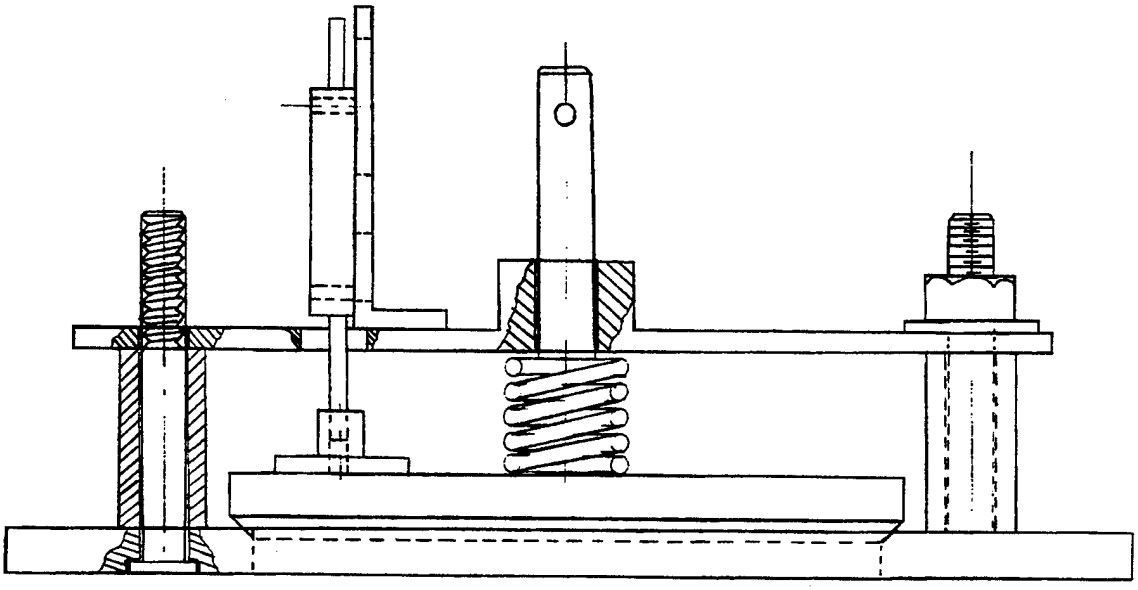

Figure 24. Sketch of the Single Compression Spring Check Valve Design

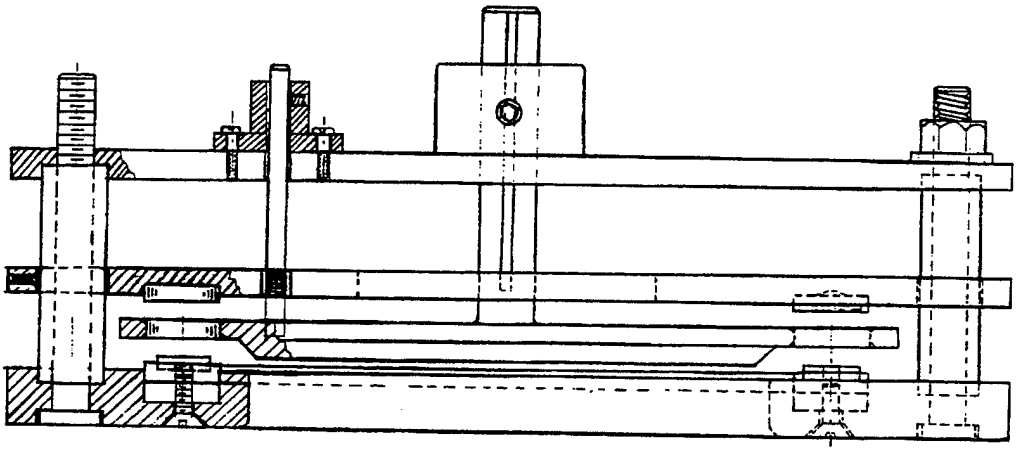

Figure 25. Sketch of the Magnetic Check Valve Design

The third prototype airbag check valve is shown in Fig. 25. This design uses magnetic attraction and repulsive forces to both adjust the pressure set points and to apply forces to restore the valve to the seat. The magnets used for the design were made from Neodymium-Iron-Boron with flux densities between 27 to 30 million gauss oersteds. The force characteristic is very nonlinear. Figure 26 contains a graph of the typical repulsion

force created as a function of displacement by a pair of ½ inch diameter 0.125 inch thick mutually opposed disc magnets.

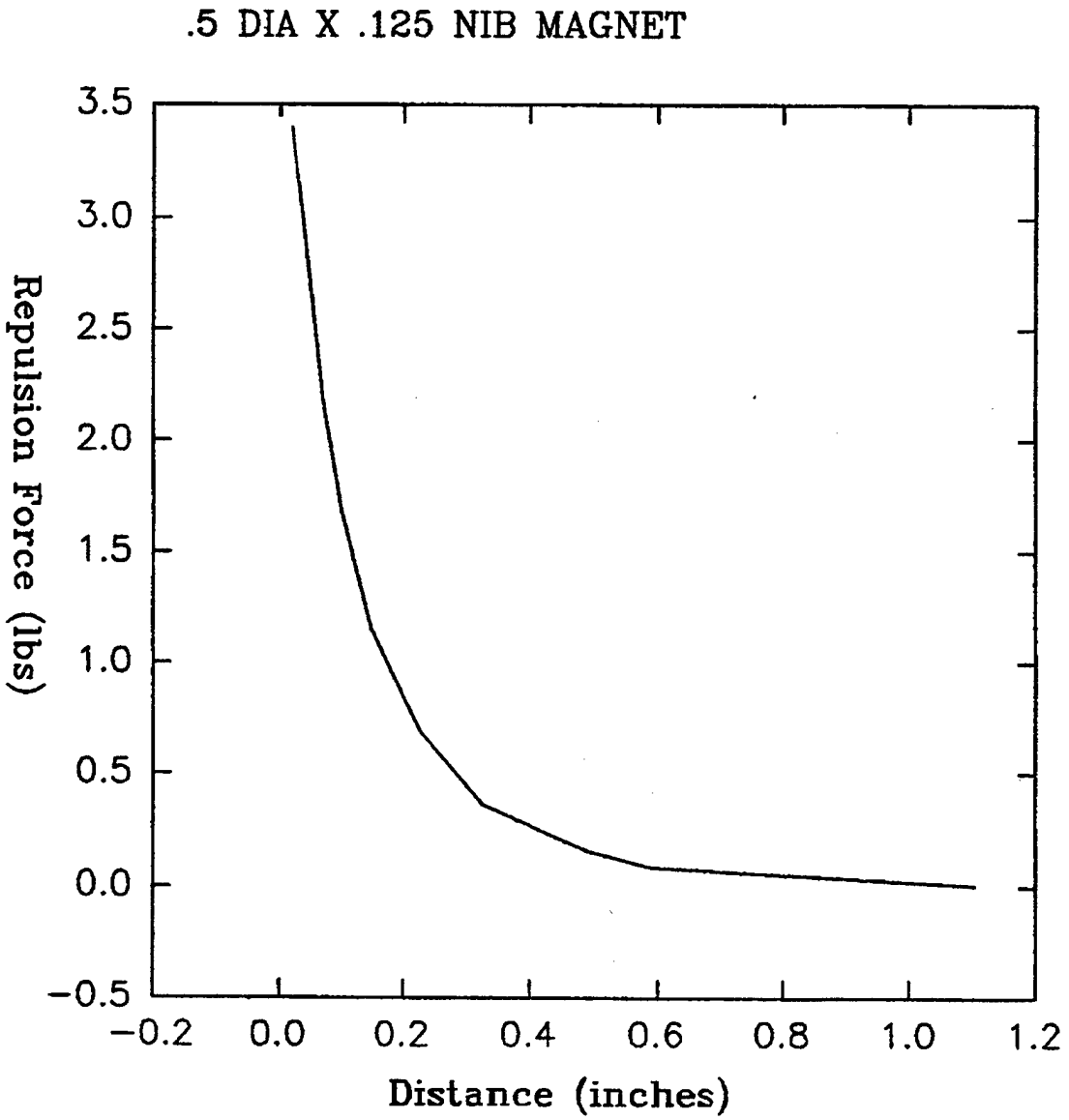

Figure 26. Graph of the Magnetic Repulsion Force as a Function of Separation Distance

The valve configuration is essentially a classical poppet design with the addition of four equally spaced disk magnets inserted near the perimeter. The sealing is accomplished on the surface of a sharp edge because of the straight bore through the valve seat. The mating surface of the valve body contains a 45-degree chamfer. The original prototype used a dog point set screw sliding in a grove on the valve stem shaft. This was done to keep the alignment of the magnet center when the valve translates from the open to closed positions. The tolerance and precision of the machining required to produce good radial alignment proved to be problematic. The valve used for experimentation was modified to incorporate a shaft parallel to the valve stem shaft. The restraint of the valve rotational displacement achieved by this design change proved beneficial.

In the second generation magneto-static design the valve stem and guide would be replaced by internal and mating external precision ground spline shafting. The result would be a single shaft providing both guiding and rotational restriction to the valve stem. The valve seat contains an annular ring whose position can be adjusted by four screws from the underside of the valve seat. Counterclockwise revolution of the elevation screws increases the length of the distance between the valve seat and the annular ring. This has the effect of lifting the attraction steel ring and increases the valve seat attractive force. This force sets the breakaway pressure level required to open the valve. Above the poppet valve there is another annular ring which is set screw secured to the stud bushings. Contained on the underside of this ring are magnets with their poles arranged to repel the valve back toward the valve seat.

Experimental Study of Valve Behavior

Two different methods of experimental measurement were used to evaluate the performance of the check valve candidates. The first consisted of building a 1.33 ft^3 enclosure connected to a 178 in^3 tank through a ½ inch internal diameter tube connected to a DC activated solenoid valve. This apparatus has the ability to inject a transient pressure pulse into the chamber. The purpose was to study the check valve dynamic vent response and to calculate the valve vent area as a function of applied pressure at the valve seat. The pressure at the underside of the check valve does not equal the chamber pressure once the valve becomes unseated. This means that analytically modeling the valve flow area change as a function of chamber pressure becomes a complicated task.

Determining the check valve exhaust flow area as a function of chamber average applied pressure using experimentation initially seemed plausible. By measuring the valves displacement as a function of pressure contained within the chamber and scaling the value by the exit valve body perimeter an exit flow area can be calculated. A steady flow pressure test would be the most accurate method to use but it requires an extremely large adjustable pressure source. Initially, the method planned to produce the exhaust areas relationship to pressure consisted of acquiring a transient valve response measurement under the application of a pressure pulse.

The displacement of the valve, the chamber pressure, and the pressure at the underside of the center of the valve body, acquired simultaneously, would enable the calculation of the exit flow area as a function of pressure. However, since the three-spring valve possesses three degrees of freedom, one vertical translation and two orthogonal rotations, a linear displacement transducer could not be used to gather the valve displacement from the seat during pulse venting.

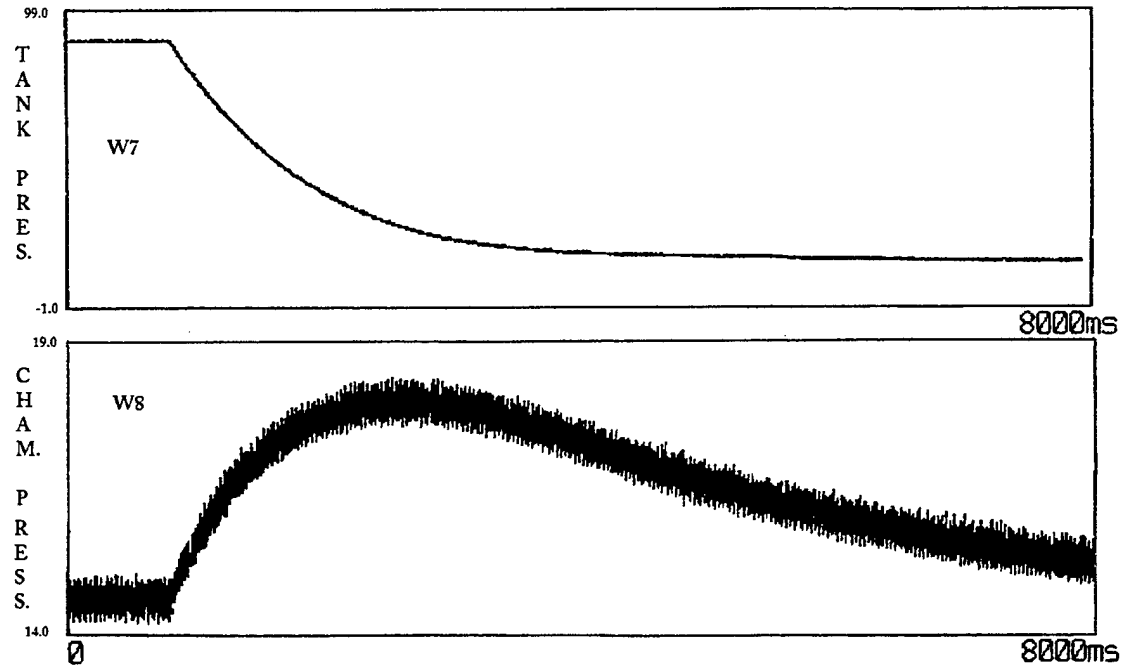

Figure 27. Graph of the 1.33 ft^3 Closed Chamber Pressure Response from the 0.103 ft^3 Filling Tank Discharge

Figure 27 shows the chamber response to the tank filling process, this was achieved by securing the three-spring valve body directly to the valve seat. Although it was impossible to create a perfectly airtight dry seal the response clearly shows a transient pulse shape. If this style valve is adapted for use as a closed volume airbag vent, the valve body will initially have to be sealed against the valve seat with a thin layer of either a floro-elastomer compound or a silicon rubber. The 0.103 ft^3 tank was initially charged to a gage indicated 80 psig level. The transducer connected to the tank indicated 89.5 psig. The solenoid valve was activated and the chamber pressure increased from the atmospheric pressure level. The average pressure being 14.6 psig as indicated by the chamber monitoring pressure transducer. It took approximately 1.6 seconds for the pressure to increase to a 17.9 psig level, which reflects a 3.26 psig change. The signal than decayed toward atmospheric as the air leaked through the valve seat. The measured chamber pressure signal possessed a 0.566 psig noise level. It was apparent from this test that the chamber transducer did not have the sensitivity to determine the pressure to within a 0.1-psig level.

A typical result of chamber testing using the three-spring check valve is shown in Fig. 28. The filling tank was charged to 80 psig as indicated by pressure gage and the solenoid valve activated. The response shown is a typical noise ridden step function.

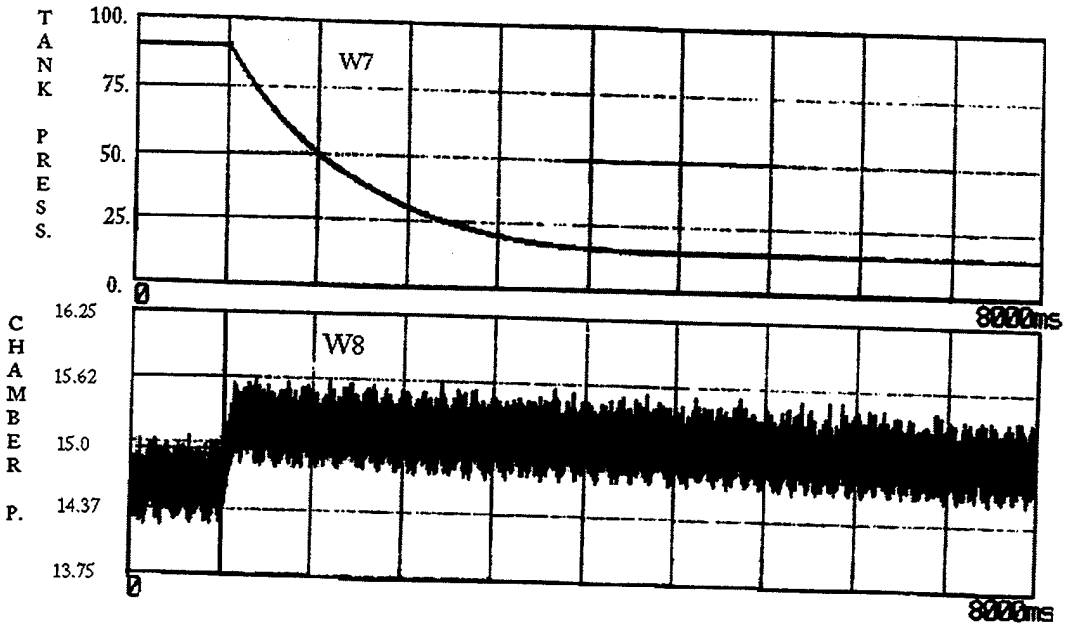

Figure 28. Graph of the Three Spring Check Valves Chamber Pressure Response Resulting from the Filling Tank Discharge

The signal has 0.6 psig of noise superimposed upon an approximate 0.6 psig pressure change. It is difficult to deduce the real character of the response from this figure.

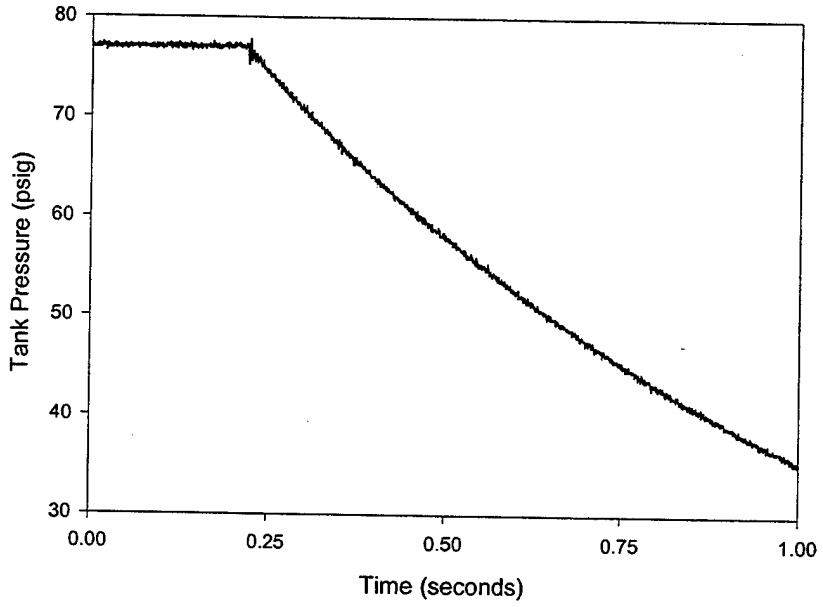

Figure 29A. Graph of the Filling Tank Discharge Pressure as a Function of Time

The single spring check valve was experimentally evaluated using the tank discharge fixed volume chamber approach. The check valve was modified to include a

linear potentiometer to measure valve translation relative to the seat. The valve body was modified to allow the ram dynamic pressure at the center of the underside to be measured during the transient. Plots of the results of subjecting the single spring check valve to the same 82 psig initial tank charge induced pressure pulse are contained in Figs. 29A-D. The four signals simultaneously observed were; Filling Tank Pressure (W7), Valve body position voltage (W5), Pressure at the Valve Body Center (W6), and the Chamber Response Pressure (W8).

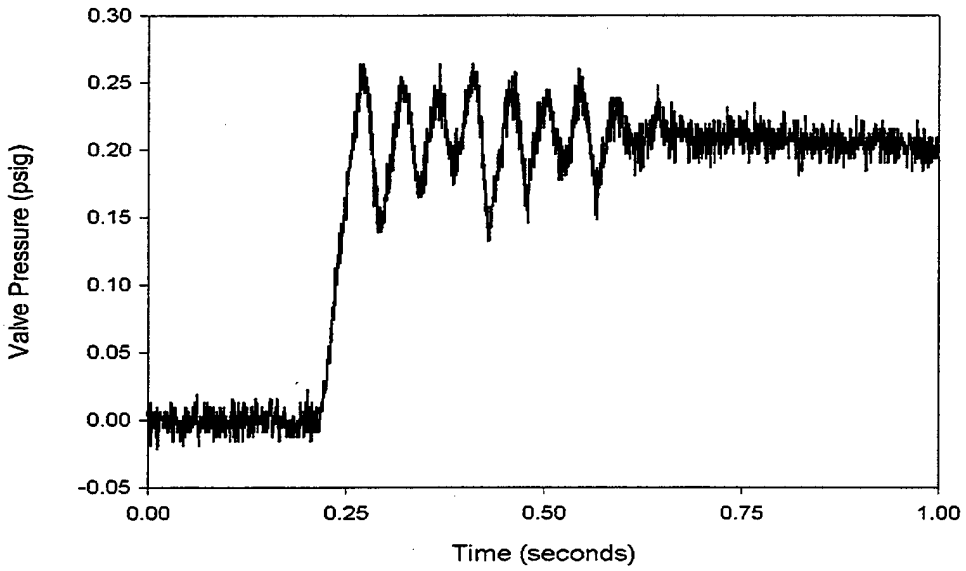

Figure 29B. Graph of the Check Valve Pressure as a Function of Time

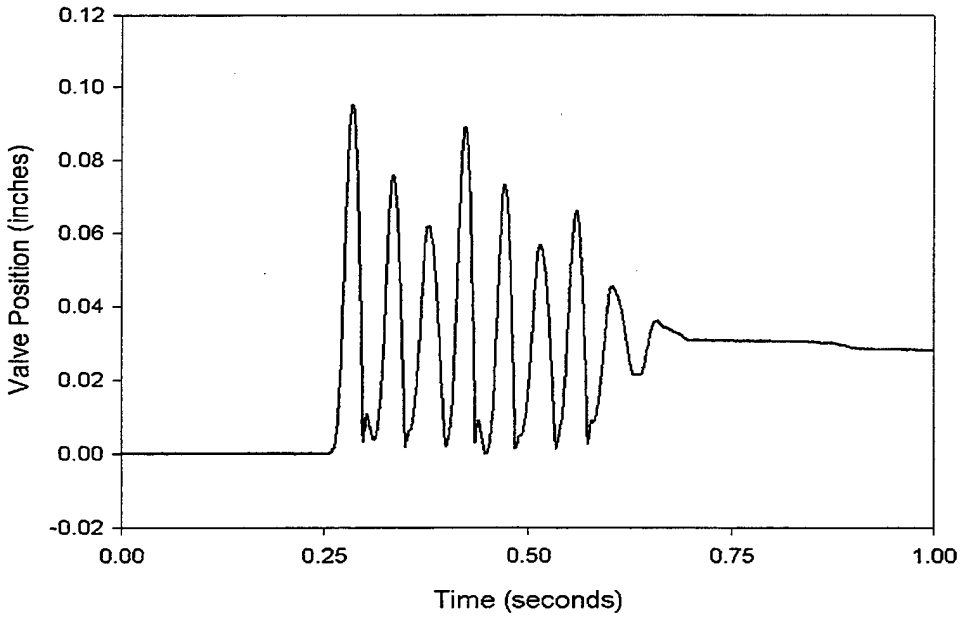

Figure 29C. Graph of the Check Valve Position as a Function of Time.

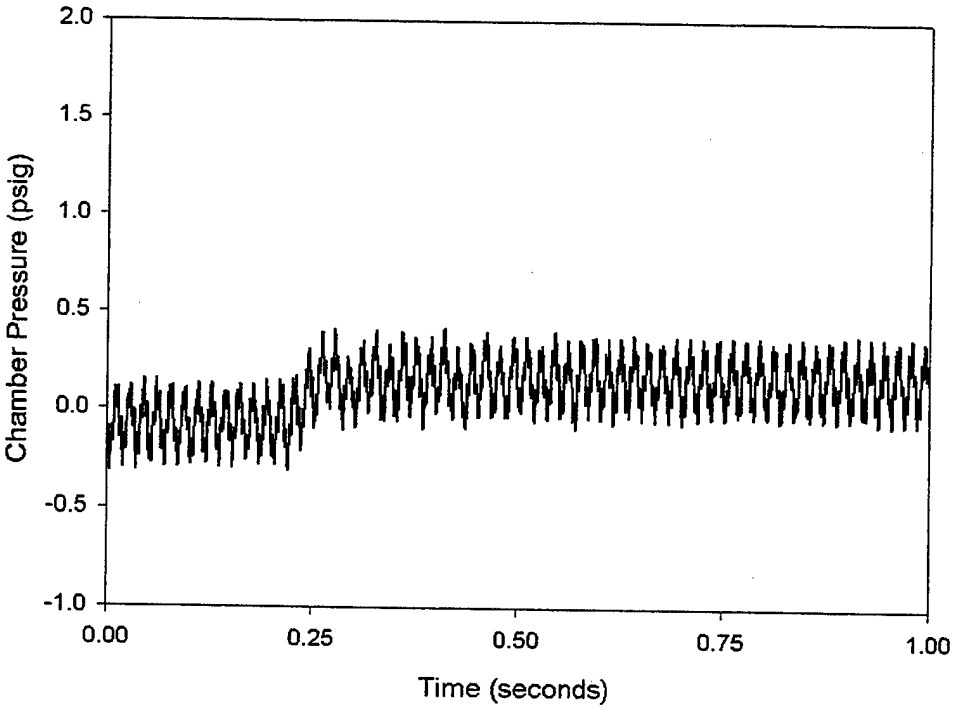

Figure 29D. Graph of the Test Chamber Pressure as a Function of Time

The filling tank discharge pressure as a function of time is plotted in Fig. 29A. The pressure transducer used for the valve body pressure measurement was changed to a higher sensitivity model for this experiment. Figure 29B shows that the shape of the pressure acting on the underside of the valve body appears as an underdamped step change. The position voltage found in Fig. 29C indicates that the valve body oscillates from an open to a closed level modulating the pressure to a constant level. As the inflow into the chamber and efflux through the valve become balanced, the valve body pressure level and the position transducer become quasi-constant. The spring rate regulated the chambers internal pressure to a 0.208 psig level.

The single spring valve was then subjected to two other tank discharges one at 60 psig and the other at 40 psig. The steady state value of valve body pressure from these tests was also found to be at the 0.21 psig level as depicted in Fig. 29B. While the steady state valve of position voltages were 0.989 & 0.868 volts respectively, compared to the original 1.084 volt level. Since the potentiometers signal gain is 0.0938 inch/volt this represents a displacement less than 0.02 inches. Depending on the alignment of the valve body, the friction and preload levels of the valve, the difference in exit flow area is less than 0.25 in^2 which is negligible. The conclusion drawn is that reduction in the magnitude of the pressure pulse magnitude, causes the modulation time to decrease while maintaining the valve convergence to the same fixed pressure and exit area levels.

Scale Model Airbag System Experiments

The second method used to experimentally evaluate the check valve candidates performance was to subject them to a pressure pulse created by an airbag landing impact. A scale model airbag system was fabricated to evaluate the behavior of the prototype air release valves and to validate the predictions determined from computer modeling. The original concept was to use the same 0.103 ft^3 tank of compressed air to inflate a 9 inch tall, 18 inch diameter, 1.33 ft^3 right cylindrical airbag. The airbag was to be inflated to a pressure level such that the deceleration work created would demonstrate an increase in airbag compression efficiency. The actual airbag used during testing consisted of a seamless right circular cylinder woven from flat Kevlar® fiber. This airbag has an estimated internal volume of approximately 2.21 ft^3, which is 66% larger than the originally intended airbag design. The volume increase was due to the manufacturing process which created a 9 inch radius hemispherical dome shaped bottom. The construction of the seamless airbag using the automated weaving process could not produce a flat bottom. Consequently the airbag could not be charged to a 2.0 psig level using an initial 100 psig tank pressure. This was due to the increase in airbag volume acting along with the system leakage. The airbag platform connection and the valve stem and seat connection were the sources of the system leakage.

The scale model airbag platform was configured to study the effects of five different exhaust vent configurations. Three sets of experiments examining the performance of the three previously mentioned prototyped check valve designs. The other two sets of experiments explored the airbag platform landing performance using two different prototyped blowout vents. The blowout style vents were constructed using components from the magnetic check valve. These vents rely upon the forces of magnetic attraction to set the pressure release level. When the internal airbag pressure exceeds the applied magnetic force level the vent becomes fully open and flow passes through a 3.5 inch diameter orifice. The first blowout style vent was fabricated by using a 4.875 inch diameter, 1/32 inch thick circular steel cover. The cover was placed directly upon the valve seat of the disassembled magnetic check valve. The second blowout style vent was constructed by using the stem and seat of the original magnetic check valve assembly with the guide and repulsion ring removed. The valve stem was unconstrained and simply placed upon the valve seat with the four magnetic pairs kept in the same alignment for all of the experiments. This configuration provided the tightest seal between the valve and seat and also possessed the highest release set point pressure.

The first set of experiments was performed using the prototype magnetic check valve attached to the airbag system. The system was elevated off of the ground at three different heights and released from rest. The calculated impact velocity level for these drops neglecting air resistance was 21.1 ft/sec, 18.1 ft/sec and 14.7 ft/sec respectively. The airbags pressure response as a function of time for these impact velocity levels are found in Fig. 30, Fig. 31, and Fig. 32 respectively. The magnetic valve was then disassembled and the valve stem clamped securely in a position ¼ of an inch from the surface of the valve seat. In this position the air is allowed to escape from the airbag through the 2.74 in^2 radial area bounded by the height of the valve stem relative to the

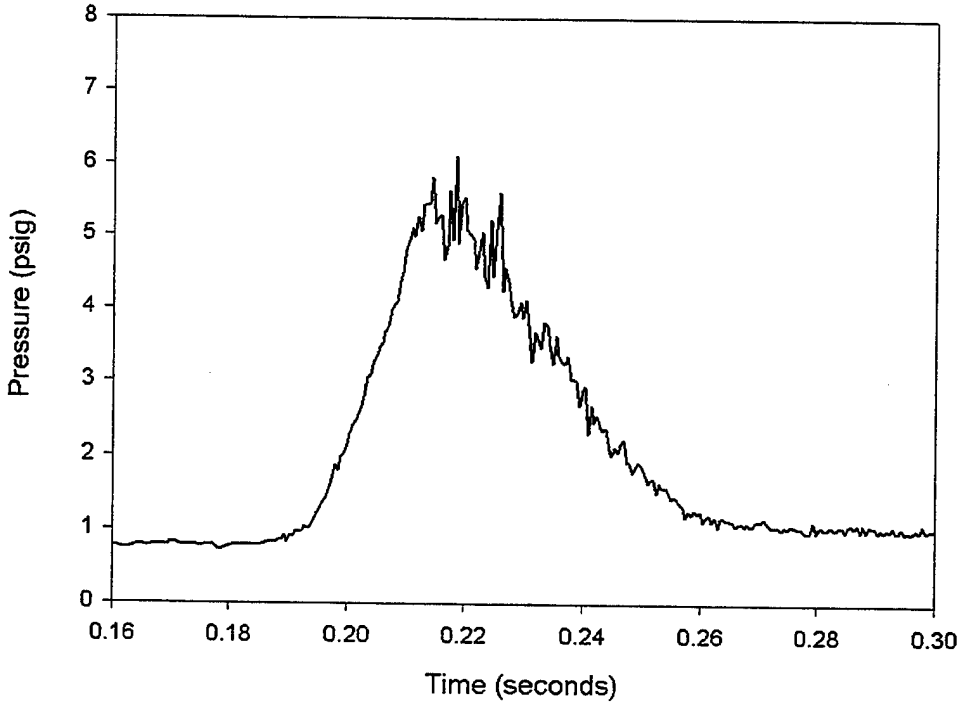

Figure 30. Airbag Pressure Response using the Magnetic Check Valve, V=21.1 ft/sec

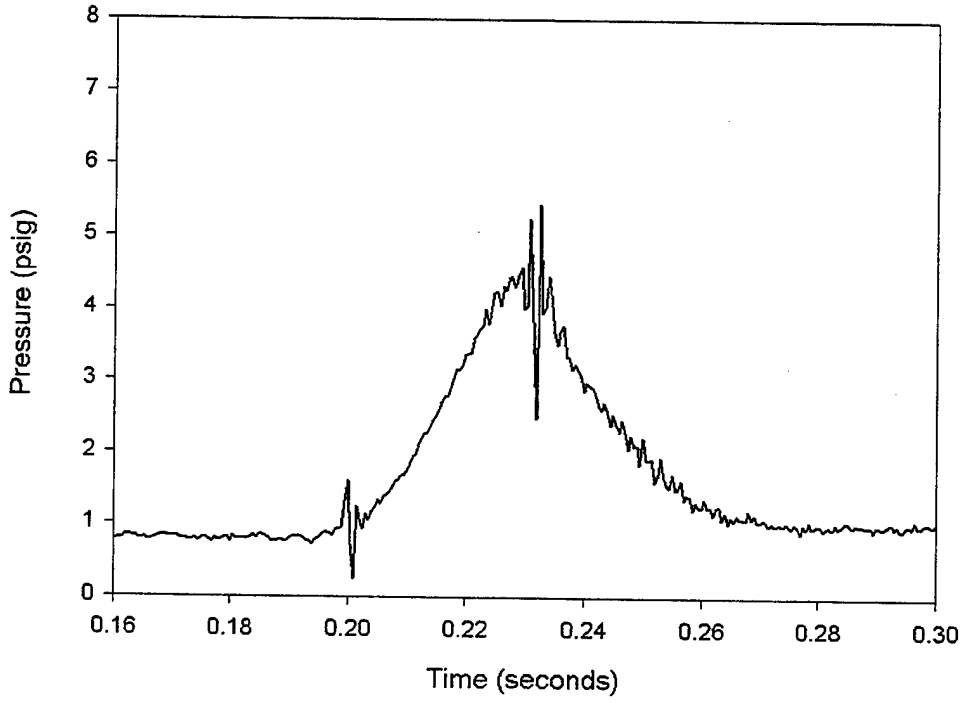

Figure 31. Airbag Pressure Response using the Magnetic Check Valve, V=18.1 ft/sec

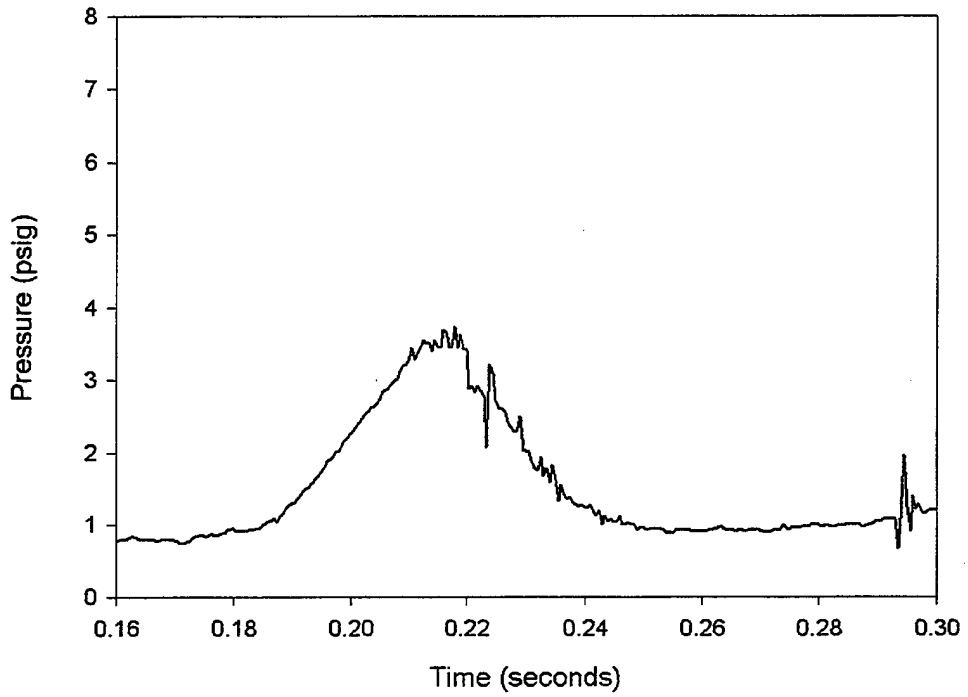

Figure 32. Airbag Pressure Response using The Magnetic Check Valve, V=14.7 ft/sec

seat. This is the typical full open position of the linear single spring check valve. The area represents a 71.5% reduction of the flow area produced by the 3.5 inch diameter exit orifice. The scale model airbag system was then subjected to another set of tests using the valve frozen open at this position. The resulting pressure response curves produced from these 21.1 ft/sec, 18.1 ft/sec and 14.7 ft/sec impacts are found in Fig. 33, Fig. 34, and Fig. 35. These results establish a baseline of pressure response curves for the scale model airbag system exhausting through a full open valve with a constant 2.74 in^2 vent area.

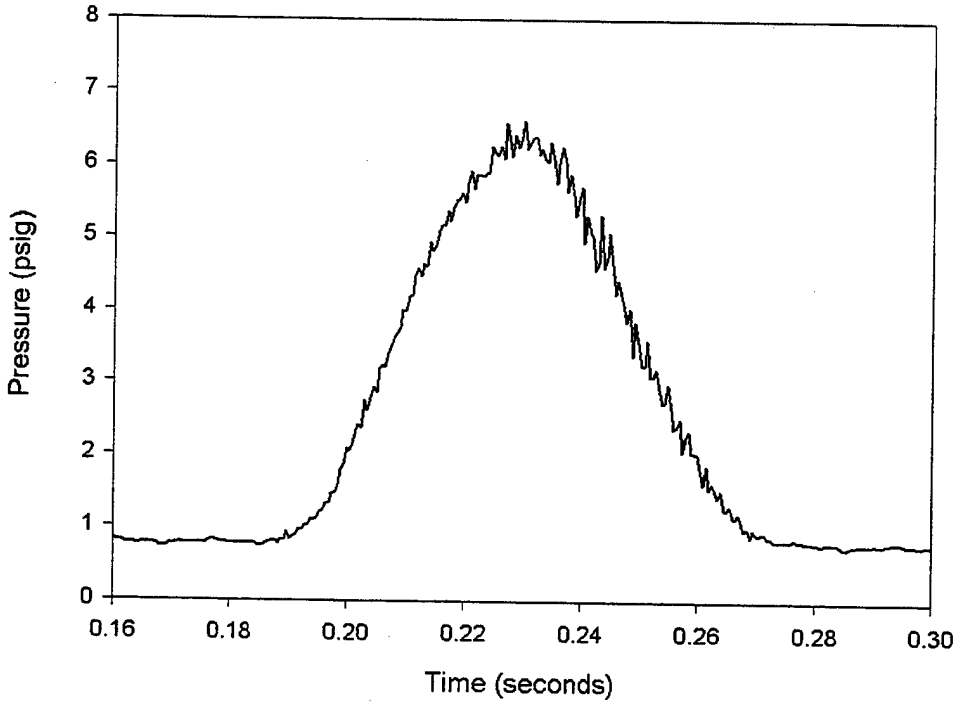

Figure 33. Airbag Pressure Response for a 2.74 in^2 Fixed Valve Opening, V=21 ft/sec

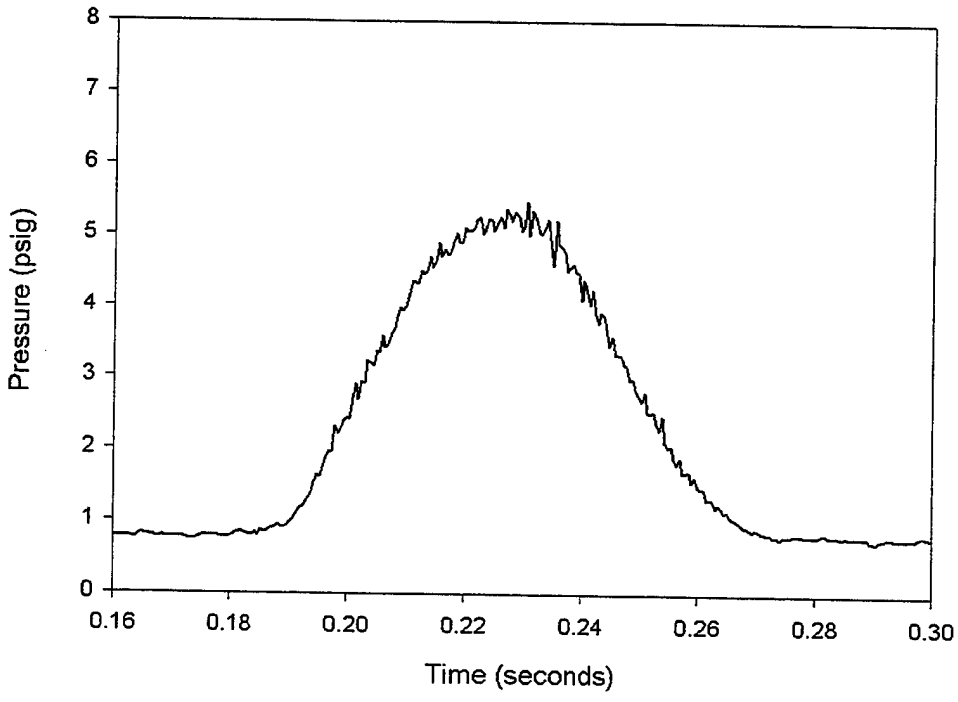

Figure 34. Airbag Pressure Response for a 2.74 in^2 Fixed Value Opening, V=18.1 ft/sec

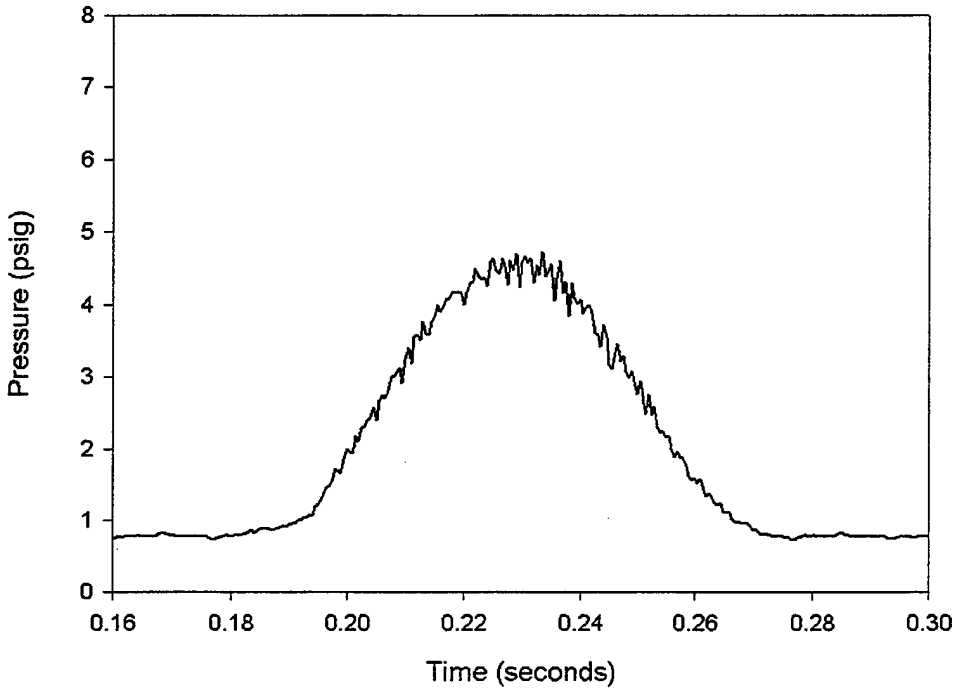

Figure 35. Airbag Pressure Response for a 2.74 in^2 Fixed Valve Opening, V=14.7 ft/sec

The performance improvement obtained by allowing the check valve candidates to modulate the exhaust airflow during impact can be seen by comparing the pressure response impact data to this baseline

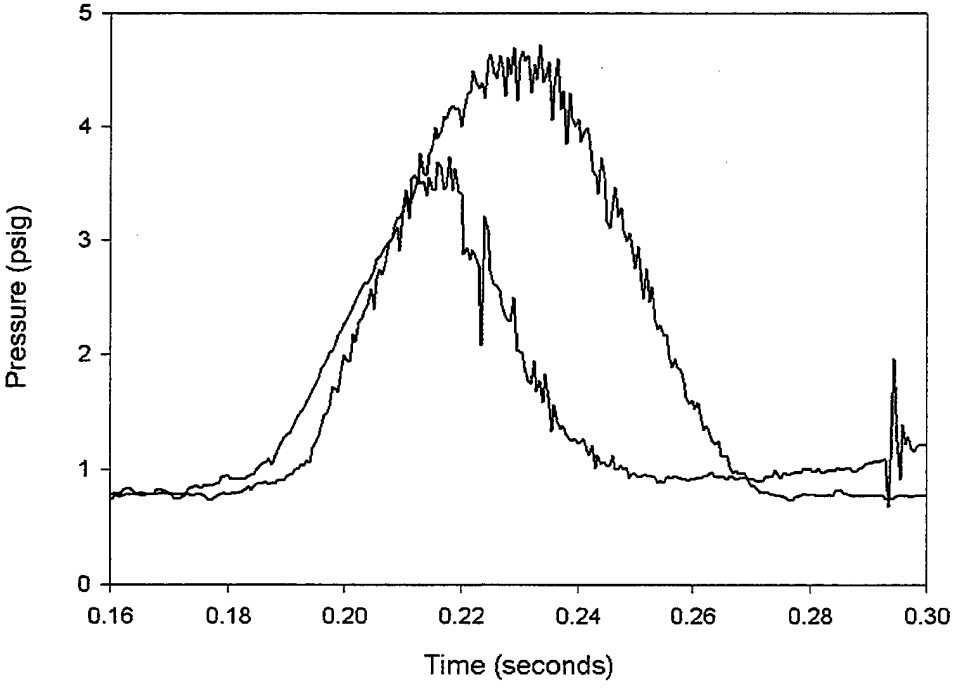

Figure 36. Airbag Pressure Responses Comparison of the Magnetic Check Valve with the 2.74 in^2 Fixed Vent Opening, V=14.7 ft/sec

Figure 36 shows the result of superimposing the pressure response of a functioning magnetic check valve with the pressure response of a valve that was fixed to maintain a 2.74 in^2 opening. The airbag impact velocity for this case was 14.7 ft/sec. The figure shows both, a significant decrease in the magnitude of the resulting airbag pressure, along with a shortening of the landing impact time duration. The pressure decrease is on the order of 1.0 psig (20%) and the duration of the pressure pulse appears to be 18 milliseconds (13.8%) shorter. The airbag system landed the payload softer and quicker when using the magnetic check valve for venting.

Similarly by comparing the superimposed airbag valve pressure responses for the 18.1 ft/sec and 21.1 ft/sec landings a 10.9% and a 14.8% reduction in peak pressure is noticed along with a 20.5% and a 14.1% decrease in their landing impact time duration's. The experiments reveal the general trend is for the check valve to convert the half sinewave shaped pressure pulse formed by fixed orifice discharge into a smaller triangular shaped pressure pulse with narrower time duration.

The next set of experiments was performed using the linear single spring check valve installed on the scale model airbag system. The drop test matrix was changed and consisted of releasing the system from 100", 83" and 61" drop heights. The resulting ground contact impact velocities produced were 23.2 ft/sec, 21.1 ft/sec and 18.1 ft/sec respectively. The airbag pressure responses resulting from these impacts are found in Fig. 37, Fig. 38, and Fig. 39.

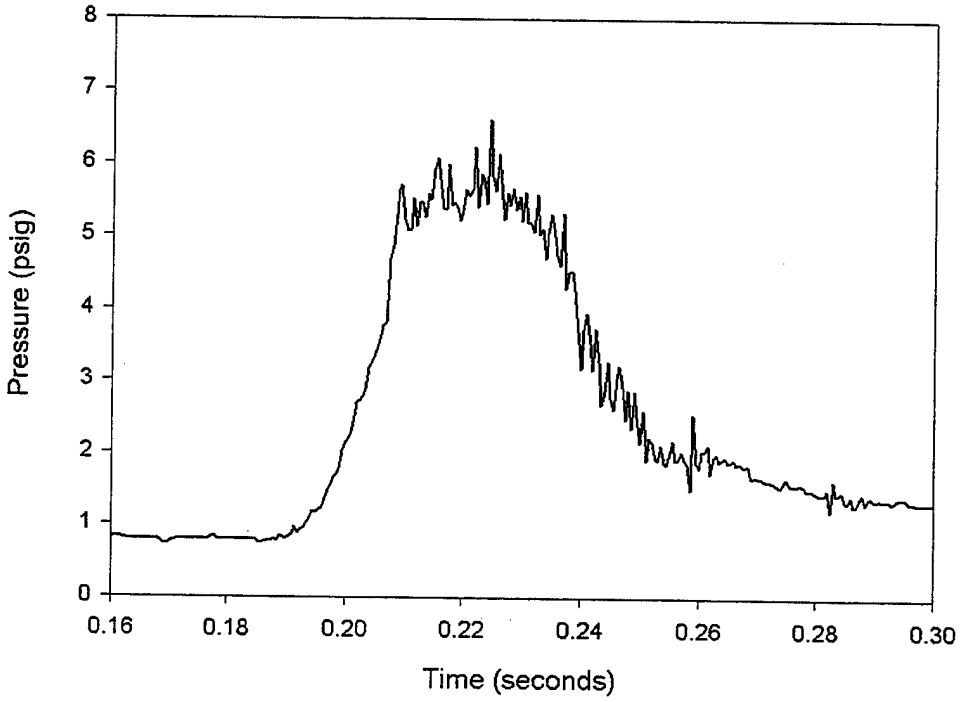

Figure 37. Airbag Pressure Response for the Single Spring Check Valve, V=23.2 ft/sec

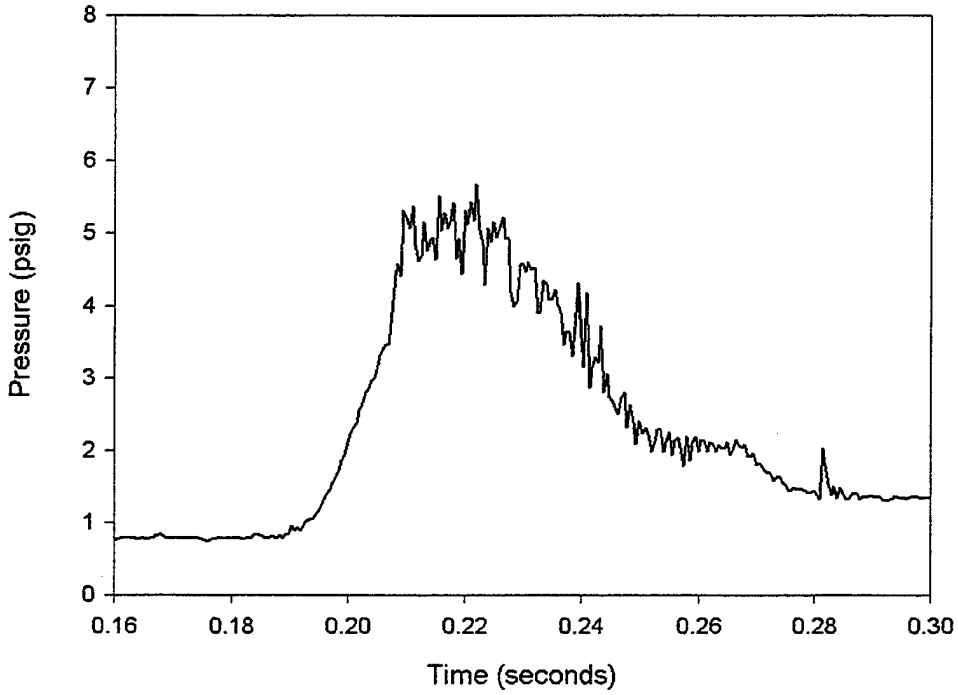

Figure 38. Airbag Pressure Response for the Single Spring Check Valve, V=21.1 ft/sec

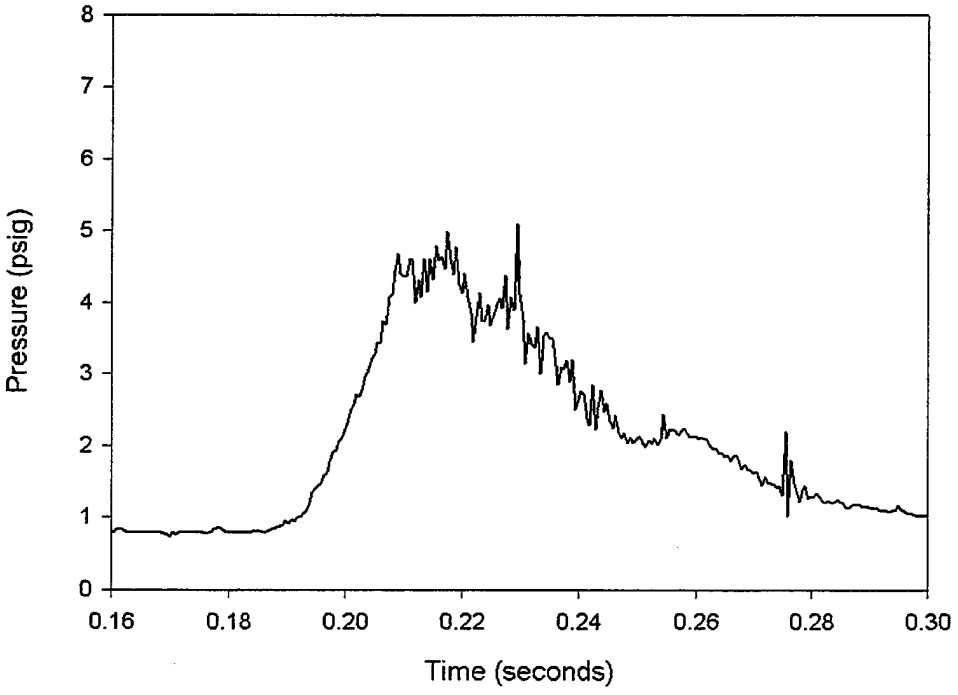

Figure 39. Airbag Pressure Response for the Single Spring Check Valve, V=18.1 ft/sec

The shape of the pressure pulses created by using this valve appears identical to those created by using the magnetic check valve. The scale model airbag system was then configured with the three linear spring check valve and subjected to the same set of

velocity impacts. The results of the airbag pressure response to these impacts are found in Fig. 40, Fig. 41, & Fig. 42.

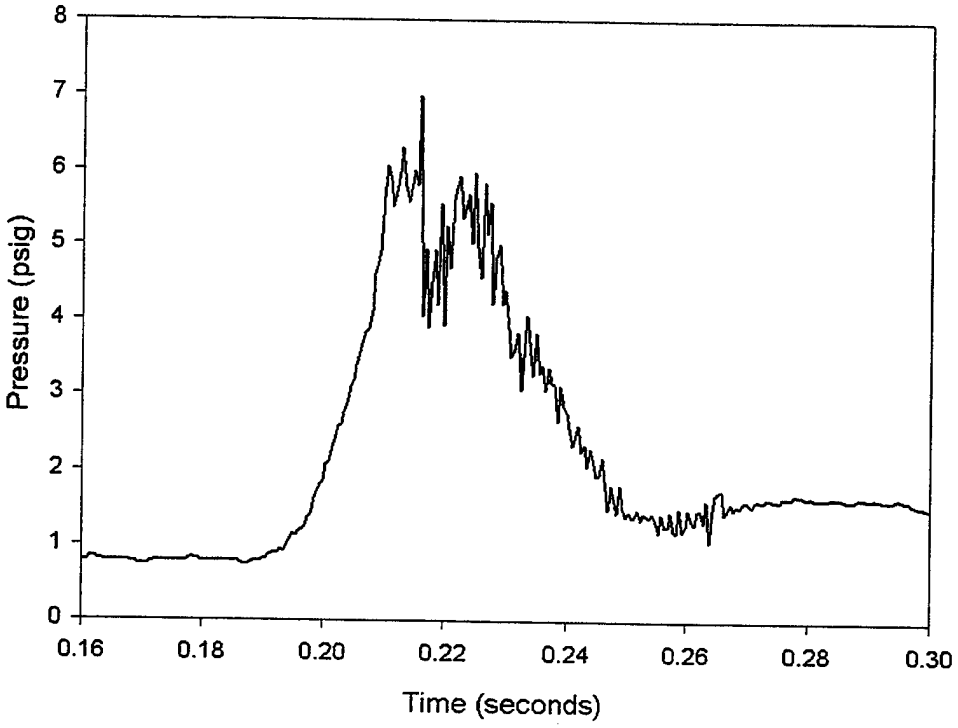

Figure 40. Airbag Pressure Response for the Three Spring Check Valve, V=23.2 ft/sec

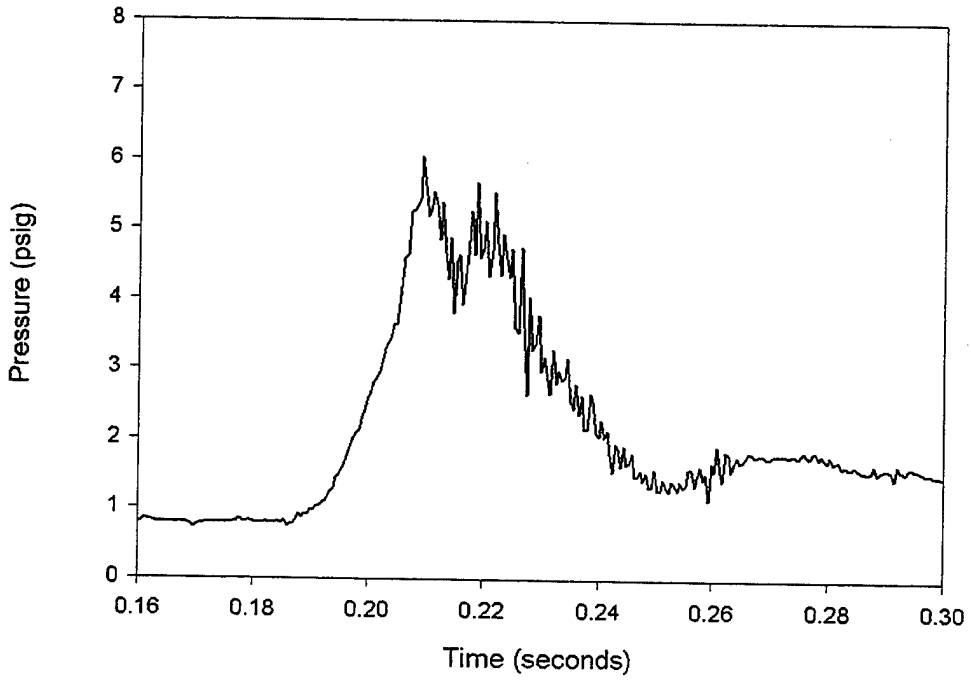

Figure 41. Airbag Pressure Response for the Three Spring Check Valve, V=21.1 ft/sec

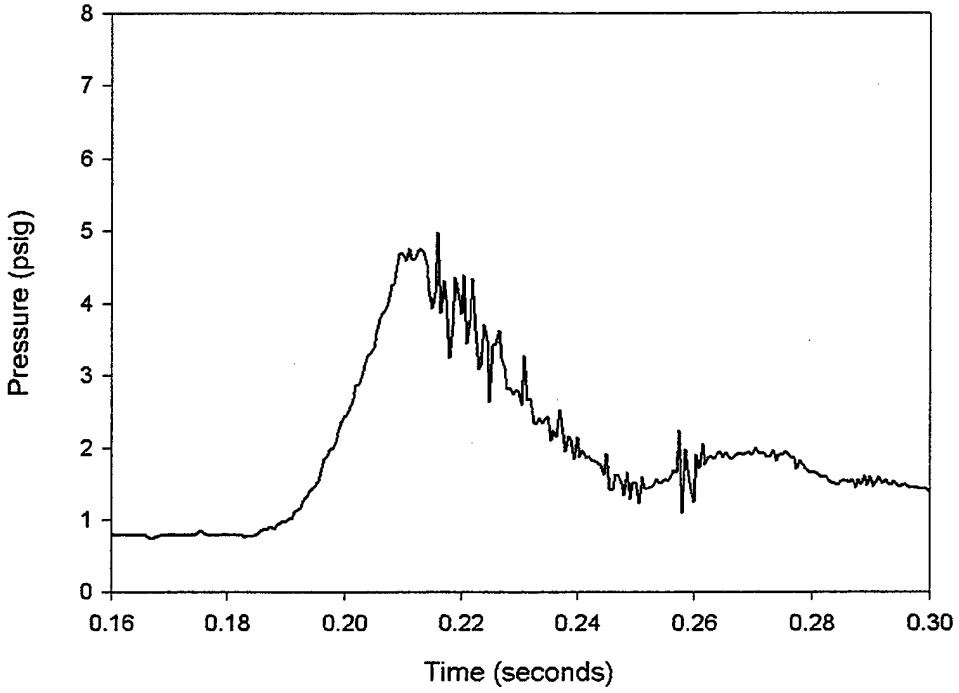

Figure 42. Airbag Pressure Response for the Three Spring Check Valve, V=18.1 ft/sec

Examination of these figures shows that the airbag pressure pulses produced have the familiar triangular shaped appearance for the 21.1 ft/sec and 18.1 ft/sec cases. The exception is in the shape of the pressure response using the single spring check valve undergoing the 23.2 ft/sec impact. For this case the pressure pulse displayed in Fig. 37, appears to dwell for a 20 millisecond interval, at a quasi-constant level before returning to zero. The shape of the resulting pressure response takes on a somewhat more rectangular appearance.

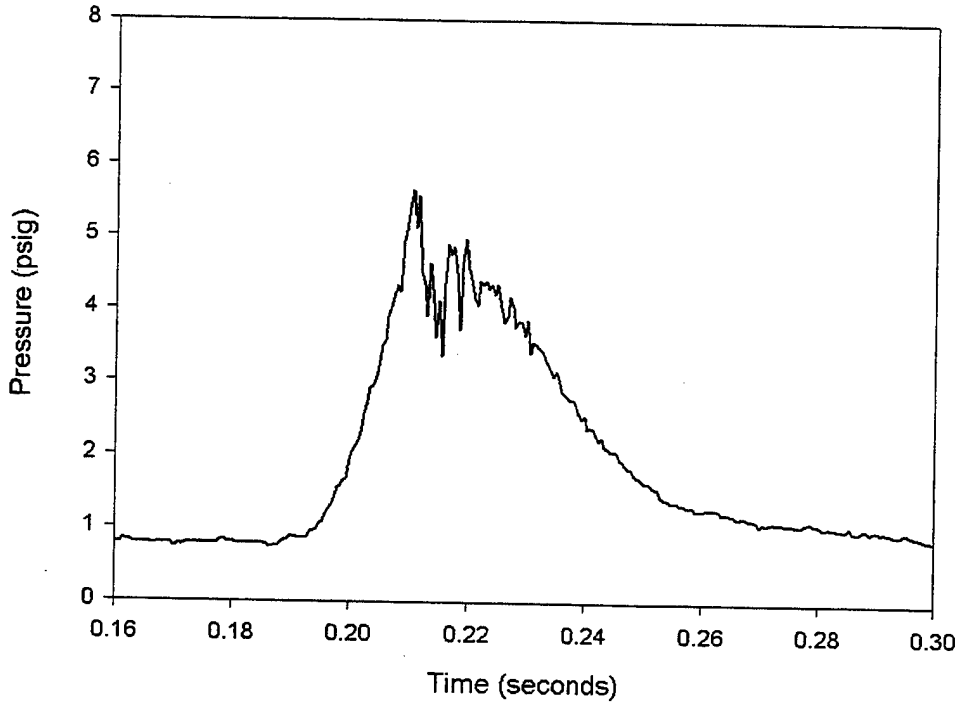

Figure 43. Airbag Pressure Response for the Steel Cover Blowout Vent, V=23.2 ft/sec

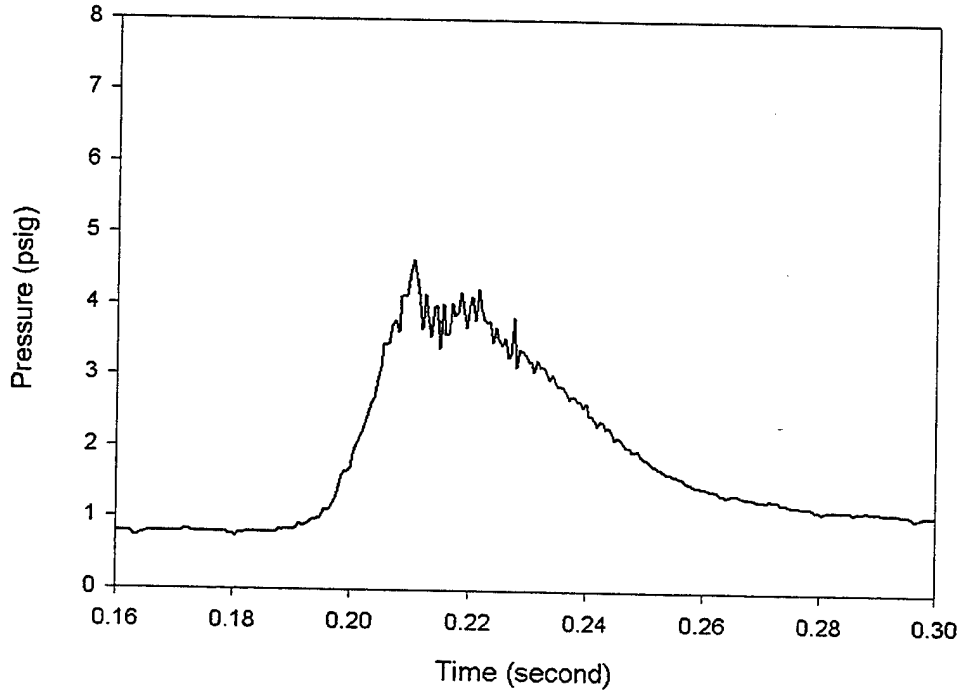

Figure 44. Airbag Pressure Response for the Steel Cover Blowout Vent, V=21.1 ft/sec

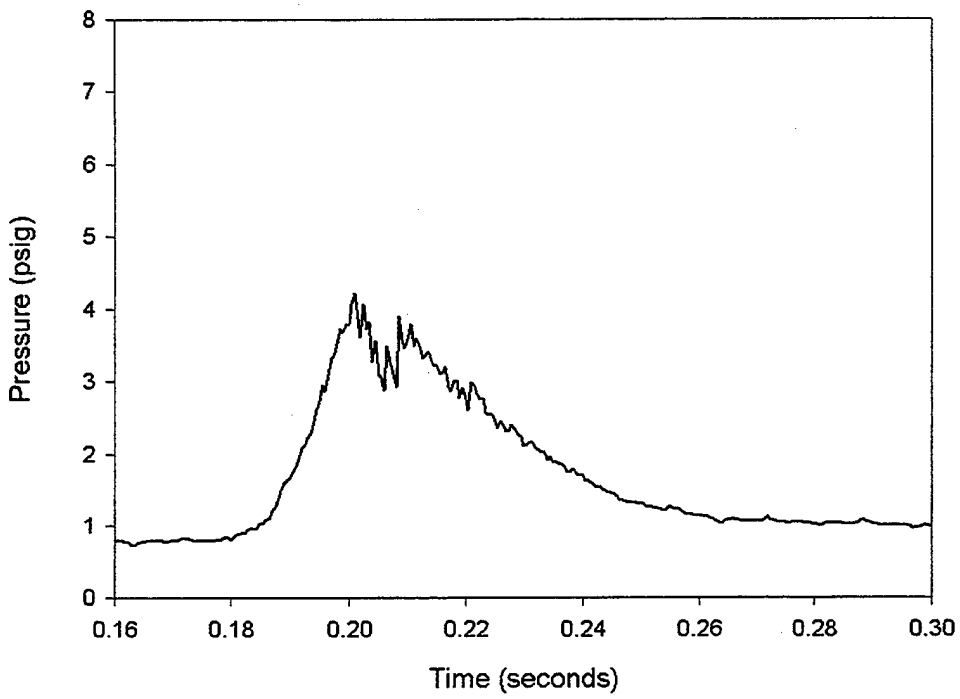

Figure 45. Airbag Pressure Response for the Steel Cover Blowout Vent, V=18.1 ft/sec

Experiments were conducted to measure the pressure response of the airbag system generated by free drop testing using the blow-out style vents. The first set of experimental results using the blow-out style vent constructed from the circular steel cover placed over the magnet valve seat are found in Fig. 43, Fig. 44, and Fig. 45. These experiments were carried out at the same 23.2 ft/sec, 21.1 ft/sec & 18.1 ft/sec impact velocity levels.

The noise averaged peak pressure level was measured from the positive sloped side of the maximum pressure level for each of the impacts. The resulting noise averaged peak pressure levels were found to be 5.7 psig, 4.7 psig and 4.3 psig respectively. The results of the experiments performed using the magnetic valve unconstrained stem and seat combination to produce the blow-out style venting appear in Fig. 46, Fig. 47, and Fig. 48 respectively.

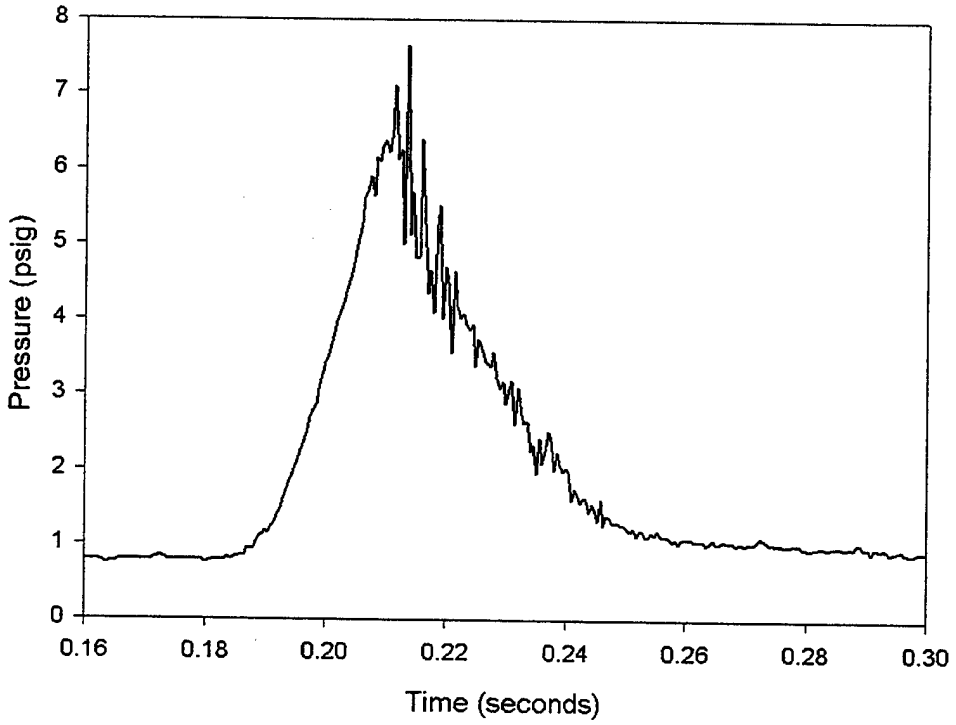

Figure 46. Airbag Pressure Response for the Free Poppet Blowout Vent, V=23.2 ft/sec

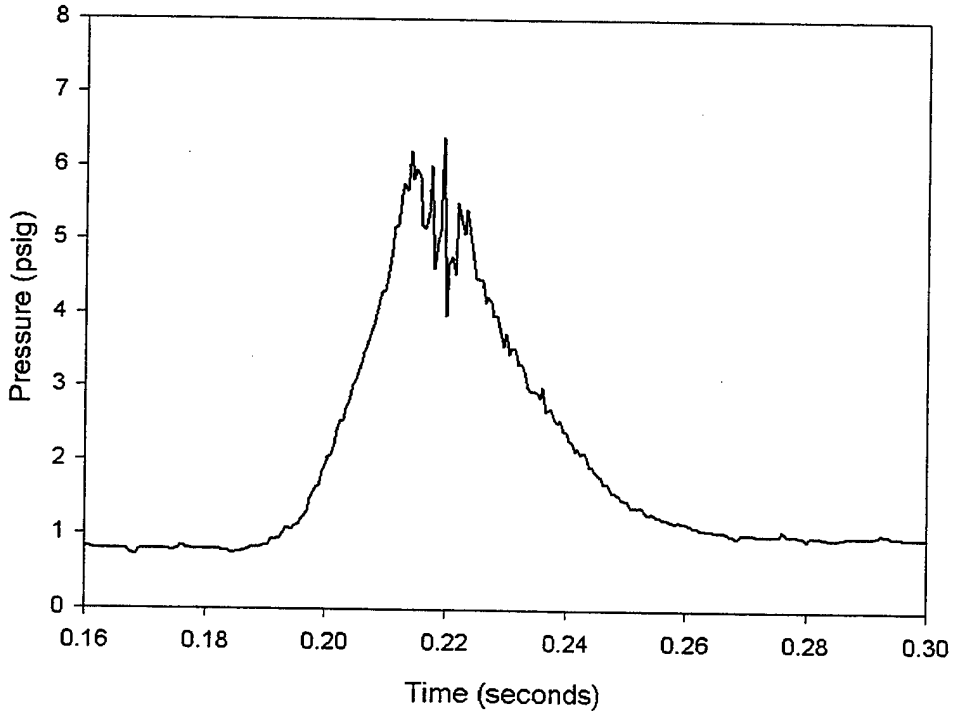

Figure 47. Airbag Pressure Response for the Free Poppet Blowout Vent, V=21.1 ft/sec

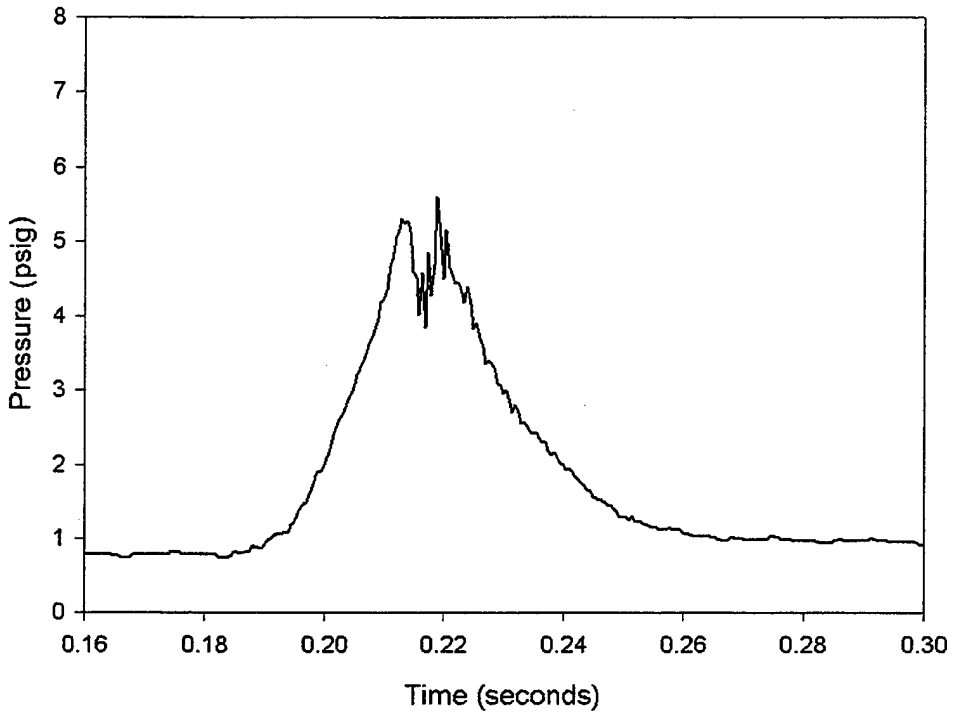

Figure 48. Airbag Pressure Response for the Free Poppet Blowout Vent, V=18.1 ft/sec

The noise averaged maximum pressure levels for this set of impacts was found to be 6.5 psig, 6.3 psig and 5.4 psig. This configuration of the blowout vent compressed the air within the airbag to higher peak pressure levels, then was previously obtained using the circular steel cover configuration. The time dependent pressure response produced by the blow-out vent configured using the stem and seat components has a greater magnitude than those produced using the steel circular cover for each of the respective impact velocities. The pressure pulses created using the blowout style vents also appears triangular shaped with respect to time.

In order to have a baseline of pressure response to compare and contrast the effects of using a blowout style vent, a set of experiments on a fixed open 9.62 in^2 vent had to be performed. Results of drop testing the scale model airbag system with a fixed 3.5" diameter orifice for the 23.2 ft/sec, 21.1 ft/sec and 18.1 ft/sec velocity impacts are contained in Fig. 49, Fig. 50, and Fig. 51.

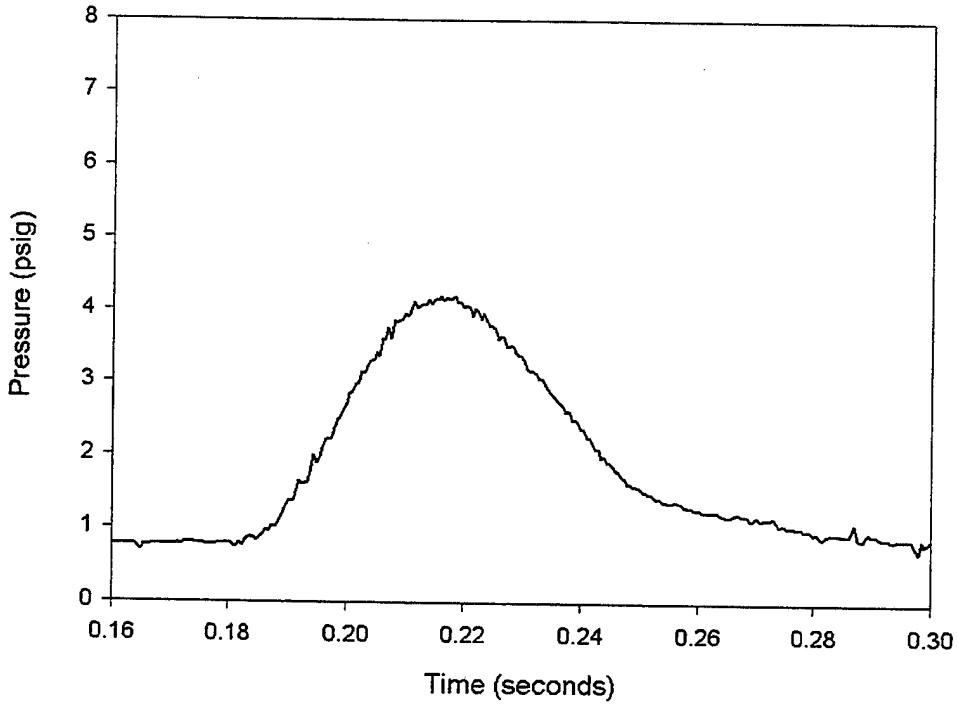

Figure 49. Airbag Pressure Response for a 9.62 in^2 Fixed Open Vent, V=23.2 ft/sec

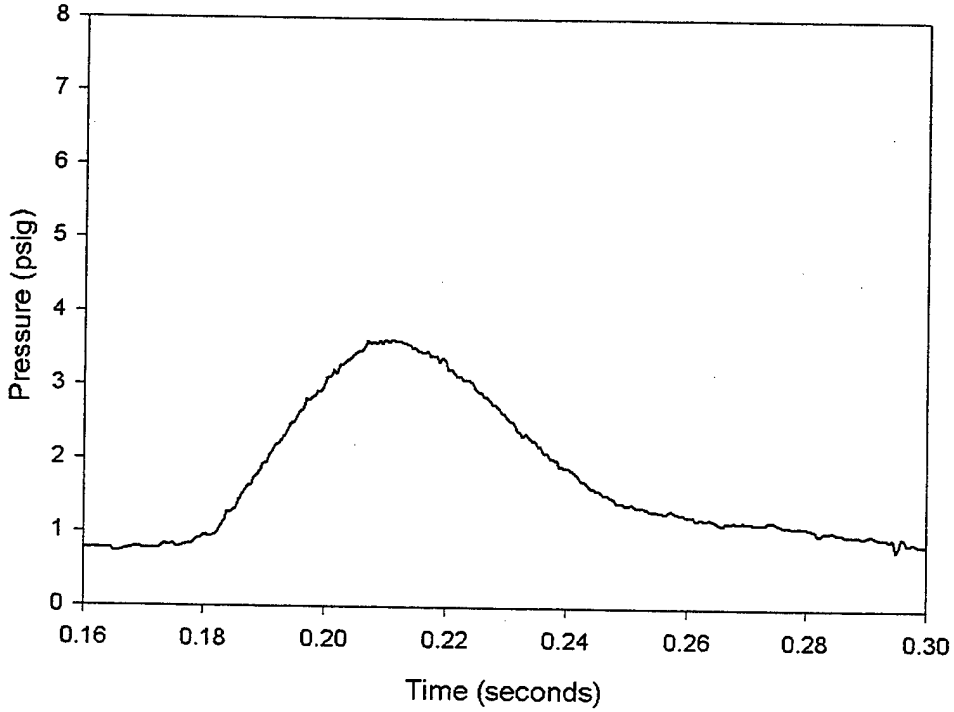

Figure 50. Airbag Pressure Response for a 9.62 in^2 Fixed Open Vent, V=21.1 ft/sec

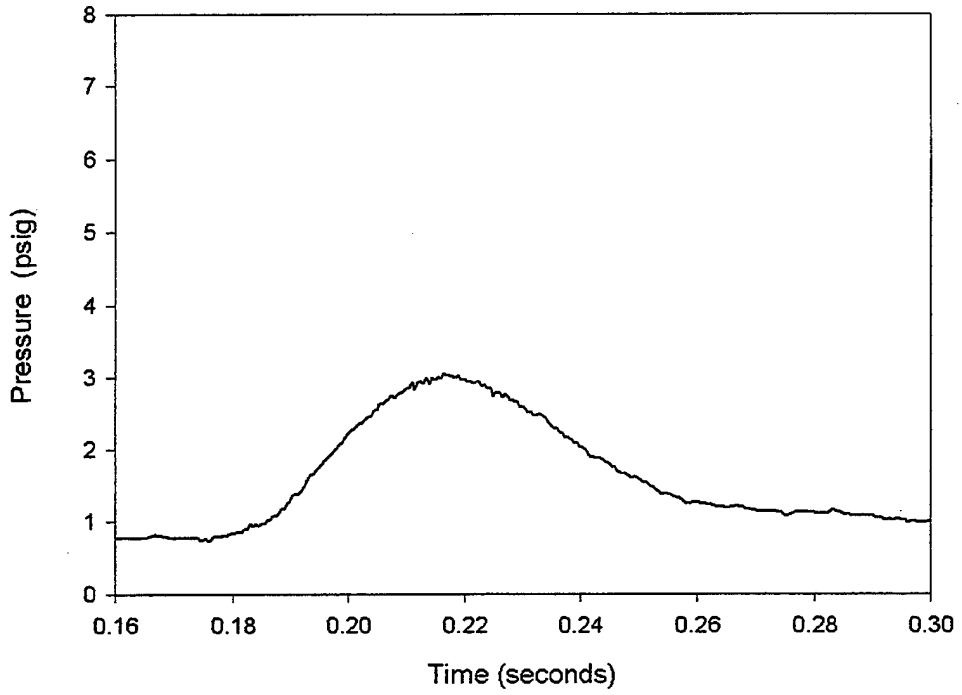

Figure 51. Airbag Pressure Response for a 9.62 in^2 Fixed Open Vent, V=18.1 ft/sec

The magnitude of the peak pressure levels attained during these experiments were measured as, 4.2 psig, 3.6 psig and 3.0 psig respectively. The general shape of the pressure response for these impacts is shown to have a smooth half sinewave character. The high frequency noise present in the airbag pressure response when using blowout style venting does not appear during these fixed open orifice compressions. The magnitude of the pressure response is found to be significantly lower than either of the responses that result using blowout style venting at each of the respective landing velocity levels. In general, this experimentation showed that the time rate of change of the pressure during the compression for an airbag that possesses a blowout style vent is greater than that achieved for its fixed open venting counterpart. The blowout style vent serves to elevate the airbag pressure to a higher maximum level in a shorter period of time, while not significantly changing the time duration of the pressure pulse.

Computer Model Validation and Verification

In order to validate the computer model a case by case comparison of similar airbag system impacts has to be conducted. The data gathered from the experiments can be used to verify the adequacy of the modeling process. In order to have a good model a large statistic of time dynamic responses must be verified. The experimental study to enable this was not conducted as part of this research process.

Since the scale model airbag used in the experimental evaluation of the check valves possessed a hemispherical dome shaped bottom the computer program was modified to accommodate this change in geometry. A subroutine was added to return the

value of the airbag internal volume as a function of airbag perpendicular compressed length. The differential equation representing the time rate of change of airbag pressure was rewritten to include this volume calculation as a function of airbag compressed length. A copy of the significant changes that were applied to the computer model source code can be found in Appendix D. The experimentally measured pressure that resulted from the airbag with the single spring check valve impacting the ground at 18.1 ft/sec was used as a test case to explore the computer models ability to predict the pressure response. The computer model was configured to calculate the pressure response from an 18.1 ft/sec impact of an airbag system connected to a spring loaded check valve. The check valve was described using three different sets of parameters to study the model behavior. The pressure response comparison that resulted from the study of effects of different model parameter changes is contained in Fig. 52.

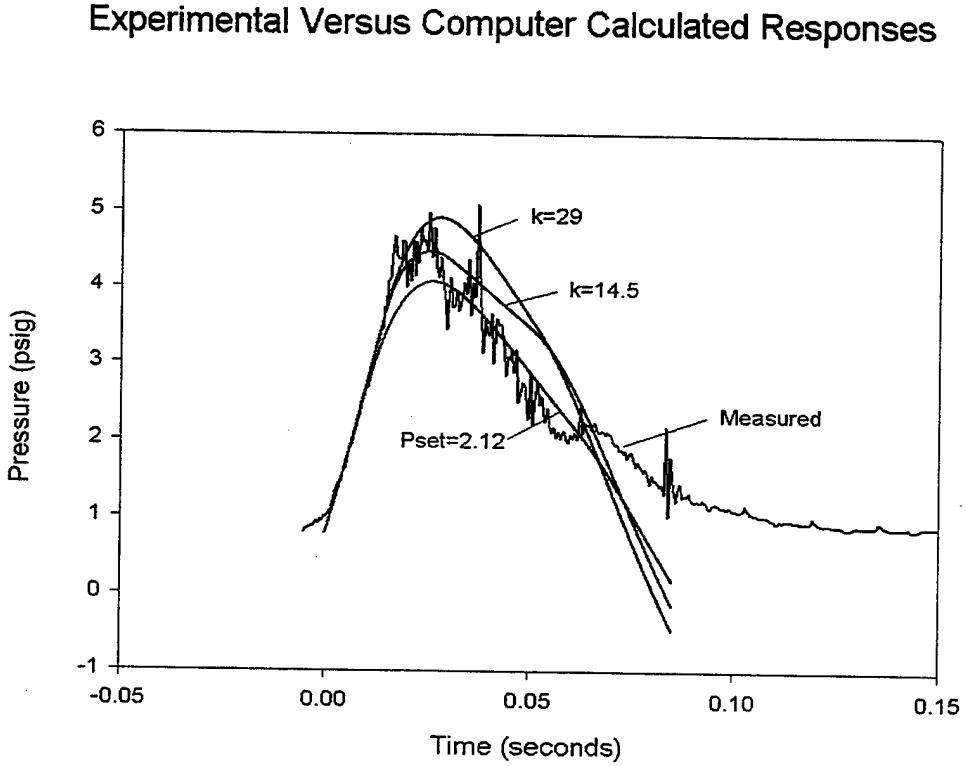

Figure 52. Single Spring Check Valve Experimental and Computer Simulated Airbag Pressure Responses V=18.1 ft/sec

The model was initially executed using a check valve that had a 14.5 lb/in spring rate and a 3.5 psig set point. The spring rate was then doubled to a 29 lb/in value while keeping the set point frozen at the 3.5 psig level. The model output showed that the effect this had on the pressure response was to better match the pressure pulses slope in the region of time found immediately after the occurrence of the peak in pressure. However, by increasing the spring rate, the magnitude of the pressure response is shown to increase significantly. An attempt to reduce the magnitude of the calculated pressure response was then accomplished by lowering the pressure set point level to a 2.12 psig level.

The computer model uses a discharge coefficient function to calculate the flow produced through an orifice in response to the pressure differential across the opening. The discharge coefficient function is composed of the sum of a two terms. The first term usually has a constant value of 0.9. The second term is hyperbolic, and consists of a fraction of the ratio of airbag pressure to ambient pressure usually given as 0.3*P. When the pressure ratio is unity the discharge coefficient function becomes 0.6, the nominal valve used to describe real world frictional losses most fluid flow experiences. The effect of increasing the second term of the discharge coefficient is to increase the pressure sensitivity of the discharge coefficient; this produces an increase in the magnitude of the computer calculated pressure response.

The computer model was executed with the parameters that model a 29 lb/in spring loaded check valve with a 1.5 psig set point and a pressure sensitive discharge coefficient of 0.6 attached to an airbag system impacting at 18.1 ft/sec. The results of the computer calculated pressure response superimposed on the experimentally measured response appear in Fig 53.

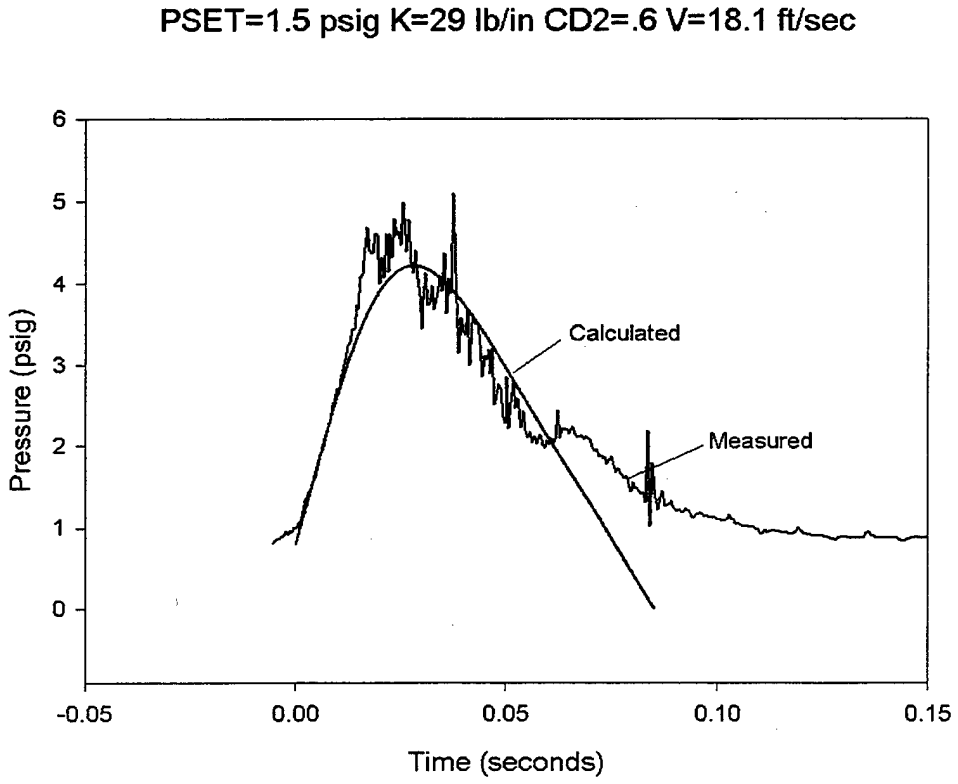

Figure 53. Single Spring Check Valve Computer Simulated Airbag Pressure Response compared with the Experimentally Measured Result, V=18.1 ft/sec

The match between the modeled an the actual pressure responses shown by this figure is quite good over the first 60 millisecond interval of the pressure pulse, after this point in time the calculated response becomes extremely divergent.

To confirm that the parameters chosen sufficiently described the system and produce a simulated pressure response, which is close to the response obtained by direct measurement, the model performance at another velocity level was examined. The computer model was executed using the same parameters to simulate the pressure response of the single spring check valve attached to the scale model airbag impacting the ground at 21.1 ft/sec. The results of superimposing the computer calculated pressure response on the experimentally measured pressure response for this higher impact velocity appear in Fig 54.

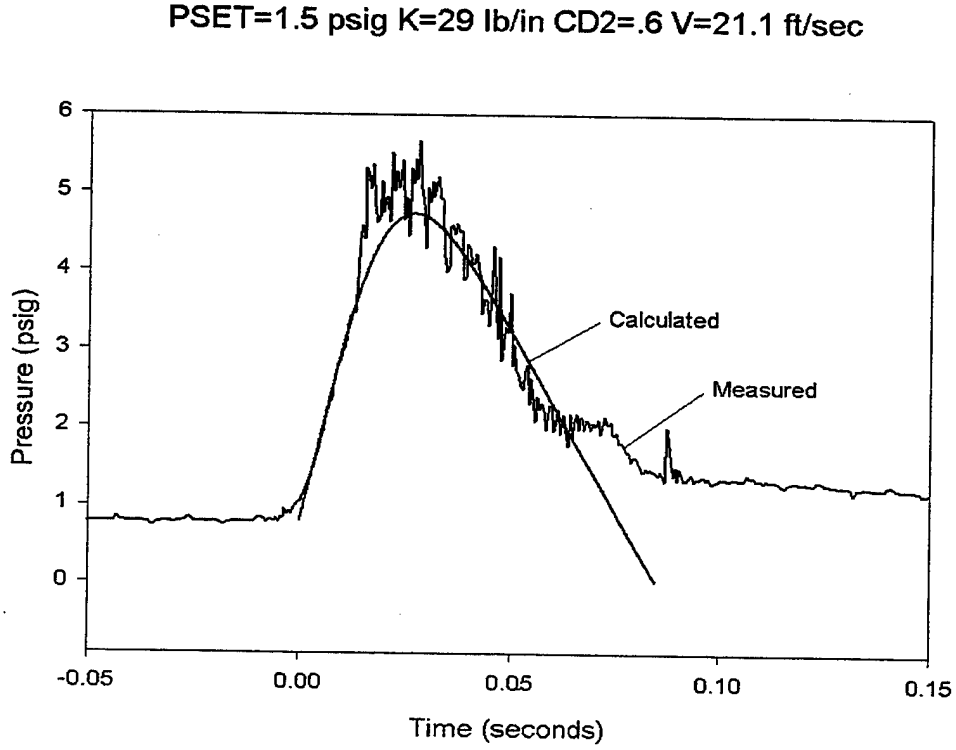

Figure 54. Airbag Pressure Response Comparison between the Computer Simulated Spring Check Valve and the Experimentally Measured Result, V= 21.1 ft/sec

The figure shows that the computer was able to reasonably predict the behavior of the airbag system at the higher impact velocity level.

The simple experiments conducted on the airbag system are somewhat of an abstraction from the velocity profiles produced in the airdrop real world. The model will never be able to predict the subtleties of the true behavior of a three dimensional airbag impact. Unless modified with case by case sets of parameters to serve as correction

factors, the model results can only be used to show the general shape and trend of the airbag system performance. The absolute value of the pressure response magnitude is impossible to predict exactly. The data for the simple vertical impacts shows that even after empirical adjustments to the model parameters are accomplished, errors as large as 0.5 psig can still exist, between the values of the measured and calculated airbag pressure responses. However, using the model to predict conservative response estimates serves as a valuable tool in the design and evaluation of various types of airbag venting hardware. The model allows an economical general study of the system performance.

Summary and Conclusions

Using spring loaded check valves as the vents on closed volume airbag systems has the effect of changing the shape of the pressure response curve. The usual shape of the pressure response obtained by discharging the airbag through a fixed vent sized at the full open valve area will appear as a smooth half sinewave. The effects of venting the same system through a spring loaded check valve will lower the magnitude of the pressure response, shorten the duration of the pressure pulse, and transform the pulse into a triangular shaped appearance.

If blowout style vents are used to release air from a closed volume airbag the pressure response generated by the impact is much higher than what is usually produced from a fixed vent of similar area. The time rate of change of the pressure experienced during the compression of an airbag that possess blowout style vents is greater than that achieved for airbags with constant open vents. The blowout style vent serves to elevate the airbag pressure to a higher maximum level in a shorter period of time, while not significantly changing the time duration of the pressure pulse.

The digital computer modeling of the airbag valve response can be used as a guide to predict its performance. Mathematically modeling the hardware response to an accurate degree involves using a blended combination of integrated device physics tuned by empirical response data. The process of obtaining the empirical response data is both costly and time consuming. Complete diagnostic study of the computer models performance would be the only way to verify that the mathematical representation of the system hardware was truly adequate.

This document reports research undertaken at the U.S. Army Soldier and Biological Chemical Command, Soldier Systems Center, Natick, MA, and has been assigned No. NATICK/TR-00/010 in a series of reports approved for publication.

REFERENCES:

1. Lee, C.K., " Methods for Improved Airbag Performance for Airdrop", Natick Technical Report TR-93/002, U.S. Army Natick Research, Development & Engineering Center, Natick, MA, October 1992.

2. Tseng, Han-Hsiu; Lee, C.K.; Lai, Francis S., "Experimental evaluation of Plastic Films for Use as Airbag Vent Blowout Patches.", Natick Technical Report TR-90/029, U.S. Army Natick Research, Development & Engineering Center, Natick, Ma, April 1990.

3. Browning, A. C., " A Vertical Approach to Air Bag Shock Absorber Design. ', Technical Note, No. Mech.Eng. 369, Royal Aircraft Establishment, Farmborough, England, February 1963.

4. Ross, Edward W., " Control Systems for Platform Landings Cushioned by Air Bags." , Natick Technical Report TR-88/021, U.S. Army Natick Research, Development and Engineering Center, Natick, MA, July 1987.

5. Lee, Calvin; Rosato, N., Lai, Fransis, "An Investigation of Improved Airbag Performance by Vent Control and Gas-injection.", AIAA PAPER 91-0892, American Institute of Aeronautics and Astronautics, January 1991.

APPENDIX A

FORTRAN COMPUTER SOURCE CODE

```
C $storage:2
C ABAG6.FOR
C
    DIMENSION DISP(1000),VEL(1000),ACC(1000),PRES(1000)
    DIMENSION FLOW(1000),TIME(1000),D(40)
    DIMENSION TA1(5),FA1(5)
C
C  PROGRAM TO CALCULATE PRESSURE, FLOW, & ACCELERATION OF
C     AIRBAGS
C  WRITTEN BY NICHOLAS ROSATO TO MODEL AIRBAG PERFORMANCE
C
    EQUIVALENCE (L,D(1)),(TEMP,D(2)),(DT,D(3)),(MASS,D(4))
    EQUIVALENCE (TO,D(5)),(H,D(6)),(B1,D(7)),(CD1,D(8))
    EQUIVALENCE (CD2,D(9)),(AMAX,D(10)),(AMN1,D(11)),(TR,D(12))
    EQUIVALENCE (TC,D(13)),(AMN2,D(14)),(TA1(1),D(15))
    EQUIVALENCE (FA1(1),D(20)),(BJ,D(25)),(GEN,D(26)),(VJIC,D(27))
    EQUIVALENCE (PSET,D(28)),(X1IC,D(29)),(X2IC,D(30)),(X3IC,D(31))
    EQUIVALENCE (P,D(32)),(SR,D(33)),(TD,D(34)),(DL,D(35)),(DI,D(36))
C
    REAL L,LAMBDA,MASS,MOUT,MDOTIN,MDINS
    CHARACTER Q,Q2
C
    DATA B1,CD1,CD2/34.667,0.9,0.3/
    DATA GAMMA,G,PA,MASS,P,DT/1.4,32.2,14.7,37.267,1.,8.5E-5/
    DATA R,TEMP,TO,L/53.3,60.,-.5,10./
    DATA H,XD1P,XD2P,XD3P/4.,0.,-32.2,0./
    DATA TC,TR,AMAX,AMN1,AMN2/1.0,0.,1.0,1.0,1.0/
    DATA J1,J2,BJ,GEN,VJIC,PSET/500,750,-1.0,-1.,-1.,15./
    DATA TA1(1),TA1(2),TA1(3),TA1(4),TA1(5)/0.,.035,.085,.1,1./
    DATA FA1(1),FA1(2),FA1(3),FA1(4),FA1(5)/0.,0.,.825,0.,0./
    DATA X1IC,X2IC,X3IC/4.,-28.,1./
    DATA SR,TD,DL,DI/14.5,.975,5.5,3.5/
C
C  THE OUTPUT DATAFILES NAMED  ABAG.DAT & JUNK  SHOULD NOT
C  EXIST  PRIOR TO THE EXECUTION OF THE PROGRAM
    OPEN(16,FILE='ABAG.DAT',STATUS='UNKNOWN')
    OPEN(14,FILE='JUNK',STATUS='UNKNOWN')
C
C
    WRITE(*,1)
  1 FORMAT(10X,'SIMULATION IN PROGRESS')
  2 WRITE(*,3)
```

```
    3 FORMAT(5X,' Do you wish to change any data?')
      READ(*,4) Q
    4 FORMAT(A1)
      IF(Q.EQ.'N') GO TO 10
      WRITE(*,*) 'Enter the number of changes.'
      READ(*,*) NC
      DO 9 IJ=1,NC
      WRITE(*,5)
    5 FORMAT(5X,' Enter the subscript & value of the variable')
      READ(*,*) K,D(K)
      WRITE(*,8) K,D(K)
    8 FORMAT(5X,'D(',I2,')=',F10.5)
    9 CONTINUE
      GO TO 2

   10 X2=-SQRT(2.*G*L)
      X1=H
      X3=P
C       X3: PRESSURE RATIO Pbag/Patm X2: VELOCITY dH/dt
C       X1: AIRBAG HEIGHT

      IF(VJIC.GT.0.) X1=X1IC
      IF(VJIC.GT.0.) X2=X2IC
      IF(VJIC.GT.0.) X3=X3IC
C
C     Density with LBM/G slugs/ft3 units
      RHO=(PA*144.)/(R*(TEMP+460.)*G)
      A1=(2.0*GAMMA)/(GAMMA-1.0)
      A2=1.-(1./GAMMA)
      A3=(GAMMA+1.)/(2.*GAMMA)
      C=SQRT(GAMMA*G*R*(TEMP+460.))
      WRITE(*,*) '   ACTIVE DATA SET'
      WRITE(16,*) '   CURRENT INPUT DATA SET'
      WRITE(*,*) ' '
      WRITE(16,*) ' '
      DO 20 KP=1,36,4
      WRITE(*,11) KP,D(KP),KP+1,D(KP+1),KP+2,D(KP+2),KP+3,D(KP+3)
      WRITE(16,11) KP,D(KP),KP+1,D(KP+1),KP+2,D(KP+2),KP+3,D(KP+3)
      WRITE(16,*) ' '
      WRITE(*,*) ' '
   11 FORMAT(3X,4('D(',I2,')=',E12.5,1X))
   20 CONTINUE
```

```
      WRITE(*, *)X1,X2,X3,RHO
      WRITE(*,*)B,LAMBDA,C,A1
      WRITE(*,*) '.....'
C     PAUSE
      WRITE(*,22)
   22 FORMAT(5X,'Do you want QWAN data displayed?')
      READ(*,23) Q2
   23 FORMAT(A1)
C
C
      DO 100 J=1,1000
      CD=CD1-CD2/P
      T=T+DT
C         AREA SCHEDULES A(t)
      CALL AREA(AOR,AMAX,AMN1,AMN2,TO,TR,TC,DT,J)
      PBLOW=(PSET/PA)+1
      PV=PA*(P-1.0)
      IF(BJ.GT.0..AND.P.LT.PBLOW) AOR=AMN1
C     IF(BJ.GT.0..AND.P.GE.PBLOW) AOR=AMAX
C         LAST TWO IF STATEMENTS REPRESENT IDEAL CHECK VALVE
C     IF(BJ.GT.0..AND.P.LT.PBLOW.AND.AOR.GE.AMAX) AOR=AMAX
C         LAST THREE IF STATEMENTS REPRESENT IDEAL BLOW OUT PATCH
      IF(BJ.GT.0..AND.P.GE.PBLOW) CALL CKVALVE(AOR,PV,SR,TD,PSET,DL,DI)
C      WRITE(*,*) J,BJ,P,PBLOW,AOR
C
      CALL LFGEN(TA1,FA1,5,T,F)
      MDINS=F
C     MDINS (slug/sec)
      IF(GEN.LT.0.) MDINS=0.
      MDOTIN=MDINS*G
C     MDOTIN (lb/sec)
C     WRITE(*,*) J,F,GEN,MDINS,MDOTIN
      B=B1-AOR
      LAMBDA=AOR/B
      BETA=P**(1./GAMMA)
      EPSILON=(1./GAMMA)*P**((1./GAMMA)-1.)
C
      CALL ALP(P,A1,A2,A3,ALPHA,CD)
      QWAN1=(-BETA*X2)/(X1*EPSILON)
      QWAN2=(MDINS/(RHO*B*EPSILON*X1))
      QWAN3=-LAMBDA*(C/SQRT(GAMMA))*ALPHA
      MOUT=-QWAN3*B*RHO*G
      XD1=X2
```

```
      XD2=(B*PA*144/MASS)*(X3-1.)-G
      XD3=-
     1(LAMBDA*(C/SQRT(GAMMA))*ALPHA+BETA*X2)/(X1*EPSILON))+QWAN2
      CALL INTEG(X1,DT,XD1,XD1P)
      CALL INTEG(X2,DT,XD2,XD2P)
      CALL INTEG(X3,DT,XD3,XD3P)
C
C     WRITE(14,24) T,XD3,QWAN1,QWAN2,QWAN3
C     WRITE(14,24) AOR,MDINS,MOUT,X1,X2
C     WRITE(14,24) RHO,ALPHA,BETA,EPSILON,XD2
C
   24 FORMAT(1X,5(E12.5,2X))
      IF(Q2.EQ.'N') GO TO 25
      IF(J.EQ.J1.OR.J.EQ.J2) WRITE(*,*) J,MDINS,QWAN1,QWAN2,QWAN3
      IF(J.EQ.J1.OR.J.EQ.J2) WRITE(*,*) ALPHA,BETA,EPSILON,LAMBDA,X1,X2
      IF(J.EQ.J1.OR.J.EQ.J2) PAUSE
C
   25 P=X3
      IF (P.LT.0.) WRITE(*,*)'PRESSURE MISCALC'
      PBAG=PA*P
      PRES(J)=PBAG-PA
      DISP(J)=X1
      VEL(J)=X2
      ACC(J)=XD2/G
      Z1=A1*C*C/GAMMA*((P**A2)-1.)
      IF (Z1.GE.0.) FLOW(J)=SQRT(Z1)
      IF (Z1.LT.0.) WRITE(*,*)'FLOW MISCALC'
      TIME(J)=J*DT
      WRITE(16,30) TIME(J),ACC(J),PRES(J),FLOW(J),DISP(J),VEL(J)
      WRITE(14,31) TIME(J),PRES(J),AOR,XD3,XD2,XD1
   30 FORMAT(6(1X,F10.5))
   31 FORMAT(F8.5,5(1X,E11.5))
  100 CONTINUE
      WRITE(*,201)
  201 FORMAT(5X,'DATA STORED IN ABAG.DAT')
C
      CLOSE(16,STATUS='KEEP')
      CLOSE(14,STATUS='KEEP')
C
      TMX=TIME(1000)
      P=1.
      XD1P=0.0
      XD2P=-32.2
```

```
      XD3P=0.
  500 CONTINUE
      STOP
      END
C
      SUBROUTINE INTEG(Z,DT,ZD,ZDP)
      Z=Z+(DT/2.)*(ZD+ZDP)
      ZDP=ZD
      RETURN
      END
C
      SUBROUTINE ALP(P,A1,A2,A3,ALPHA,CD)
      IF (P.LT. 1.894) THEN
      Z1=A1*((P**A2)-1.)
      IF(Z1.GE.0.) ALPHA=SQRT(Z1)*CD
      IF(Z1.LT.0.) WRITE(*,*)'ALPHA MISCALC'
      ENDIF
      IF (P.GE.1.894) THEN
      ALPHA=ALPHA*1.894*(P/1.894)**A3
      ENDIF
      RETURN
      END
C
      SUBROUTINE AREA(AOR,AMAX,AMN1,AMN2,TO,TR,TC,DT,J)
      T=DT*J
      S1=(AMAX-AMN1)/(TR-TO)
      S2=(AMN2-AMAX)/(TC-TR)
      IF(T.LE.TO) AOR=AMN1
      IF(T.GT.TO .AND. T.LE.TR) AOR=S1*(T-TO)+AMN1
      IF(T.GT.TR .AND. T.LE.TC) AOR=S2*(T-TR)+AMAX
      IF(T.GE.TC) AOR=AMN2
C     WRITE(*,*) T,AOR
C     PAUSE
      RETURN
      END
C
      SUBROUTINE LFGEN(X,Y,N,XIN,YOUT)
      DIMENSION X(N),Y(N),SLP(5),OFS(5)
      NINT=N-1
      DO 10 J=1,NINT
      IF(XIN.LT.X(J+1).AND.XIN.GT.X(J)) I=J
      IF(XIN.EQ.X(J)) I=J
   10 CONTINUE
```

```
SLP(I)=(Y(I+1)-Y(I))/(X(I+1)-X(I))
OFS(I)=Y(I)-SLP(I)*X(I)
YOUT=SLP(I)*XIN+OFS(I)
RETURN
END


SUBROUTINE CKVALVE(AOR,P,SR,TD,PSET,DL,DI)
DATA PIE,DS,RO,TL/3.1416,.25,.03704,.25/
AI=(PIE/4.)*DI*DI
VL=(PIE/4.)*DL*DL*TL
WL=RO*VL
FP=AI*PSET
DX=FP/(3.*SR)
F=P*AI
X=(WL+F-3.0*SR*DX)/(3.*SR)
AOR=X*(PIE*DL-3.*DS)/144.
IF((X+DX).GE.TD) AOR=(TD-DX)*(PIE*DL-3.*DS)/144.
RETURN
END
```

List of Symbols

L	Drop Height of Airbag Platform (ft)
TEMP	Ambient Temperature (^{o}F)
DT	Simulation Time Increment (seconds)
MASS	Mass of the Payload (slugs)
TO	Point in time corresponding to AMN1 (seconds)
H	Airbag height (ft)
B1	Airbag Cross-sectional Area (ft^2)
CD1	Airbag orifice coefficient
CD2	Airbag orifice coefficient
AMAX	Orifice area when simulated time equals TR(ft^2)
AMN1	Orifice area when simulated time is less than or equals TO (ft^2)
TR	Point in time corresponding to AMAX (seconds)
TC	Point in time corresponding to AMN2 (seconds)
AMN2	Orifice area when simulated time is exceeds or equals TC (ft^2)
TA1()	Flow Table time array
FA1()	Output flow level array corresponding to TA1( ) time points
BJ	Subroutine Switch (BJ > 0.) makes orifice behave as an ideal blow out patch

GEN Program switch (GEN < 0.) shuts off input mass rate of flow source
VJIC Program Switch (VJIC > 0.) loads initial conditions X1=X1IC, X2=X2IC, X3=X3IC
PSET Exhaust Valve Vent Pressure Level (psig)
X1IC Initial value of airbag displacement (ft)
X2IC Initial value of velocity (ft/sec)
X3IC Initial value of airbag pressure ratio (Pbag/Pambient)
P Ratio of internal bag pressure to ambient pressure

MODEL SUBROUTINE OPERATING INSTRUCTIONS

The model contains a SUBROUTINE AREA that allows the user to schedule the airbags exhaust area as a function of time. The subroutine was originally designed to behave like a classical signal limiter. The subroutine can produce step or ramp functions in vent exhaust area as a function of time. It allows the study of variable open loop control of exhaust vents.

Only two configuration modes of the area subroutine were used during the modeling. The first mode was used to describe a constant fixed vent area of a simple airbag landing. In order to achieve this state the variables AMN1, AMN2, and AMAX are all set equal to the same value. The subroutine was originally written to describe an orifice changing shape as a function of time. In this normal state the subroutine sets the exhaust area to constant levels between three points in time. The AMAX, AMN1, and AMN2 levels of output area correspond to the TO, TR and TC points in time.

IDEAL BLOW OUT PATCH AND CHECK VALVE MODELING

In order to model the response of a check valve that is frictionless, massless with the ability to accelerate close in zero time, two commented IF Statements have to be enabled and the code recompiled before execution. The If Statements change the vent area either to a full open or full closed value depending on the level of the pressure ratio. If the pressure ratio is above the PBLOW level the valve opens, if below the level it closes. The only difference between an ideal blow out patch and an ideal check valve is once the blow out patch ruptures the area must remain open during the simulation.

To simulate the action of an ideal blow out patch rupturing when the internal bag pressure exceeds a given threshold three commented Fortran statements have to be enabled and the code recompiled and executed. The case that models a blow out patch as an ideal step change in flow exhaust area requires that the variable BJ must be positive. (BJ > 0.) In addition to enable this type of response, the burst pressure threshold has to be prescribed in the variable PSET, and the AMAX & AMN1 levels of area need definition.

The blow out patch model consists of the AMN1 being a small near zero value representing some leakage effective area typically .001 ft^2. The final blow out area value is contained within AMAX.

The internal gage pressure within the airbag must exceed the value contained in PSET for the IF Statements to switch the flow area from AMN1 to the full open area AMAX. The PSET is specified as a gage pressure (i.e. 1.0, 2.0 3.0 psig) for a typical simulation. A true representation of the physics of the blow out patch involves more detailed modeling. To accomplish this the feature enabling an area-time rupture to occur as a function of internal airbag pressure. A=A(P, t) requires some knowledge of blow out patch real world performance.

MASS INJECTION OPERATION

The SUBROUTINE LFGEN was designed to perform a single variable mapping of output flow level as a function of input time. The mass injection of air into the airbag is accomplished by setting the GEN parameter greater than zero. When GEN is positive a linearly interpolated mass rate of flow time history is inserted into the airbag volume. The mass rate of flow addition to the dimensionless version of the continuity equation that incorporates Bernoulli's steady state energy equation was used to define the bag's time rate of change dimensionless pressure reaction.

To enable the mass rate of air into the airbag a mass time profile has to be defined using a table look-up process. The table contains five points in time defining the continuously interpolated flow curve. The linear vector arrays TA1 & FA1 can be changed to accommodate various shapes of flow. The most effective profile was one that ramps or linearly increases with time. This models an ideal supply source of mass flow.

The default setting are contained within the two equivalence arrays TA1() and FA1(). The function map has typical units of time as the absyssa in real seconds while the ordinate or input mass rate of airflow has units of [slug/sec] since the model density is in $lbm/ft^3/g$ or $slug's/ft^3$.

SUBROUTINE CKVALVE

The subroutine is used to simulate a linear spring loaded check valve made from compression springs. The model was originally made to simulate the three spring design but can be used in general by applying one third the value of spring rate SR to simulate a single spring. The three spring design possessed ¼ inch diameter studs with a plastic valve. The default values for the density of the valve material and the stud diameter are contained in the subroutine data statement (RO & DS).

P	Pressure applied to the valve (psi)
SR	Spring Rate (lb/inch)
AOR	Output Flow Area (ft^2)
PSET	Valve opening Set point pressure level (psi)
DL	Diameter of Valve (inch)
DI	Diameter of valve seat orifice (inch)

Figure 18B contains a plot of a computer simulated spring loaded check valve area output response as a function of pressure for various spring rates. The simulation was performed using a 5.5 inch diameter valve. Examination of plot shows that soft springs those that possess smaller spring rates yield larger curtain flow areas for the same applied valve pressure. A plot of exit area as a function of position shows that springs with long free lengths under large differences in total spring deflection and solid height produce larger flow area due to the increased deflection possible using these springs.

The check valve model was based upon the assumption that the pressure applied to the valve was equal to the pressure upstream of the valve seat orifice. A force balance using this assumption was applied to the valve as a free body. The exit flow area was essentially the diameter of the valve minus the projected area of the three supporting studs. The model pressure was not adjusted to incorporate the effect due to the velocity change of the fluid.

By increasing the valve diameter the curtain flow area can be increased. The model does not account for the decrease in applied pressure at the underside of the valve as a function of vertical distance from the valve seat orifice. Frictional effects such, as loss coefficients through the opening and the bending of the flow through a 90-degree turn are not taken into account in this crude ideal check valve model.

This Page Intentionally Left Blank

APPENDIX B

CLOSED VOLUME AIRBAG COMPRESSION ANALYSIS

A polytropic compression of a closed volume Airbag, subjected to 70% change in original volume. An adiabatic process both frictionless and thermodynamically reversible for pure air or nitrogen can be evaluated using the same k=1.4 specific heat ratio.

$$PV^k = const = P_iV_i^k = P_i(AS)^k = P_fV_f^k$$

$$V_i = AS$$

$$V_f \equiv .3 * AS$$

$$P(V) = P_iV_i^k(V)^{-k}$$

$$P(V_f) = P_i(AS)^k(.3SA)^{-k} = 5.395 * P_i$$

$$Work = \int PdV = \int P_i(AS)^k V^{-k} dV$$

$$Work = P_i(AS)^k \int_{V_i}^{V_f} V^{-k} dV = [\frac{V^{-k+1}}{-k+1} P_iV_i^k]\Big|_{Vi}^{Vf} = \frac{V_f^{1-k} - V_i^{1-k}}{1-k}(P_iV_i)^k$$

$$Work = \frac{(.3SA)^{1-k} - (AS)^{1-k}}{1-k} P_i(AS)^k = \frac{(SA)^{1-k}(.3^{1-k} - 1)}{1-k} P_i(AS)^k$$

$$Work = \frac{P_iSA * (.3^{1-1.4})}{1-1.4} = -1.547 * P_i * S * A \qquad \text{Equation (I)}$$

The work done at the moving boundary for the ideal gas with a ratio of specific heats of 1.4.

The Average pressure over the assumed 70% volume change:

$$P_{av} = \frac{\int P(V)dV}{\int dV} = \frac{-1.547 * P_i * SA}{(.3-1.0)SA} = 2.209 * P_i \qquad \text{Equation (II)}$$

Energy Balance for the closed volume Airbag undergoing the polytropic compression:

$$\frac{1}{2} * \frac{W}{g}(2gh) + W(c+S) - 1.547P_i * SA = W(c+.3S) \qquad \text{equating terms yields,}$$

$$Wh + WS = 1.547P_i * SA + .3WS$$

APPENDIX B (Cont'd)

Solving for the initial value of pressure: $$P_i = \frac{1}{1.547}\frac{W}{A}\left(\frac{h}{S} + .7\right)$$ Equation (III)

Equation (III) represents the amount of initial pressure required to stop a payload of weight W using an airbag of crossectional area A, and stroke S. The airbag must undergo an adiabatic compression and consume 70% of its initial stroke.

A mass injection airbag system with initially closed vents that is charged with compressed nitrogen or air prior to ground impact was analyzed. The analysis is a simplified calculation based upon the conservation of energy applied to the airbag mass system found in the figure below. The energy available at ground contact when the airbag system is allowed to free fall from a drop height h above the ground consists of two components. The first being the kinetic energy of motion where the velocity is specified by $\sqrt{2gh}$.

The second term consists of the potential energy of the vertical position of the

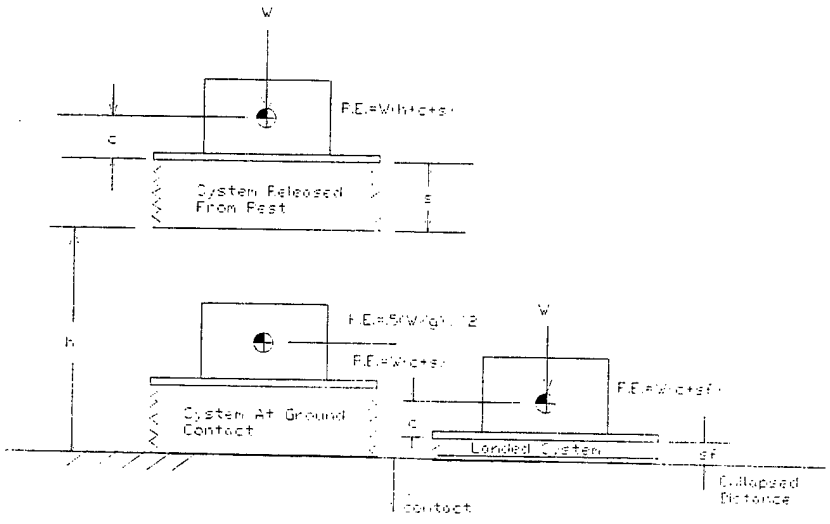

weight above the bag. The sum of this energy must be equated to the pressure-volume work the bag performs and the residual potential energy of the bag in the collapsed position.

APPENDIX B (Cont'd)

The final collapsed distance was chosen to be 30% of the original airbag height. This would range from 10.8 inch to 5.4 inches for airbags with 3 ft to 1.5 ft heights The energy balance provides an average pressure requirement to effectively absorb the vertical energy in pressure-volume changes. Equation (III) describes the relationship of initial pressure required to absorb the airbag systems landing energy. Equation (II) relates the average pressure of the polytropic compression process to the initial airbag pressure charge. Combining both of these equations yield the average airbag pressure produced during the compression.

$$P_{av} = \frac{W(h+.7S)}{.7AS} \qquad \text{Equation (IV)}$$

Equation (IV) shows that the average pressure required to stop a payload is inversely proportional to the airbags crossectional area. The equivalent g-force applied to the payload due to this pressure is calculated by dividing the force produced by the product of the pressure times the airbag crossectional area by the payloads weight.

$$g_{av} = \frac{P_{av} * A}{W} = \frac{h+.7S}{.7S} = 1 + \frac{h}{.7S}$$

Using the equations formulated for the closed volume airbag analysis, landing responses for two different airbag configurations were studied. A comparison between a single rectangular 8 ft long by 4 ft wide (32 ft^2) airbag, and two 4 ft diameter round airbags each having a 12.566 ft^2 area, for a total platform contact area of 25.1 ft^2 was performed. The drop height chosen was 13 ft which produces a 28.9 ft/sec vertical impact speed. This is the typical terminal velocity range used for airdrop cargo delivery. The average value of pressure generated was calculated using equation (IV). Table (A) contains the results for various airbags heights for both the 1000 lb and 2000 lb payload weight cases.

Height	1000 Lb	1000 Lb	2000 Lb	2000 Lb
Ft	Rect. Psi	Cir. Psi	Rect. Psi	Cir Psi
3	1.56	1.987	3.121	3.974
2.5	1.829	2.329	3.658	4.658
2	2.232	2.842	4.464	5.684
1.5	2.904	3.697	5.808	7.395

This Page Intentionally Left Blank

APPENDIX C

COMPUTER SIMULATION DERRIVATION

The basis of the Fortran Source Code was originally derived by Powell found in reference [3]. The assumptions made were that the airbag remains cylindrical during impact and the vent area stayed constant. The continuity equation was applied to the airbag as a system.

$$\frac{dM}{dt_{sys}} = \frac{\partial M}{\partial t_{C.V.}} + \int_{c.s.} \rho V_N dA \ , \quad \text{Continuity Equation}$$

$$-\frac{d(\rho_{bag} hB)}{dt} = \rho_{orif} \cdot a \cdot q_{orif} \cdot C_D$$

Combing continuity with the Adiabatic Relationship between pressure and density,

$$P_{bag} = \rho_a \cdot (\frac{P_{bag}}{P_a})^{\frac{1}{\gamma}}$$

inside the airbag in relation to the outside ambient conditions. Yielded an orifice flow equation expressing the time rate of change of the ratio of bag internal pressure to the ambient pressure outside the bag.

$$\frac{d(\frac{P_{bag}}{P_{atm}})}{dt} = \frac{dP}{dt} = -\frac{(\frac{\rho_{or} a}{\rho_a B} q C_D + P^{\frac{1}{\gamma}} \frac{dh}{dt})}{\frac{h}{\gamma} P^{\frac{1}{\gamma}-1}}$$

Applying Bernoulli's equation for a steady streamline solving for q_{or};

$$\frac{\gamma}{\gamma-1} \cdot \frac{P_{bag}}{\rho_{bag}} = \frac{\gamma}{\gamma-1} \cdot \frac{P_{or}}{\rho_{or}} + \frac{1}{2} \cdot q_{or}^{\ 2}$$

then simplifying and collecting terms, formulates the nonlinear differential equation relating the time rate of change of the pressure ratio as a function of that pressure ratio and the velocity of the airbags collapsing height.

Equation (I)

$$\frac{dP}{dt} = -\frac{\frac{aC_D}{B}\cdot\sqrt{\frac{2\gamma}{\gamma-1}\cdot\frac{c^2}{\gamma}(P^{1-\frac{1}{\gamma}}-1)}+P^{\frac{1}{\gamma}}\cdot\frac{dh}{dt}}{\frac{h}{\gamma}\cdot P^{\frac{1}{\gamma}-1}}$$

Newtons second Law of motion was then applied to the payload mass being supported by the airbag:

$$\sum F = ma \text{, which resulted in,}$$

Equation (II)

$$-Mg + (P_{bag} - P_a)B = M\frac{d^2h}{dt^2}$$

Simultaneously solving Equations (I) and (II) with respect to time was the basis of the original airbag model. The model has since been coded into various computer programs in the quest to develop techniques to optimize and theoretically study the cushioning performance.

To study the phenomena of mass injection an additional term representing the velocity of the inflow must be added to the existing terms in Equation (I) numerator. This term is specified as: $-\frac{\frac{dm_{in}}{dt}}{\rho_{atm}\cdot B}$ The numerator being [slug/sec] of mass inflow, scaled by the product of atmospheric density in [slug/ft^3] multiplied by the airbag crossectional area in [ft^2] producing units of [ft/sec]. The addition of this term in the computer model allows gas-injection studies to be theoretically analyzed this results in Equation (IA). The equation accounts for both the inflow as well as efflux of mass into the airbag volume.

Equation (IA)

$$\frac{dP}{dt} = -\frac{\frac{aC_D}{B}\sqrt{\frac{2\gamma}{\gamma-1}\frac{c^2}{\gamma}(P^{1-\frac{1}{\gamma}})}+P^{\frac{1}{\gamma}}\frac{dh}{dt}-\frac{\frac{dm_{in}}{dt}}{\rho_{atm}\cdot B}}{\frac{h}{\gamma}\cdot P^{\frac{1}{\gamma}-1}}$$

In the search for optimization of the deceleration, Ross[4] constrained the velocity of the airbag to be the following fourth order polynomial:

$$\frac{dh}{dt} = u_0[-\frac{t}{t_f}]^4 + 2.0[\frac{t}{t_f}]^2 - 1]$$

then solved Equations (I) and (II) for the optimum open loop vent area as a function of time that maximized the deceleration.

The current computer model does not constrain the change of height to any prescribed function it integrates the equations simultaneously in time, by reducing Equation (II) into two first order differential equations. The model solves three simultaneous differential equations in time using simple rectangular integration.

$$x_1 \equiv h$$

$$x_2 \equiv \frac{dh}{dt} = \frac{dx_2}{dt}$$

$$x_3 \equiv P$$

$$\frac{dx_1}{dt} = x_2$$

$$\frac{dx_2}{dt} = \frac{B}{M}(P_{bag} - P_a) - g$$

$$\frac{dx_3}{dt} = \frac{dP}{dt}$$

The model uses the Equation (IA) representation for the time rate of change of pressure ratio. This enables analytical computer study of the airbag gas inflation process.

This Page Intentionally Left Blank

APPENDIX D

FORTRAN SOURCE CODE CHANGED TO ACCOMIDATE THE SCALE MODEL AIRBAG HEMISPHERICAL DOME

```
    ...
    ...
    HBA=H/2.
    CALL VOLU(X1,V1,HBA)
    XD1=X2
    XD2=(B*PA*144/MASS)*(X3-1.)-G
    XD3=-
((AOR*(C/SQRT(GAMMA))*ALPHA+BETA*X2)/(V1*EPSILON))+QWAN2
    CALL INTEG(X1,DT,XD1,XD1P)
    CALL INTEG(X2,DT,XD2,XD2P)
    CALL INTEG(X3,DT,XD3,XD3P)
C
....
....
....
   STOP
   END

    SUBROUTINE CKVALVE(AOR,P,SR,TD,PSET,DL,DI)
    DATA PIE,DS,RO,TL/3.1416,.25,.03704,.25/
    AI=(PIE/4.)*DI*DI
    VL=(PIE/4.)*DL*DL*TL
    WL=RO*VL
    FP=AI*PSET
    DX=FP/(3.*SR)
    F=P*AI
    X=(WL+F-3.0*SR*DX)/(3.*SR)
    AOR=X*(PIE*DL-3.*DS)/144.
    IF((X+DX).GE.TD) AOR=(TD-DX)*(PIE*DL-3.*DS)/144.
    RETURN
    END

    SUBROUTINE VOLU(X1,V,A)
    PI=3.1415926
    X=2.*A-X1
    H=2.*A
    IF(X1.LE.H.AND.X1.GE.A) V=(5./3.)*PI*A*A*A-(PI*(X*A*A-X*X*X/3.))
    IF(X1.LT.A) V=PI*A*A*X1
    RETURN
    END
```